ResearchOnline@JCU

JAMES COOK UNIVERSITY AUSTRALIA

This file is part of the following work:

Lechene, Marine (2025) ***Spatio-temporal dynamics of coral demography across environmental gradients on the Great Barrier Reef and the Torres Strait.*** **PhD Thesis, James Cook University.**

Access to this file is available from:

https://doi.org/10.25903/tfap%2Dyq25

Copyright © 2025 Marine Lechene

The author has certified to JCU that they have made a reasonable effort to gain permission and acknowledge the owners of any third party copyright material included in this document. If you believe that this is not the case, please email researchonline@jcu.edu.au

Spatio-temporal dynamics of coral demography across environmental gradients on the Great Barrier Reef and the Torres Strait

Thesis submitted by

Marine Anna Alice Lechene

B.Sc., M.Sc.

In February 2025

For the Degree of Doctor of Philosophy

College of Science and Engineering, James Cook University

The Australian Institute of Marine Science

Townsville, Queensland, Australia

Acknowledgements

Firstly, I would like to thank my supervisor Renata Ferrari for your unwavering support, guidance, and unconditional availability – even at the very last minute! Thank you for thinking of me when the opportunity arose to take on your first PhD student, despite the years that had passed since my master's degree. Knowing each other beforehand made my PhD journey incredibly enjoyable, as if I were guided by an old friend looking out for me. I am especially grateful for your all-encompassing advice, from scientific insights to life hacks and navigating academia as an international female student. I will be forever thankful for your mentorship.

A special thanks to my co-supervisor, Nicholas Murray. Your impressive research background and academic experience, combined with your nurturing nature, were invaluable throughout my PhD. Thank you for providing me with opportunities to gain teaching experience, which I greatly enjoyed, and for always offering advice on becoming a better scientist. Your encouragement to think about the broader impact and resonance of my research has been incredibly meaningful.

I would like to extend my heartfelt thanks to my co-supervisor, Mia Hoogenboom. Despite your incredibly busy schedule, you took me under your wing and provided invaluable guidance. Your input has always been insightful and on point, a testament to your extensive experience in supervising students and your deep knowledge of coral ecology. One of the most valuable lessons I learned from you is the power of summarising key findings in a table – something I will carry forward in all my future work!

A big thank you to my external co-supervisor, Will Figueira. Will, thanks for being so approachable from day one, back in 2016 when at the end of a lecture I asked if you had a research project opportunity for me in your lab. Turns out you did, and the rest is history. Thank you for your support during both my master's degree and PhD, for your good ideas, enthusiasm and also humour.

I am immensely grateful to the EcoRRAP team for their support in the field and in the office. A special thanks to Sophie Gordon, Mariana Álvarez-Noriega, Maren Toor, Tiny Remmers, Madison Becker, Eoghan Aston, and Deborah Burn for sharing successes and frustrations, for always supporting one another, and for pushing each other to grow both personally and professionally. We quickly became close friends, and I cherish the joy of working alongside

people I admire and care about. Seeing each other grow has been an incredible experience – I love you all.

To my friends in Townsville, Sydney, New-Zealand, France and New-Caledonia, thank you for your unwavering support throughout this PhD journey. You kept me sane during the tough times and made the good times unforgettable. I will forever cherish our camping trips, rock climbing adventures, dinners, celebrations, shared laughter and tears, as well as the moments of joy and sorrow. You have truly been my family away from home.

I am also grateful to the staff at JCU and the former Centre of Excellence for Coral Reef Studies (ARC CoE) for their support during my candidature. A special thanks to Morgan Pratchett—your guidance in forming and structuring this project, particularly during my first (and most challenging) year, was invaluable.

A heartfelt thank you to the AIMS@JCU team for your support. Being part of this student cohort was a truly special experience, thanks to your dedication and care. You made our PhD journey so much more enriching. I am particularly grateful for the prizes and awards offered by the program, which allowed me to attend conferences each year and collaborate with other research teams—opportunities that greatly shaped my academic experience. On this, I am very grateful to have received the Leviathan Grant, in collaboration with the artist Shezad Dawood that allowed me to collaborate with the 3DX Lab at the University of New South Wales. Thank you, Benjamin Bailey, for turning the 3D coral reef models into virtual reality!

This thesis was made possible through the AIMS@JCU Postgraduate Scholarship, with additional financial support from the ARC CoE, College of Science and Engineering, and the AIMS@JCU program. Fieldwork, data processing, and management were made possible thanks to the Reef Restoration and Adaptation Program's subprogram EcoRRAP and the Australian Institute of Marine Science. I would also like to acknowledge and pay my respects to the Traditional Owners of the Sea Country from which this data was collected from, with free informed prior consent. I specifically acknowledge and thank the following Traditional Custodians groups: Masigalgal, Porumalgal, Warraberalgal (Torres Strait); Gunggandji, Ngurruumungu, Gingaal (Northern Great Barrier Reef); Manbarra, Bindal (Central Great Barrier Reef); and Woppaburra, Bailai, Gurang, Gooreng Gooreng, Taribelang Bunda (Southern Great Barrier Reef).

Finally, I owe immense gratitude to my family and partner. A special thanks to my grandmother, whose support made it possible for me to pursue my master's degree in Australia. To my mum – thank you for always being proud of me, no matter how lost I may have seemed at times. Your unwavering belief in me has been a constant source of strength. To my partner, fiancé, and future husband – words cannot express how grateful I am for your support over these last 11 years. You stood by me through every decision, from my first move to Australia to relocating to Townsville, even when it meant we had to live apart for a time. Thank you for always following me, believing in me, and being my pillar when I doubted myself – which, let's be honest, is most of the time.

So, to all of you who have been part of this incredible journey – I cannot thank you enough. This project is the thread that connected it all, and I am forever grateful.

Statement of the Contribution of Others

This thesis was conducted under the supervision of Dr. Renata Ferrari, A/Prof. Nicholas Murray, A/Prof. Mia Hoogenboom and A/Prof. Will Figueira. Please see the table below for specific contributions by supervisors and other collaborators.

Chapter	Contributor	Nature of Assistance
Chapter 1: General introduction	Renata Ferrari[1] Nicholas Murray[2] Mia Hoogenboom[1,2]	Conceptualisation/chapter preparation Conceptualisation/chapter preparation Conceptualisation/chapter preparation
Chapter 2: Colony morphology and habitat drive coral size patterns *(under review)*	Mariana Álvarez-Noriega[1] Madison Becker[1] Maren Toor[1] Sophie Gordon[1] Tiny Remmers[1,2] Will Figueira[3] Mia Hoogenboom[1,2] Renata Ferrari[1]	Conceptualisation/data collection/ data analysis/manuscript preparation Data extraction/manuscript preparation Data collection/ data extraction/manuscript preparation Data collection/data extraction/manuscript preparation Data collection/manuscript preparation Data analysis/manuscript preparation Conceptualisation/data analysis/manuscript preparation Data collection/conceptualisation/data analysis/manuscript preparation
Chapter 3: Evaluating error sources to improve precision in the co-registration of underwater 3D models *(published)*	Will Figueira[3] Nicholas Murray[2] Eoghan Aston[1,2] Sophie Gordon[1] Renata Ferrari[1]	Conceptualisation/data analysis/manuscript preparation Conceptualisation/data analysis/manuscript preparation Data extraction/manuscript preparation Conceptualisation/data collection/data extraction/manuscript preparation Data collection/conceptualisation/data analysis/manuscript preparation
Chapter 4: Legacy effects of a mild mass bleaching event on	Mariana Álvarez-Noriega[1] Deborah Burn[1]	Data collection/conceptualisation/data analysis/manuscript preparation

coral survival and growth *(in prep.)*	Madison Becker[1] Maren Toor[1] Sophie Gordon[1] Tiny Remmers[1,2] Mia Hoogenboom[1,2] Renata Ferrari[1]	Conceptualisation/data analysis/manuscript preparation Data extraction/manuscript preparation Data collection/ data extraction/manuscript preparation Data collection/data extraction/manuscript preparation Data extraction/manuscript preparation Conceptualisation/data analysis/manuscript preparation Conceptualisation/data analysis/manuscript preparation
Chapter 5: General discussion	Renata Ferrari[1] Nicholas Murray[2] Mia Hoogenboom[1,2]	Conceptualisation/chapter preparation Conceptualisation/chapter preparation Conceptualisation/chapter preparation

[1] Australian Institute of Marine Science, Townsville, QLD 4810, Australia
[2] College of Science and Engineering, James Cook University, Townsville, QLD 4811, Australia
[3] School of Life and Environmental Science, The University of Sydney, Sydney, NSW 2006, Australia

This thesis was also supported by Januar Harianto and Zal Cowasji who assisted in the data extraction in Chapter 3. Project proposal formulation assistance and advice from Prof. Morgan Pratchett.

This thesis was funded by an AIMS@JCU Scholarship provided to Marine Lechene. Data collection, processing and extraction was supported by the Reef Restoration and Adaptation subprogram Ecological Intelligence for Reef Restoration (EcoRRAP, https://gbrrestoration.org/program/ecorrap/).

Abstract

The ongoing degradation of coral reef ecosystems, characterised by a significant shift in coral community composition and species habitat distributions, poses serious threats to the structure and function of these biodiverse ecosystems. Monitoring the condition/state of coral reefs typically relies on one common metric, change in hard coral cover as a percentage of area, that is relatively easy to measure in a standardized way across different reef habitats and regions. While change in coral cover provides a snapshot of reef condition at different points in time and space, it is of very limited use for unravelling the mechanisms behind coral loss or recovery. This is because coral size structure influences reproductive potential, and thus population viability, and measures of coral cover do not capture the necessary size and vital rate information required to predict population and community dynamics. To understand and predict key drivers of coral reef trajectory, there is a need to adopt demographic and trait-based approaches.

The overarching objective of this thesis was to assess how environmental gradients shape coral reef demographics at multiple scales to enable better predictions of coral reef trajectories over the coming decades of ocean warming. To address this objective, three distinct studies (presented in data Chapters 2, 3 and 4 of the Thesis) were undertaken to: (1) examine the spatial variation in size structure of dominant coral taxa across environmental gradients, linking coral traits to habitat conditions; (2) introduce novel methods for accurate detection of changes of coral populations and communities in millimetre resolution and across reefscapes over time; and (3) investigate how colony level bleaching responses, as well as colony size, affected coral survival and growth across environmental gradients. For (3), the mild bleaching event experienced on the Great Barrier Reef in 2022 provided a unique opportunity to assess colonies experiencing a wide range of temperature stress conditions that resulted in a broad spectrum of bleaching responses with relatively high survival and allowed a detailed assessment of the sub-lethal effects of bleaching on growth. Overall, this thesis advances ecological theories of landscape and population dynamics, develops an unprecedented coral demographic dataset, and provides valuable insights for the management of coral reefs in the face of ongoing environmental change.

Understanding the size structure of coral populations is critical for assessing resilience, yet our knowledge of how environmental conditions influence coral size structure remains limited. In

Chapter 2, spatial patterns in the size structure of six dominant morphotaxa were quantified across 85 sites on the Great Barrier Reef and the Torres Strait. Large-area orthomosaics, were used to measure the planar area of 5880 coral colonies that naturally occurred along gradients in key environmental factors such as depth, cross-shelf position, latitude and wave exposure. This study tested three hypotheses: (1) are larger corals more prevalent at higher latitudes; (2) do inshore reefs favour larger corals due to environmental conditions; (3) are larger corals more prevalent in less exposed habitats; and do size variation patterns vary with colony morphology. The results show that larger corals were more prevalent in inshore reefs and less exposed habitats except at higher latitude locations. These patterns were particularly pronounced in 'top-heavy' morphologies like large tabular *Acropora*, which are more vulnerable to breakage in high-exposure environments. As larger colonies produce more gametes, these results can be used to identify reefs, and/or habitats within reefs, that disproportionally contribute large numbers of larvae to replenish coral populations.

Understanding how environmental forces shape coral populations in space and time helps inform management strategies. To accurately measure the demographics that shape coral population dynamics at meaningful spatial scales requires advanced image processing methods to reconstruct coral colony morphology and reef topography. Detecting change from photogrammetry products, such as change in coral colony planar area, requires accurate alignment of 3D reconstructions of reef sites collected at different times using a process referred to as temporal co-registration. However, achieving precise co-registration is difficult in reef habitats due to practical challenges intrinsic to underwater surveys. **In chapter 3**, an efficient co-registration workflow for 3D models derived from underwater structure-from-motion methods is presented to address these challenges. This workflow was also tested by using 3D models from across a wide range of coral reef habitats covering all those that one may encounter in shallow reefs (15 m depth and above). Four key sources of error in the workflow were identified, empirically estimated and tested to investigate their relative contribution to the overall protocol error: co-registration, 3D processing, image acquisition, and reference and scaling features (RSF) placement. The proposed co-registration workflow aims to minimise these sources of errors and had a mean precision of 1.37 ± 16.55 mm. Image acquisition and RSF placement errors contributed the most to the total workflow error (37 % and 53 %, respectively), while the contribution of co-registration and 3D processing errors was minimal (3 % and 7 %, respectively).

The co-registration workflow from chapter 3 enabled the extraction of coral colony size data between 2021 and 2023 at permanent sites along the GBR. In early 2022, a mild mass bleaching event occurred in the central region of the GBR, providing the unique opportunity to assess thousands of colonies experiencing a range of bleaching responses, where relatively high survival allowed a unique opportunity to investigate the sub-lethal effects of bleaching on growth. An extra survey of the permanent sites at the peak of bleaching was done, enabling the quantification of bleaching extent and severity. By generating and analysing a unique dataset including colony size fifteen months prior, three months prior and nine months after the peak of the bleaching event, as well as information on mortality, **chapter 3** investigated the lethal and sublethal effects of the bleaching event on dominant and susceptible coral taxa in this region of the GBR. Specifically, this study tested (1) how heat stress impacts survival and growth of healthy (i.e., not bleached) colonies, and (2) how bleaching severity affects survival and growth and how this effect is modulated by key biological, environmental and biophysical variables such as taxonomic identity, initial colony size, depth, reef slope, turbidity and sea surface temperature. Results showed that survival probabilities were strongly linked to initial colony size, with larger corals more likely to survive post-bleaching. Heat stress negatively affected growth, particularly in corals that fully bleached or experienced partial mortality. Environmental variables generally had negative effects on growth and sometimes interacted with bleaching severity, amplifying, or unexpectedly, mitigating impacts. These findings emphasize the necessity of incorporating colony size, along environmental data, into population dynamic models to better predict coral demography under changing conditions.

In conclusion, this thesis advances coral reef science by quantifying the critical role of coral colony size in demographic processes and leveraging photogrammetry to precisely monitor colonies across diverse environments. It provides scalable tools for ecological research, informs conservation strategies to protect source reefs and habitats, and offers a comprehensive framework for understanding and managing coral populations in the face of climate change.

Table of Contents

Acknowledgements 2
Statement of the Contribution of Others 5
Abstract 7
Table of Contents 10
Chapter 1. General introduction 14
Chapter 2. Colony morphology and habitat drive coral size patterns 24
2.1 Abstract 24
2.2 Introduction 25
2.3 Methods 29
2.3.1 Data collection and processing 29
2.3.2 Statistical analysis 32
2.4 Results 35
2.4.1 Influence of latitudinal gradient 37
2.4.2 Influence of cross-shelf position 39
2.4.3 Influence of habitat 40
2.5 Discussion 42
2.5.1 Influence of cross-shelf gradient on coral size frequency distribution 43
2.5.2 Influence of wave exposure and depth gradients 44
2.5.3 Ecological implications 46
Chapter 3. Evaluating error sources to improve precision in the co-registration of underwater 3D models 49
3.1 Abstract 49
3.2 Introduction 50
3.3 Methods 53
3.3.1 Sources of error examined 54
3.3.2 Study plots 58
3.3.3 Data collection 58
3.3.4 3D processing 60
3.3.5 Deviation analysis 61
3.4. Results 63
3.5 Discussion 69
3.5.1 Context of study 69
3.5.2 Good practices guidelines for co-registration workflows 72
3.5.3 Important considerations 78
3.6 Conclusion 79
Chapter 4. Legacy effects of a mild mass bleaching event on coral survival and growth 80
4.1 Abstract 80
4.2 Introduction 81
4.3 Methods 84
4.3.1 *In situ* sampling 84
4.3.2 Image processing 86
4.3.3 Environmental variables 88
4.3.4 Data analyses 89

4.4 Results 94
4.4.1 Effect of heat stress on survival and growth of healthy colonies 94
4.4.2 Effect of bleaching severity, colony size and environmental variables on survival and growth of coral colonies during a mild mass bleaching event 97
4.5 Discussion 104
Chapter 5. General Discussion 110
References 115
Appendix A. Supplementary material to Chapter 2 133
Appendix B. Supplementary material to Chapter 3 138
Appendix C. Supplementary material to Chapter 4 143
Appendix D. Publications arising from this thesis 144
Appendix E. Publications not arising from this thesis 145

List of Figures

Figure 1. 1. Conceptual diagram showing temporal and spatial scales on which biophysical processes influencing coral demography operate (orange), our current observational capacity for a given survey method (blue) and the different types of demographic data (green) available in corals. 21

Figure 2. 1. Nested sampling design used in this study to examine the size structure of six dominant morphotaxa on the Great Barrier Reef and Torres Strait. 30
Figure 2. 2. Six coral morphotaxa (and their code) used in this study..... 31
Figure 2. 3. Difference in size structure between clusters. 37
Figure 2. 4. Effect of cross-shelf position (inshore versus offshore) on three size classes of two morphotaxa in two different latitudinal regions of the GBR (Central and South). 39
Figure 2. 5. Difference size structure of six morphotaxa between habitats..... 40

Figure 3. 1. Conceptual diagram detailing the experimental design around the four sources of error tested in the field and in the office. 56
Figure 3. 2. In-depth workflow diagram detailing all the steps and parameters used from image collection in the field to precision evaluation. 57
Figure 3. 3. Design and setup of a sphere-tree. 59
Figure 3. 4. Diagram of equipment, plot setup and swim patterns used during image acquisition. 60
Figure 3. 5. Distributions of the model-to-model deviations by plots (P01-P10) and source of error (a-d)..... 65
Figure 3. 6. Example of deviation analysis output..... 67
Figure 3. 7. Distribution of model-to-model deviations..... 68

Figure 4. 1. Study sites 85
Figure 4. 2. Survival probability between years and taxa.. 95
Figure 4. 3. Size at t_1 as a function of size at t_0, year and taxa. 96
Figure 4. 4. Survival and growth model outputs for A. staghorn.. 99
Figure 4. 5. Survival and growth model outputs for A. corymbose..... 100
Figure 4. 6. Survival and growth model outputs for P. damicornis. 101
Figure 4. 7. Survival and growth model outputs for P. verrucosa..... 102
Figure 4. 8. Survival and growth model outputs for S. hystrix. 103

List of Tables

Table 1. 1. Summary of key advantages and limitations of the most common methods to quantify coral colony size through time. 20

Table 2. 1. Summary statistics for each morphotaxon. 36

Table 3. 1. The four key sources of error examined in this study, how test models were created, what the inferred error was, and if each of the key sources of error included other sources of error. 55
Table 3. 2. Summary statistics (mean, median, standard deviation - SD - and median absolute deviation - MAD -) of model-to-model deviations calculated across all 10 plot pairs for each source of error 66

Table 4. 1. Survival model formula of the best-fit model for each taxon. Models were compared using AIC. 93
Table 4. 2. Growth model formula of the best-fit model for each taxon. Models were compared using AIC. 94
Table 4. 3. Summary table of the significant effects of tested predictors on survival probability and growth of five morphotaxa 104

Chapter 1. General introduction

Coral reefs in the Anthropocene

Coral reefs are critical ecosystems both ecologically and socioeconomically. They provide a wealth of ecosystem goods and services such as the support of biodiversity and habitat (Fisher et al., 2015; Gillis et al., 2014), the provision of coastal protection (Ferrario et al., 2014), food and income (Golden et al., 2016; Spalding et al., 2017), and cultural significance (Cinner, 2014; Gregg et al., 2015). However, coral reefs are no exception to the overall declining integrity of ecosystems worldwide and are rapidly degrading in response to climate change-induced stressors (Bellwood et al., 2004; Hoekstra et al., 2005).

Coral reefs' loss of integrity is mainly quantified as declines in the abundance and diversity of habitat-forming corals (e.g., De'ath et al., 2012; Gardner et al., 2003; Mellin et al., 2019). The causes of sustained habitat degradation vary regionally, although localised disturbances and pressures are increasingly being compounded by apparent and emerging effects of global climate change (Bellwood et al., 2019; Hoegh-Guldberg et al., 2017). Since the 1998 global mass bleaching event (although earlier warnings were made by researchers, e.g., Glynn, 1991), climate change and associated stressors have been recognised as the greatest threats to the integrity of coral reef ecosystems globally (Anthony et al., 2020; Burke et al., 2011; Hoegh-Guldberg et al., 2023). Climate-induced mass coral mortality is often followed by sustained declines in structural complexity, due to erosion and decomposition of dead coral skeletons, and ultimately affects the abundance and diversity of reef-associated organisms (Graham et al., 2007; Pratchett et al., 2009, 2018; Stella et al., 2011).

Coral population dynamics and demography

Demography is a critical framework for understanding population dynamics within ecosystems. By quantifying processes such as birth, death and fecundity, demographic studies provide insights into the factors driving population growth or decline (Leslie, 1945; Lotka, 1931; Roughgarden, 1975). For keystone species, changes in age structure have far-reaching consequences for ecosystem functioning and trophic dynamics (e.g., Paine, 1969). For example, the loss of large and mature framework-building individuals – such as old trees in forests or large corals on reefs – can disrupt habitat availability, diminish resource supply and

alter ecological processes, highlighting the interconnectedness between population demography and ecosystem health (Dietzel et al., 2020; Lindenmayer & Laurance, 2017).

Demographic studies typically rely on detailed data about population size, composition and vital rates. While this information is readily available for human populations through censuses, it remains sparse and spatially restricted for most wild animal and plant species, especially invertebrates and marine taxa (Cardoso et al., 2012; Régnier et al., 2015; Webb & Mindel, 2015). Coral populations exemplify these challenges. As benthic colonial organisms with size-dependent rather than age-dependent life-histories (Hughes, 1984), reef-building corals rely on larval dispersal for habitat recolonisation and exhibit a wide range of colony sizes, often varying by orders of magnitude (Meesters et al., 2001; Soong, 1993). Larger colonies, which are disproportionally fecund, play a critical role in sustaining populations by contributing significantly to reproduction, resisting complete mortality through partial survival, and in some cases, persisting for centuries despite recruitment failures (Hughes & Tanner, 2000).

The reproductive strategies of corals further complicate demographic assessments. Broadcast-spawning species release gametes into the water column, enabling fertilised larvae to disperse across vast distances (up to hundreds of kilometres), while brooding species retain fertilised embryos within the colony and release fully developed larvae that settle near the natal reef (Harrison & Wallace, 1990). These differences in dispersal patterns influence how coral species recolonise habitats and recover from disturbances, underscoring the importance of spatial and temporal scales in demographic studies (Darling et al., 2012; Edmunds & Riegl, 2020; Pearson, 1981). However, limited in-water survey coverage and the inherent complexity of coral life histories make it challenging to collect demographic data at scales that capture critical processes such as recruitment dynamics and responses to reef disturbances. Consequently, knowledge gaps remain in our understanding of interspecific and intraspecific variation and the underlying ecological mechanisms of population change.

Recent large-scale studies have begun to quantify changes in coral demographic across regional and decadal scales. For instance, Dietzel et al. (2020) documented a significant and sustained decline in large coral colonies on the Great Barrier Reef, with implications for reproductive potential and population recovery. These studies provide critical baselines but often rely on aggregate metrics or interpolated survey data, which may obscure fine-scale variation in colony responses and environmental context. As such, there remains a need for approaches that resolve

individual-level demographic processes to clarify how corals respond to environmental change in space and time.

There can be synergistic, additive and opposing effects of different environmental variables on demographic rates (e.g., Chase et al., 2014; Negri & Hoogenboom, 2011). For instance, coral survival and growth require a specific set of conditions in temperature, light, water flow, water chemistry and nutrient levels (Anthony & Fabricius, 2000; Hoogenboom & Connolly, 2009; Lough & Barnes, 2000). In addition, reefs experience significant environmental variability over small spatial and temporal scales. Gradients in depth and turbidity affect levels of irradiance at scales of centimeters to meters (Anthony et al., 2004), resulting in changes in species composition among habitats (e.g., Browne et al., 2013). During acute storms, such as tropical cyclones, wave energy can intensify rapidly and break or dislodge more vulnerable colonies (Madin et al., 2014; Madin & Connolly, 2006) resulting in mortality across large spatial scales and substantial decreases in coral cover, especially at sites where susceptible corals are the most abundant (Madin et al., 2014). In addition, climate change is increasing the frequency of environmental change with direct consequences on demographic rates. For instance, increasing temperature or decreasing calcification rates may reduce coral growth rates, skeletal density or increase susceptibility to dislodgement or breakage (Pratchett et al., 2015). Consequently, knowledge gaps also remain in our understanding of the effects that different components of environmental change will have on demography.

Impact of heat stress on coral demographics

Climate change, principally ocean warming and acidification, threatens coral reef ecosystems. Elevated sea surface temperatures drive widespread coral bleaching events. Bleaching arises when the symbiotic relationship between corals and their dinoflagellate algae symbionts (family Symbiodiniaceae) breaks down. These algae are crucial for their hosts, supplying energy through photosynthesis and providing essential nutrients (Muscatine et al., 1997; Wiedenmann et al., 2023). However, extreme environmental conditions, such as increased temperatures or intense light, can damage the algae's photosynthetic systems, reducing their capacity to supply energy to the coral host (Iglesias-Prieto et al., 1992). This damage leads to cellular stress in both the algae and the coral, ultimately reducing algal density within coral tissues (Warner et al., 2002) or causing the symbiosis to collapse entirely (Lesser, 2006), exposing the coral's white skeleton – hence the term 'coral bleaching'.

Since 1998, the GBR has experienced six mass bleaching events, with four occurring since 2016. The increasing frequency of thermal stress events leaves coral reefs with limited recovery periods, resulting in overlapping disturbances that compound their effects (Emslie et al., 2024). Climate projections suggest that most reefs will suffer recurrent or annual bleaching by 2050 (Donner et al., 2005; Kwiatkowski et al., 2015; van Hooidonk et al., 2016). These conditions are expected to cause substantial declines in live coral cover, shifts in species composition toward more stress-tolerant species (Logan et al., 2014; Pandolfi et al., 2011) or individuals adapted to higher temperatures (Thomas et al., 2018). In extreme cases, reefs may undergo local extinction (Pratchett et al., 2020) or phase shifts to ecosystems dominated by non-coral species (McManus & Polsenberg, 2004). Although some coral populations show potential to adapt to warming seas (Fox et al., 2021; Palumbi et al., 2014; Romero-Torres et al., 2020), the cumulative impact of repeated bleaching events most likely impairs coral physiological performance over time rather than promoting acclimatization (Grottoli et al., 2014). Severe thermal stress can lead to bleaching-induced mortality, creating population bottlenecks that restrict opportunities for adaptation (Burn et al., 2023; Dietzel et al., 2021). Even following successive moderate-intensity heatwaves, evidence of acclimatisation is often absent at ecologically meaningful scales, underscoring the limited capacity of many reefs to recover in the face of increasing thermal stress.

Monitoring individual corals through marine heatwaves provides valuable insights into the drivers and prevalence of coral acclimatisation to heat stress. While many coral bleaching studies rely on population-scale metrics, such as the percentage of colonies bleached (e.g., Marshall & Baird, 2000; Pisapia et al., 2019), fewer focus on tracking the fate of individual colonies over time (but see Byrne et al., 2025; Morais et al., 2021, 2024). This approach is often constrained by the difficulty of precisely relocating and measuring the size and health status of many individual coral colonies *in situ*. Advancements in large-area imaging technologies, such as photogrammetry, address these challenges by enabling researchers to create detailed georeferenced 3D models and 2D orthomosaics of reef benthos. These models allow for the accurate identification and monitoring of individual coral colonies over time and have been successfully applied to study growth and mortality (e.g., Cresswell et al., 2020; Ferrari et al., 2017; Lange & Perry, 2020). This approach also enhances our understanding of how intraspecific diversity in bleaching responses influences ecological outcomes and identify key drivers of well acclimated corals. While numerous studies highlight interspecific differences in bleaching susceptibility as predictors of mortality—where resistant species

experience lower mortality than susceptible ones (Baker et al., 2008; Hughes et al., 2019; Loya et al., 2001; McClanahan et al., 2004)—this method reveals the critical role of individual traits and their variation within species in shaping reef resilience.

The onset of another global bleaching event in 2023-2024 has underscored the urgent need for action (Hoegh-Guldberg et al., 2023). International commitments such as the UN Decade for Ecosystem Restoration (https://www.decadeonrestoration.org/) and the Coral Reef Breakthrough 2023 (https://coralbreakthrough.org/), which aim to restore natural ecosystems, have spurred reef restoration efforts. Restoration of coral reefs is typically aimed at aiding the recovery of reef structure, function and key species under stress, while promoting resilience (Shaver et al., 2022) and sustaining ecosystem services (e.g., tourism, fisheries, coastal protection, Hein et al., 2021). These efforts range from mitigation and rehabilitation to fostering long-term resilience to climate change impacts through strategies like assisted evolution (van Oppen et al., 2015). Reef restoration relies on two key disciplines: ecological restoration, which focuses on supporting the recovery of degraded, damaged or destroyed ecosystems, and restoration ecology, the science that informs and guides these practices (Suggett et al., 2024). Both are essential for ensuring the success of restoration projects and achieving their stated objectives.

Despite this, some critics argue that small-scale restoration projects are costly distractions that fail to address the root causes of reef decline (Bellwood et al., 2019; Hughes et al., 2017). These critiques often conflict with growing evidence that restoration can support ecological recovery, including for coral reefs (Lange et al., 2024; Toth et al., 2022). This scepticism partly stems from challenges such as limited resources to monitor long-term ecological outcomes and the difficulty of distinguishing the effects of restoration from natural recovery processes, until recently mostly due to inadequate methods and lack of empirical data across thousands of coral colonies. Ultimately, simply protecting ecosystems at risk of collapse is no longer sufficient. The focus of ecosystem management for integrity represents a shift from maintaining biodiversity to protecting key functions (e.g., roles of predators, Ritchie & Johnson, 2009).

In coral reefs, variations in coral colony taxa, shape and size (i.e., growth and partial mortality) explain variations in performance, function and response to disturbance (Zawada, Madin, et al., 2019). Active interventions are increasingly important for ecological restoration, yet critical baseline knowledge such as drivers of coral demographics to guide coral reef restoration efforts

and validate predictive models remains scarce. Emerging technologies such as underwater photogrammetry present an exciting tool to gather data needed to quantify restoration success (Ferrari et al., 2021) and validate coral population and community demographic models under increased environmental stress (Edmunds et al., 2014; Riegl et al., 2017).

Advances in reef monitoring technologies

Photogrammetry-based surveys offer a significant advantage for ecosystem monitoring by providing a comprehensive, permanent, two-dimensional (2D) or three-dimensional (3D) representation of a system, replacing the fragmented view offered by individual photos (Baltsavias et al., 2001; Barker et al., 1997; Collins & Moon, 1979; Painter et al., 1974). This method can generate various outputs depending on the intended application. 3D models, created from overlapping images of a scene, allow for the estimation of surface area and volume and enable tracking of changes over time to measure topographical shifts (e.g., Bythell et al., 2001; Hoshikawa et al., 2024; Rossi et al., 2020). Orthomosaics, another product, are high-resolution, large-scale orthorectified images derived from the original photos and 3D models (Westoby et al., 2012). Unlike satellite-based aerial surveys, orthomosaics offer millimetre resolution due to their close-range remote sensing approach (Remmers et al., 2024). Unlike standard photos, orthomosaics integrate depth information, essentially providing a flattened version of a 3D model. This enables accurate individuals' size estimation, regardless of the distance between the camera and the coral.

Given the significant role of coral colony size in demographic processes, it is important that monitoring approaches prioritise accurate and precise size measurements over time (Edmunds & Riegl, 2020). Traditional *in situ* approaches for measuring coral colony size rely on rulers or transect tapes to measure one-dimensional (1D) colony diameter, from which 2D planar area can be estimated by assuming each coral colony is elliptical. While simple, this method often underestimates coral size, particularly for large or irregularly shaped colonies (Chandler et al., 2024). Photoquadrats offer improved planar area estimates but often distort colony size due to perspective effects and relocation of the same colonies through time remains challenging. In contrast, photogrammetry-based methods generate 2D orthomosaics and 3D models, allowing thousands of coral individuals to be tracked through time with millimeter-scale accuracy (Burns et al., 2015; Ferrari et al., 2017; Lange et al., 2022; Sandin et al., 2020). Since 2012, the growing adoption of underwater photogrammetry-based surveys has highlighted their effectiveness and

reliability for monitoring underwater ecosystems, overcoming limitations of earlier methods (Couch, 2021; Remmers et al., 2024). A summary of the key advantages and limitations of each method to quantify coral colony size through time is provided in Table 1.1 below.

Table 1. 1. Summary of key advantages and limitations of the most common methods to quantify coral colony size through time.

Method	Advantages	Disadvantages	Examples
In situ (transect tape, callipers)	Simple, low-cost, no post-processing	Assumes elliptical shape, underestimates size, low precision, bottom time limitations	Bak & Meesters 1998; Grimsditch et al., 2017; Dietzel et al., 2020
Photoquadrats	Better 2D size estimation	Perspective distortion, hard to relocate colonies	Edmunds, 2019; Morais et al., 2021 ; Lachs et al., 2024
Photogrammetry	High precision, scalable, tracks individuals through time	Requires processing power, expertise, more costly upfront, data storage	Cresswell et al., 2020; Sandin et al., 2020; Lange et al., 2022

Purpose of thesis and outline

Despite growing concerns about the impacts of climate change on coral reefs, critical knowledge gaps remain in understanding how coral populations respond to environmental stressors over time. Recent large-scale studies, such as Dietzel et al. (2020), have provided invaluable insights into regional shifts in coral size structure and population decline over decadal timescales. However, such approaches typically rely on interpolated survey data, coarse taxonomic resolution and aggregated population-level metrics, limiting their ability to resolve the fine-scale drivers of demographic change. These thesis addresses these limitations by focusing on colony-level demographic responses to disturbance and environmental variability. Rather than examining population trends alone, it investigates the processes that drive population change, and how these vary with colony size and environmental context. By tracking thousands of individuals through time using photogrammetry, this work provides novel, process-based complement to broad-scale studies. The goal is to produce fine-scale empirical data and analysis that strengthen demographic models and support restoration and conservation strategies under climate change.

Coral demographic processes are inherently size-dependent: larger colonies tend to have higher fecundity and lower mortality but may also face greater vulnerability to physical damage or bleaching. These processes are also modulated by environmental gradients. For example, wave exposure can increase mechanical damage in large, top-heavy colonies; turbidity and depth influence light availability and in turn, energy acquisition and growth; water flow affects nutrient delivery and sediment removal. Yet, few studies have empirically quantified how environmental context and colony size interact to shape demographic rates across taxa. This interaction is a key mechanism underlying variation in reef recovery potential, especially in the face of increasingly frequent disturbances (Figure 1.1).

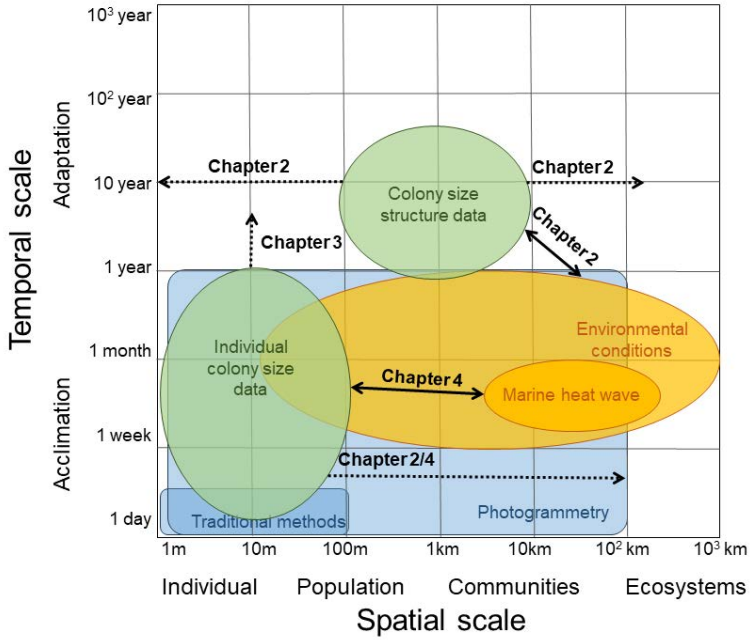


Figure 1. 1. Conceptual diagram showing temporal and spatial scales on which biophysical processes influencing coral demography operate (orange), our current observational capacity for a given survey method (blue) and the different types of demographic data (green) available in corals. Dotted arrows represent datasets expanded in this thesis chapters and the solid arrows represent hypotheses tested in this thesis chapters.

To address these gaps, this thesis asks three interlinked questions: (Q1) How does coral colony size vary across environmental gradients? (Q2) How can we track colonies through time to quantify demographic rates (growth, survival) accurately and precisely? (Q3) How do colony size, bleaching severity and environmental conditions interact to influence coral demography?

These questions are evaluated through three testable hypotheses: (H1) Coral size structure varies with environmental gradients such as turbidity, temperature and wave exposure. (H2) High-resolution photogrammetry can be used to quantify demographic rates accurately and

precisely. (H3) The legacy effects of bleaching are mediated by both initial size and local environmental conditions.

The three data chapters of this thesis each address a core research question, combining spatial surveys, methodological innovation, and disturbance response analysis to explore how colony size and environmental shape coral demography.

In **Chapter 2**, I developed a large coral colony size dataset with an extensive spatial extent and analysed those data to unveil patterns in colony size structure across latitudinal, cross-shelf and habitat gradients. I found that larger corals were typically found in inshore reefs and less exposed habitats, highlighting the importance of these areas as potential source reefs. Coral size structure varied by taxon and environmental conditions but was generally skewed towards smaller colonies – a pattern consistent with prior studies. This underscores the rarity and ecological significance of larger colonies, which are crucial for the reproductive output of the population, increased resilience to bleaching and faster recovery post-disturbance.

In **Chapter 3**, I developed an innovative and efficient workflow for tracking thousands of colonies over time, enabling cost-effective, large-scale monitoring with high precision. This workflow enables for the first time temporal and spatial assessments of coral demographic processes providing critical insights into the effect of environmental stressors on demographic rates across populations and communities.

In **Chapter 4**, I quantified the lethal and sub-lethal effects of a mild mass bleaching event. I found that survival probabilities were strongly linked to initial colony size, with larger corals more likely to survive post-bleaching. Bleaching severity negatively affected growth, particularly in corals that fully bleached or experience partial mortality. The environmental variables tested (water velocity, temperature and turbidity) had only marginal effects on growth and survival. Only temperature interacted with bleaching severity and initial size to either amplify or mitigate heat stress impacts on growth depending on the taxon. These findings emphasize the necessity of incorporating colony size into population and community models to better predict coral demography under climate change.

This thesis advances coral ecology by highlighting the importance of colony size in demographics and using photogrammetry for precise change detection. It provides scalable

research tools, informs conservation strategies, and enhances understanding of coral population dynamics and recovery amid climate change.

Chapter 2. Colony morphology and habitat drive coral size patterns

This chapter is under review in Ecosphere as:

Marine Lechene, Mariana Álvarez-Noriega, Madison Becker, Maren Toor, Sophie Gordon, Tiny Remmers, Will Figueira, Mia Hoogenboom, Renata Ferrari (in review). Colony morphology and habitat drive coral size patterns. Ecosphere.

2.1 Abstract

Coral reefs are essential ecosystems that provide important ecological services and support the livelihoods of millions of people worldwide. Understanding the size structure of coral populations is critical for assessing recovery potential, yet our knowledge of how environmental conditions influence coral size structure, across a range of coral taxa, remains limited. This study tested three hypotheses: due to environmental forcing larger corals are more prevalent at (1) higher latitudes, (2) on inshore reefs, and (3) in sheltered habitats, but coral taxa with different morphologies vary in their sensitivity to specific environmental conditions. We thus examined spatial patterns in the size structure of six dominant morphotaxa across 84 sites on the Great Barrier Reef and the Torres Strait. We used large-area orthomosaics to measure the planar area of 5880 coral colonies, across gradients in latitude, cross-shelf position, wave exposure and depth. Our main findings indicate that larger corals are more prevalent on inshore reefs and less exposed habitats but not at higher latitude. These patterns were particularly pronounced in top-heavy morphologies, which are more vulnerable to breakage in high-exposure environments. As larger colonies produce more gametes these results can be used to identify reefs, or habitats within reefs, that disproportionately contribute large numbers of larvae to replenish coral populations. Understanding how environmental forces shape coral populations helps inform resilience-based management by identifying source reefs.

2.2 Introduction

Demography serves as a fundamental tool in understanding the dynamics of populations within ecosystems (Edmunds & Riegl, 2020). The characterisation, comparison, and assessment of populations require the quantification of key demographic traits, such as age structure, birth and death rates, fecundity, sex ratio, and density. Understanding the age structure of a population holds particular significance due to its direct influence on reproductive potential, thereby enabling estimation of future population growth or decline (Hinde, 1998). Examining change in age-structure is especially relevant for keystone species given their pivotal roles in ecosystem functioning and the subsequent cascading effects on dependent organisms. For instance, the decline of large, mature trees may precipitate habitat loss, diminish food availability, and reduce carbon sequestration, exemplifying the intricate interplay between demographic shifts and ecological processes (Lindenmayer & Laurance, 2017).

Scleractinian corals, analogous to trees in tropical forests, play a pivotal role in supporting entire marine ecosystems by serving as primary providers of habitat structure upon which marine organisms rely (Hutchings et al., 2019). However, the literature has extensively documented the decline in coral cover (Bruno & Selig, 2007; De'ath et al., 2012), habitat complexity (Álvarez-Filip et al., 2009), and the abundance of large, fecund corals (Dietzel et al., 2020). Corals are colonial organisms for which demographic rates such as growth and mortality depend more strongly on size rather than age (Babcock, 1991; Hughes & Connell, 1987; Hughes & Jackson, 1980). Consequently, examining the size structure of coral populations is invaluable for understanding and predicting their state and trajectory, as well as the implications for associated species and ecosystem services (Woodhead et al., 2019). For instance, a risk of population decline may be indicated by either the lack of small colonies, which can result from high juvenile mortality rates or declines in recruitment (Chong-Seng et

al., 2014; Hughes & Tanner, 2000; Miller et al., 2016), or by the lack of large colonies, which may suggest size-dependent mortality that disproportionally affects the largest and most fecund colonies (Hall & Hughes, 1996). Recovery after disturbances is dependent on the asexual and sexual reproduction of surviving coral populations. This highlights the critical importance of large, fecund colonies, which boost larval availability, and post-settlement survival and growth rates. Together, these factors increase the likelihood of successful recruitment (Connell et al., 1997; Doropoulos et al., 2016).

The size structure of corals varies not only among species (Meesters et al., 2001) but also within species due to differences in environmental contexts (Bak & Meesters, 1999; Bauman et al., 2013; Gilmour, 2004). For instance, according to Bergmann's rule (Bergmann, 1848) which states that larger body sizes are associated with colder climates, it is expected that colony size increases with latitude (Chong et al., 2023; Meiri, 2011). A strong environmental factor in corals is water movement. The relationship between water movement, colony size and shape dictate mass exchange of metabolically important gases and metabolites between seawater and coral tissue (Patterson, 1992). However, strong water movement generated by high wind events such as storms and cyclones, can also limit coral colony size by causing breakage and disproportionally impact large, top-heavy colonies (Madin et al., 2014; Madin & Connolly, 2006; Massel & Done, 1993). As a result, habitats frequently exposed to high wind and wave activity are expected to have lower abundances of vulnerable size classes and morphologies. Previous studies have also found marked differences in coral size structures with depth (Adjeroud et al., 2007, 2015; Kramer et al., 2020). While consistent patterns in coral size structure between depths have not been clearly established, depth likely influences coral size due to variations in key physiological factors such as light, temperature and water velocity along the water column (Hoogenboom & Connolly, 2009). Corals, that derive most of their energy from photosynthesis, are expected to decrease in size with depth (Kramer et al., 2020).

Variations in environmental conditions can also influence the size structure of corals. For instance, reefs in sub-optimal and variable conditions such as high-latitude, marginal reefs experience a shift in size structure towards larger corals (Chong et al., 2023; Sommer et al., 2024) because of harsher conditions causing higher mortality rates for the smallest corals (Connell, 1973) and lower sexual recruitment rates (Abrego et al., 2021; Cant et al., 2022). Moreover, mean coral colony size can decrease with increasing distance from shore due to increased wave energy on reefs closer to the edge of the continental shelf (Lirman & Fong, 2007; Sommer et al., 2024). Similarly, inshore reefs can have a high relative abundance of larger colonies because of higher mortality rates of juveniles and lower recruitment rates due to sedimentation, poor water quality, variable conditions in temperature and high turbidity (Fabricius et al., 2005). Such complex interactions between numerous putative drivers of coral vital rates highlights the need for empirical data across large environmental gradients to better understand the relative contributions of life-history traits (e.g., morphology, growth strategy, mortality susceptibility, reproductive strategy) and environmental factors (e.g., water velocity, light, temperature) in shaping coral population size structures and dynamics (Anderson & Pratchett, 2014; Bauman et al., 2013).

Traditional methods for measuring coral colony size *in situ* involve using rulers or transect tapes to measure one-dimensional (1D) colony diameter, from which two-dimensional (2D) planar area can be approximated under the assumption that every coral colony is an ellipse (Adjeroud et al., 2015; Linares et al., 2011). While this single-dimensional approach is straightforward, it often fails to capture the true size or corals, particularly for large colonies and morphologies that deviate significantly from an elliptical shape (Chandler et al., 2024). The use of photoquadrats offer an improvement by providing a more accurate measure of coral colony planar area. However, relocating photoquadrats to track individual colonies over time is difficult, and the use of individual photos can distort size estimates due to variation in

distance and angle between the camera and corals (e.g., colonies further from the camera appear smaller). Since the 2010s, advancements in underwater imaging and photogrammetry techniques have improved coral monitoring. Structure-from-motion (SfM), a close-range photogrammetry technique, enables the creation of high-resolution, large area 2D orthomosaics and 3D models of the benthos. These products allow researchers to permanently mark and track the same coral colonies over time, increase sample size, and reliably measure planar area as a size estimate by projecting colonies onto the same 2D plane (Burns et al., 2015; Ferrari et al., 2017; Lange et al., 2022). Since 2015, the widespread adoption of SfM-based surveys has demonstrated the technique's effectiveness and reliability for monitoring underwater ecosystems (Remmers et al., 2024).

Here, we investigated the spatial patterns in the size structure of six dominant coral morphotaxa with contrasting life history strategies on the Great Barrier Reef (GBR) and the Torres Strait. We used high-resolution orthomosaics to extract colony planar area of 5880 coral colonies across 85 sites, encompassing three environmental gradients (wave exposure, turbidity and temperature). Our spatial analyses advance our understanding of major environmental forcings believed to shape the size structure of hard corals. We specifically examined three hypotheses, founded on existing biogeographical knowledge, on the expected relationships of coral size frequency distribution, taxa and their environment: 1) Larger corals are found at higher latitudes (i.e., southern region of the GBR). Populations in higher latitude reefs are exposed to colder environments (Sunday et al., 2012) and to greater variation in temperature than tropical populations (Stevens, 1989). This could favour larger colonies over small ones through higher rates of small colony mortality and lower recruitment levels (Abrego et al., 2021; Chong et al., 2023; Connell, 1973). 2) Larger corals are found inshore. Inshore reefs are characterised by sedimentation and high variation in environmental conditions (e.g., temperature, turbidity), which could favour larger colonies over small ones through lower recruitment rates and higher

juvenile mortality (Fabricius et al., 2005). 3) Larger corals are found in sheltered habitats, compared to exposed habitats. We expect coral size structure to vary across a gradient of wave exposure with size decreasing as exposure increases. We also anticipate morphotaxa- and depth-specific responses to the three environmental gradients (Hypotheses 1-3). For instance, differences in size between habitats may be more pronounced in corals with top-heavy morphologies as they are disproportionally susceptible to breakage compared to bottom heavy morphologies (Madin & Connolly, 2006). Similarly, size differences may be depth-dependent, in deeper habitats where light availability is lower, corals are expected to be smaller (Kramer et al., 2020).

2.3 Methods

2.3.1 Data collection and processing

Imagery was collected as part of the Ecological intelligence for reef restoration and adaptation (EcoRRAP) sub-program (https://gbrrestoration.org/program/ecorrap/) following photogrammetry imaging procedures described in (Gordon et al., 2023). The total study sampling size included nine reefs along the Great Barrier Reef and three in the Torres Strait grouped into six clusters (Torres Strait, Offshore North, Offshore Central, Inshore Central, Inshore South and Offshore South; latitude range: -23.917571 to -9.73404). Within each reef, sites on the reef slopes and in lagoons were chosen across a wave exposure (to the prevailing wind direction) gradient (Front = high, Flank = mid, Back = low and Lagoon = lowest exposure) and depths (shallow ~5 m and deep ~12 m – where possible). The combination of site and depth is hereafter referred to as habitat (e.g., back shallow becomes low exposure shallow) (Figure 2.1). Reefs were considered offshore or inshore based on water clarity assessment (i.e., inshore more turbid). The total sampling size was 85 sites with four replicates each, hereafter referred to as plots, or a total surface area of approximately 23900 m^2 (340 plots

of 72 m^2 each) sampled in the period between January and May 2021 when no known major disturbance was recorded.

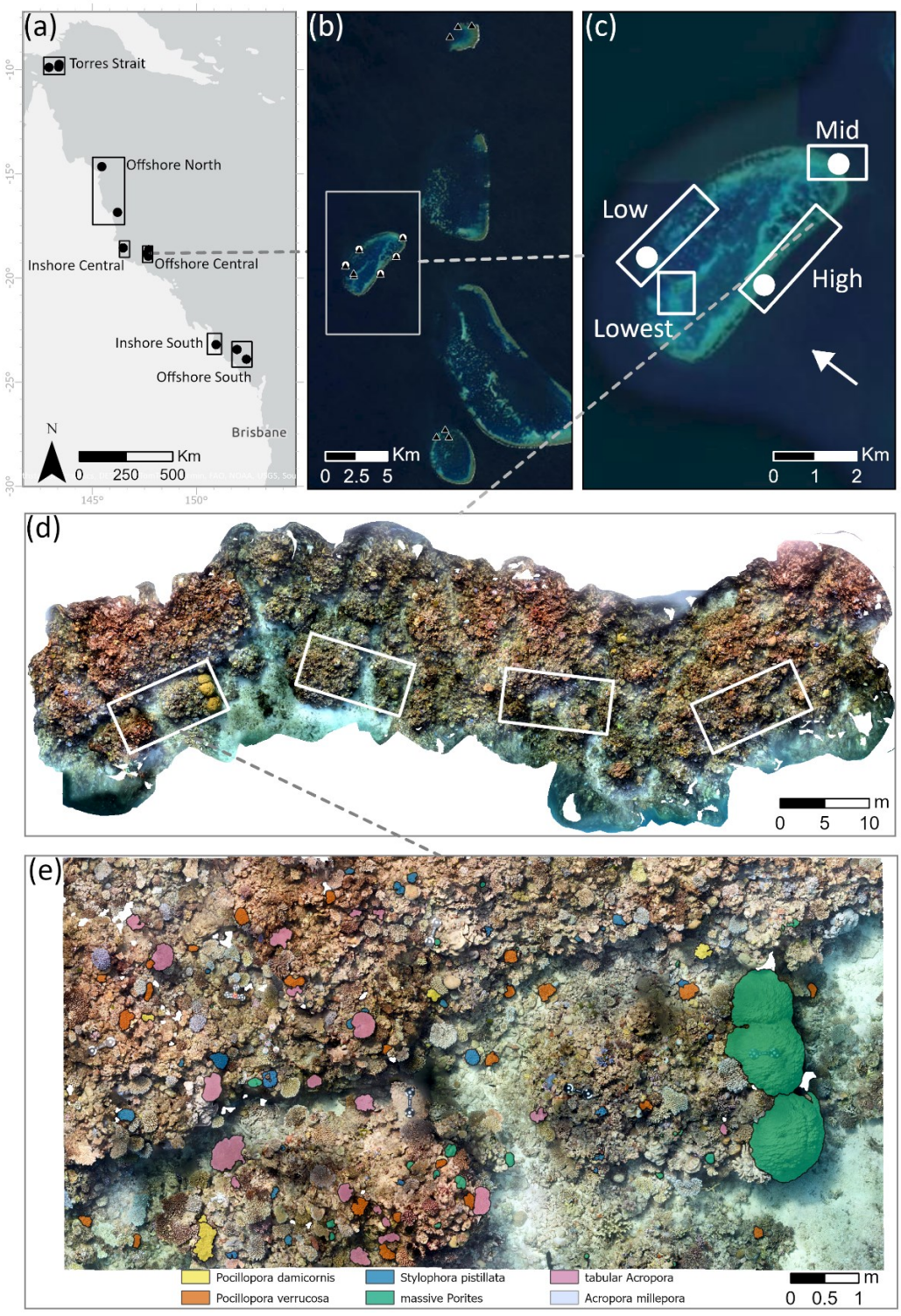


Figure 2. 1. Nested sampling design used in this study to examine the size structure of six dominant morphotaxa on the Great Barrier Reef and Torres Strait. (a) map of reefs organized in six clusters, (b) example of a cluster of

three reefs (offshore central), (c) example of different habitats sampled around Davies reef across a gradient of wave exposure (black triangles represent shallow habitats while white circles represent deep habitats), the white arrow indicates the direction of the wind, (d) example of a high exposure, shallow habitat comprising four plots (unit surveyed using photogrammetric technique) and (e) example of a 12 x 6 m plot (orthomosaic) with digitized colonies for six morphotaxa. Colonies were digitized only if they were reliably identifiable, sizable and entirely visible and within the boundaries of the orthomosaic. Note, white polygons are holes in the orthomosaic.

A total of 2000-3000 images were taken at each plot and imported into Agisoft Metashape version 1.7.4 (Agisoft LLC, 2023) for 3D processing. For each plot, a two-dimensional orthomosaic was created from acquired images using custom python scripts with the parameters described in (Lechene et al., 2024). Each orthomosaic was standardized to a size of 12 x 6 m and imported into TagLab v2022.04.21 (Pavoni et al., 2022) for coral colony tracing.

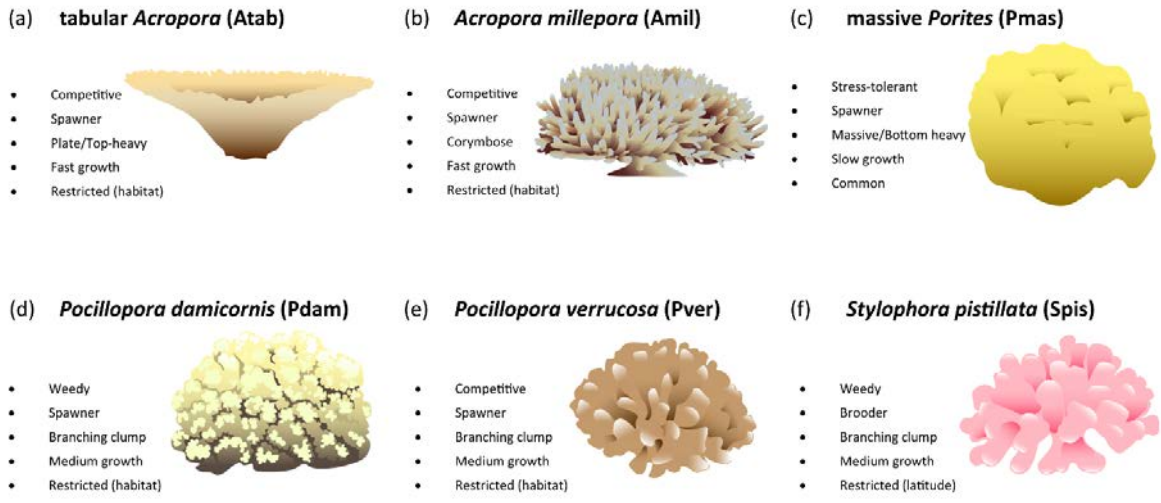


Figure 2. 2. Six coral morphotaxa (and their code) used in this study. These morphotaxa were chosen for their contrasted life-history strategies and morphologies, their different levels of resistance to disturbance and their relatively high abundance in most habitats.

Corals were identified to the highest taxonomic resolution possible using six focal morphotaxa: tabular *Acropora*, *Acropora millepora,* massive *Porites*, *Pocillopora damicornis, Pocillopora verrucosa*, and *Stylophora pistillata (*Figure 2.2*).* These taxa were selected based on their high abundance across sites – quantified from 2021 orthomosaics (see details about species selection in Toor et al. (2025) section 5.2) – and their representation of contrasting life-history strategies. For instance, *Acropora spp.* exhibit rapid growth and higher susceptibility to mechanical and

thermal disturbances, while massive *Porites* grow slowly but are generally more resistant to stress (Figure 2.2). A subset of colonies was identified by a highly trained benthic ecologist from the high-resolution images and the orthomosaics. This subset was then validated by a highly trained taxonomist *in situ*. When the *in situ* ID did not match the orthomosaic ID, the later was corrected. Validation analyses showed all morphotaxa were identified from images with 80-95 % accuracy.

On each plot, colonies were digitized by delineating them with polygons using TagLab and assigned a class. In TagLab, the '4-clicks segmentation' tool was used to trace colonies rapidly. This tool only requires the user to click on the four extremes of each colony before using an interactive segmentation model to trace its complex boundaries. These boundaries were then manually adjusted using the 'Edit border' tool for each colony. Colonies were digitized if they could be assigned to a class with at least 80% certainty, clearly reconstructed (i.e., not blurry or distorted), clearly visible (i.e., not obscured or overtopped by another organism or substrate) and entirely within the boundaries of the orthomosaic. Finally, colony sizes were extracted as 2D planar area in square meters using ArcGIS Pro version 3.0 (ESRI, 2023) and custom ArcPy and python scripts.

2.3.2 Statistical analysis

To examine spatial patterns and the relationship between environmental gradients and coral size structure, we ran three analyses that match the objectives and hypotheses' structure presented in the introduction. With these three analyses we explored: 1) whether coral size varied between reef clusters distributed along a latitudinal gradient; 2) whether coral size varied between inshore and offshore locations; and 3) whether coral size varied between habitats distributed across gradients of wave exposure (back, deep sites = lowest exposure). Each of these analyses included different coral taxa (and morphologies). For all analyses, we fitted

Bayesian Generalized Linear Mixed Effect Models (bGLMMs) using the packages *brms* (Bürkner 2017) and *rstan* version 2.26.22. (Stan Development Team, n.d.) within the R Statistical and Graphical Environment version 4.3.1 (R Core Team, 2023). Colonies with partial mortality on the periphery were included, but our method precluded us from accurately determining the size of colonies with central partial mortality (mainly massive *Porites*), which were subsequently excluded from the analyses (n = 162). We also checked that these excluded colonies were evenly spread among sites therefore it is unlikely that their exclusion would change any observed patterns. It should therefore be noted that we may be slightly overestimating average colony size for massive *Porites*. Because of higher uncertainty associated with the taxonomic identification of smaller colonies from orthomosaics and to ensure results are not impacted by our ability to detect smaller corals using this method, colonies smaller than 10 cm in diameter (~78 cm^2) were excluded from the analyses (n = 3606). Instead of partitioning size data into arbitrary size classes and to keep size as a continuous variable, we performed quantile regressions for three quantiles corresponding to three size classes: smallest: quantile = 0.1 (i.e., the smallest 10%); median: quantile = 0.5 (i.e., the middle of the size distribution) and largest: quantile = 0.95 (i.e., the largest 5%). While other quantiles could have been selected (i.e., 0.25 or 0.75), we opted for more extreme quantiles to emphasize the tails of the distribution where shifts in size structure might be most informative for detecting demographic responses. All models used the same response variable, Coral Colony Planar Area, which was log-transformed and modelled using an asymmetric Laplace distribution adequate for quantile regression. Default priors were used (with the function *get_prior* of the *brms* package). Please note, not all taxa were included in all analyses, as for some combination of clusters, sites and cross-shelf position certain taxa were absent and would cause the models to not converge.

Spatial variation in the size structure of coral morphotaxa across a latitudinal gradient was analysed by fitting three bGLMMs (one for each quantile or size class) with predictor variable Cluster interacting with Taxa and nested random effects of Plot within Site. *P. verrucosa* and S. *pistillata* were excluded as they were not present at all reef clusters. A total of 20,000 iterations with a warmup of 5,000 and thinning of 12 were performed on each of three chains of each model. Posterior contrasts were calculated for each model to compare the estimated marginal means of colony size between clusters using the functions *emmeans* and *pairs* of the package *emmeans* v. 1.8.7 (Lenth, 2023).

Spatial variation in the size structure of coral morphotaxa between inshore and offshore locations was analysed by fitting three bGLMMs with predictor variables: Cross-shelf position interacting with Taxa and Latitudinal cluster and nested random effects of Plot within Site. Cross-shelf position had two levels: inshore and offshore and Latitudinal cluster had two levels: central and south. Only tabular *Acropora* and *P. damicornis* were included as they were present at each combination of Cross-shelf position and Latitudinal cluster. A total of 20,000 iterations with a warmup of 5,000 and thinning of 12 were performed on each of three chains of each model except the model corresponding to the smallest size class which needed a total of 50,000 iterations with a warmup of 5,000 and thinning of 20. Posterior contrasts were calculated for each model to compare the estimated marginal means of colony size between inshore and offshore locations.

Spatial variation in the size structure of coral morphotaxa between habitats was analysed by fitting three bGLMMs with predictor variables Habitat interacting with Taxa and nested random effects of Plot within Site within Reef. Habitat was a combination of wave exposure (lowest, low, mid and high) and depth (shallow and deep). All morphotaxa were included. A total of 20,000 iterations with a warmup of 5,000 and thinning of 10 were performed on each

of three chains of each model. Posterior contrasts were calculated for each model to compare the estimated marginal means of colony size between habitats.

For all models in all analyses, chains mixing, and convergence were checked using Markov Chain Monte Carlo diagnostics using the *rstan* package. All chains were well mixed and converged upon a stable posterior (all Rhat values < 1.05). For each model, goodness of fit was checked visually using posterior predictive checks and all models were validated using the *DHARMa* package version 0.4.6 (Hartig, 2022) to check simulated residuals. The random effect structure in each model was tested and chosen to capture non-independence due to spatial grouping at multiple scales and reflects the expectation that plots within the same reef or site are more similar. We conducted visual inspections of residuals for spatial patterning and overdispersion using randomised quantile residuals. While these checks did not reveal obvious spatial structure or model misspecification in the residuals, we acknowledge that residual spatial autocorrelation may persist even with appropriate random effects.

2.4 Results

A total of 5880 colonies were retained for the analyses: 1059 tabular *Acropora*, 351 *A. millepora*, 726 *P. damicornis*, 2343 massive *Porites*, 859 *P. verrucosa* and 542 *S. pistillata*. Colony sizes ranged from 78.6 cm^2 to 27140.2 cm^2 or approximately 10 cm to 185.9 cm in diameter. The median colony size was 255.5 cm^2 or approximately 18 cm in diameter. The descriptive statistics for each morphotaxon are provided in Table 2.1.

Table 2. 1. Summary statistics for each morphotaxon.

	min size (cm²)	**median size (cm²)**	**max size (cm²)**	**min diameter (cm)**	**median diameter (cm)**	**max diameter (cm)**
Tabular *Acropora*	79.5	666.9	27140.2	10.1	29.1	185.9
A. millepora	79.2	336.2	4403.8	10.05	20.7	74.9
P. damicornis	79	257.6	3607.9	10	18.1	67.8
Massive *Porites*	78.6	234.9	23761.9	10	17.3	173.9
P. verrucosa	78.7	229	1598.3	10	17.1	45.1
S. pistillata	78.6	141.8	855.7	10	13.4	33.

2.4.1 Influence of latitudinal gradient

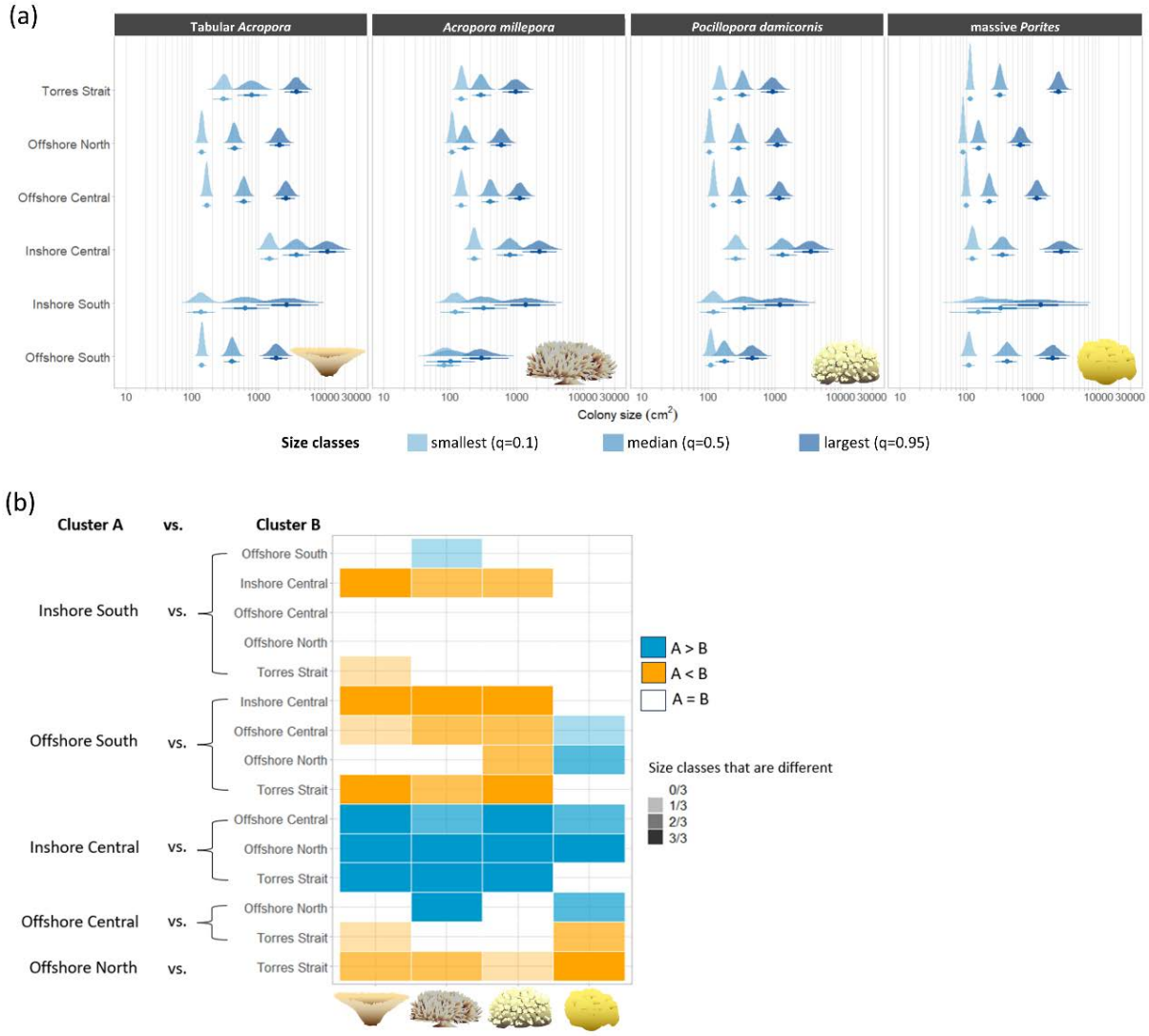


Figure 2. 3. Difference in size structure between clusters. (a) Marginal posterior distributions of colony sizes for each cluster for all morphotaxa. Points represent estimated marginal means; thick and thin lines represent 66% and 95% highest probability density (HPD) credible intervals respectively. Clusters are ordered from north (top) to south. (b) Pairwise comparisons of colony sizes (estimated marginal means) between clusters at 95% HPD. Contrasts are ordered as the cluster expected to have larger corals is the first cluster A of each pair A versus B (i.e., all differences should be positive given our hypothesis that corals are larger in higher latitude). When cells are blanked there is no evidence of a difference in size between clusters. When cells are blue there is a positive difference and coral size is larger in the first cluster compared to the second (hypothesis confirmed). When cells are orange, there is a negative difference and coral size is smaller in cluster A compared to B. The opacity of each cell denotes for how many of the three size classes (smallest, median and largest) there is evidence of a difference between clusters.

To test whether coral size varied between clusters with expectation that corals were larger at higher latitude, a total of 4479 colonies were considered across all locations (Figure 2.1): 1059

tabular *Acropora*, 351 *A. millepora*, 726 *P. damicornis*, and 2343 massive *Porites*. There was a general trend for colony size to be larger in the Torres Strait and the Inshore Central clusters (Figure 2.3a). There was evidence of a difference in size between clusters (Figure 2.3b), especially colony size in Inshore Central which was consistently larger for all three size classes and morphotaxa except massive *Porites* which was only larger in Inshore compared to Offshore Central (Appendix A: Supplementary Figure S1). Massive *Porites* was also the only morphotaxa that displayed larger colonies in Offshore South compared to Offshore Central and Offshore North. There are also interesting nuances to highlight regarding the variation in size structure between clusters. For massive *Porites*, the largest corals are found in Torres Strait and Inshore Central (true for all three size classes) and the population size structures of the northern and central regions are skewed towards small colonies (i.e., the distributions of smallest and median sizes are closer together). For *P. damicornis*, sizes are equally distributed except for Inshore Central where populations are dominated by large colonies. For *A. millepora*, northern populations are dominated by small colonies whereas central populations are dominated by large colonies.

2.4.2 Influence of cross-shelf position

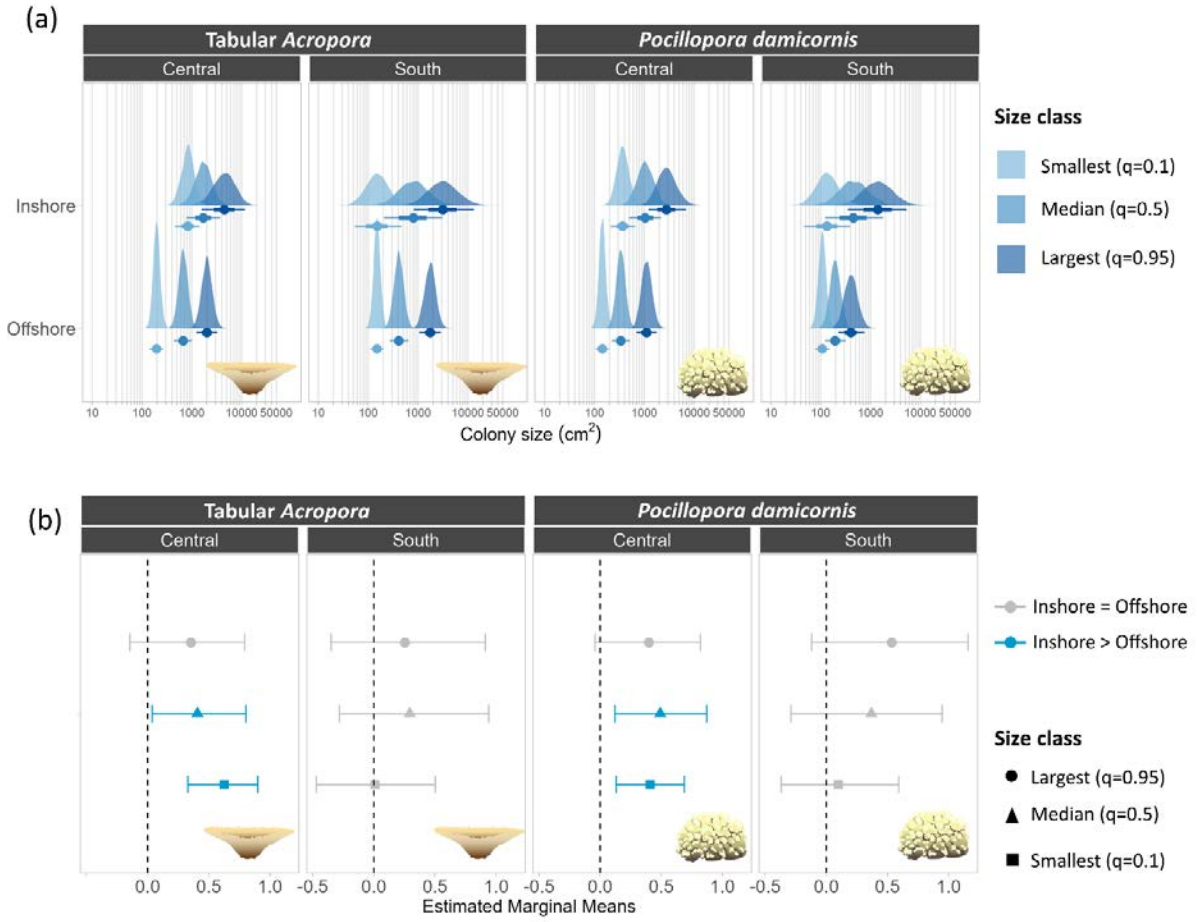


Figure 2. 4. Effect of cross-shelf position (inshore versus offshore) on three size classes of two morphotaxa in two different latitudinal regions of the GBR (Central and South). (a) Marginal posterior distributions for the interaction between cross-shelf position, latitudinal region and colony for each morphotaxa and size class. Points represent estimated marginal means; thick and thin lines represent 66% and 95% HPD credibility intervals respectively. (b) Pairwise comparisons of colony sizes (estimated marginal means) between inshore and offshore habitats for each morphotaxa and size class. Whiskers represent 95% HPD credible intervals. When intervals do not cross zero and are positive, there is strong evidence that colony size inshore is larger than offshore (hypothesis validated).

To test whether corals were larger inshore compared to offshore locations, with the expectation that corals would be larger inshore, we used a total of 795 tabular *Acropora* and 524 *P. damicornis* colonies. There was a consistent trend for corals to be larger inshore for all three size classes and both morphotaxa (Figure 2.4a). For the small and median size classes in the Central region, there is strong evidence that coral size is larger inshore (Figure 2.4b), for the other size classes and South region, there is statistical evidence that size inshore is larger than

offshore, but the distributions' overlap is greater than 5% (Appendix A: Supplementary Figure S2).

2.4.3 Influence of habitat

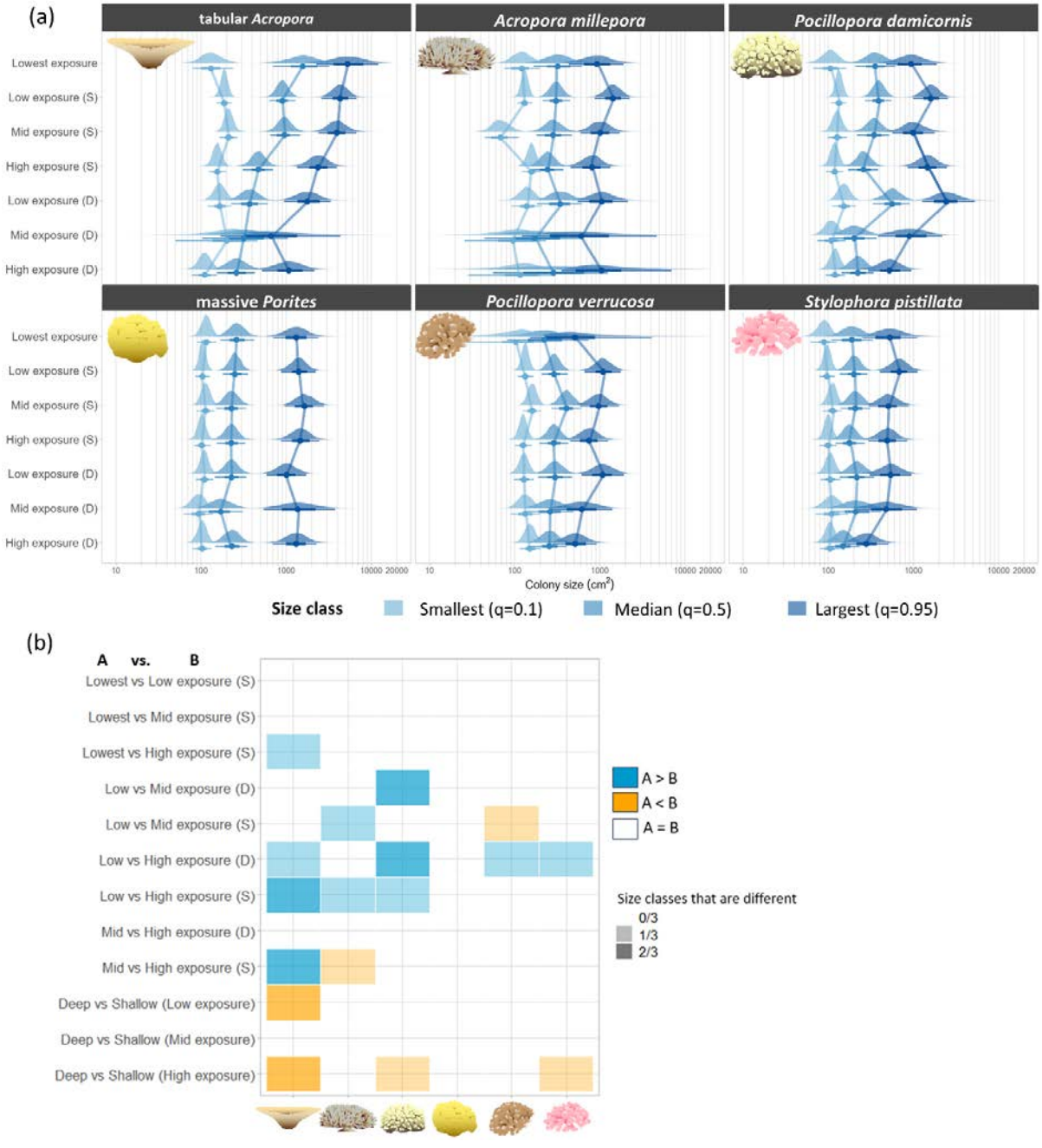


Figure 2. 5. Difference size structure of six morphotaxa between habitats. (a) Marginal posterior distributions for the interaction between habitats and colony sizes for each morphotaxa and size class. Points represent estimated marginal means; thick and thin lines represent 66% and 95% confidence intervals respectively. Depth for each habitat is coded as: S = shallow and D = deep. Habitats are ordered along the y-axis by depth and expectation that

size increases with decrease in exposure. Vertical lines connect the means of each distribution to highlight patterns and ease visual interpretation. (b) Planned contrasts of colony sizes (estimated marginal means) between habitats for each morphotaxa. Contrasts are ordered as the habitat expected to have larger corals is the first habitat A of each pair A versus B (i.e., all differences should be positive given our hypothesis that corals are larger in less exposed habitats). When cells are blanked there is no evidence of a difference in size between habitats. When cells are blue there is a positive difference and coral size is larger in the first habitat compared to the second (hypothesis confirmed). When cells are orange, there is a negative difference and coral size is smaller in habitat A compared to B The opacity of each cell denotes for how many of the three size classes (smallest, median and largest) there is evidence of a difference between habitats.

To test whether coral size varied between habitats with the expectation that corals would be larger at lower level of exposure for the same depth zone, a total of 5880 colonies were considered across all locations: 1059 tabular *Acropora*, 351 *A. millepora*, 726 *P. damicornis*, 2343 massive *Porites*, 859 *P. verrucosa* and 542 *S. pistillata*. There was a general trend for colonies to be larger in less exposed, shallow habitats. Exceptions to this trend were massive *Porites* and *P. verrucosa* which were largest in mid exposure habitats and *P. damicornis* which was largest in low exposure, deep habitats (Figure 2.5a). Strong evidence of differences in size between habitats was rare (Figure 2.5b) (but see Appendix A: Supplementary Figure S3 for comparisons result at HPD 90% and HPD 66%). Coral colony size decreased consistently with increasing exposure on deeper slopes for tabulate *Acropora, P. verrucosa*, *P. damicornis* and *S. pistillata*. However, the trend was most prominent in tabular *Acropora,* and varied across size classes for all taxa, with a stronger effect on the largest size class. Contrastingly, *A. millepora* corals tended to increase in size with increasing exposure, but the difference was only evident between medium and high exposure. For this taxon, the influence of exposure was only consistent across all size classes in deeper slopes, where only the smallest size class corals were larger in highly exposed habitats in shallow slopes.

Differences in size structure between habitats were apparent in tabular *Acropora* where low exposure habitats were dominated by large colonies (median and largest size distributions were closer together). While high exposure habitats were dominated by small colonies (smallest and median size distributions are closer together), deep habitats were consistently dominated by

small colonies. P. *damicornis* also exhibited these patterns in shallow habitats. The other morphotaxa displayed consistent size structures across exposure, especially massive *Porites* and S. *pistillata*, and with populations dominated by small colonies. Overall, the effect of habitat on size increases with colony size and is only apparent for median and largest colonies (Figure 2.5, Appendix A: Supplementary Figure S3).

Despite these nuances, comparisons of size between habitats revealed that differences were marked mostly between low and mid to high exposure habitats (Figure 2.5b). Interestingly, there seems to be a size threshold under which exposure has no effect. Moreover, in some cases, the effect of exposure on small colonies differs from that on medium and large colonies (e.g., see tabular *Acropora* in Lowest versus Low exposure and Lowest versus Mid exposure). Contrary to our hypothesis, deep habitats (considered less exposed) contained smaller colonies than their shallow equivalents.

2.5 Discussion

Table 2.2. Predicted and observed drivers of colony size. *Only two taxa tested.

Driver	**Hypotheses**	**Supported by size structure data**
Latitudinal gradient	Increases with latitude	No
Cross-shelf gradient	Larger inshore	Yes
	Taxon-specific trends	No*
Wave exposure gradient	Larger in less exposed habitats	Yes/No (taxon dependent)
	Taxon-specific trends	Yes
Depth gradient	Larger in deeper habitats	Yes/No (taxon dependent)
	Taxon-specific trends	Yes

For corals, the largest fecund colonies contribute disproportionally to the reproductive output of the population and are the primary broodstock to replenish diminished populations. Our study used leveraged novel methods to develop an unusually large coral colony size dataset (N = 5880 colonies) with an extensive spatial extent (23900 m^2 surveyed across 14.2 degrees of latitude) and analysed those data to unveiled patterns in colony size structure of some dominant Indo-Pacific corals across latitudinal, cross-shelf and habitat gradients. Our results demonstrate that spatial variation in coral size is consistent among taxa along latitudinal and cross-shelf gradients, but that trends are taxon-specific in response to spatial variation in exposure and depth (see Table 2.2 for summary). These new insights into how environmental factors shape the spatial distribution of large colonies can help identify source habitats for coral larvae and contribute to adaptive and resilience-based conservation and management.

2.5.1 Influence of cross-shelf gradient on coral size frequency distribution

Both the cluster and the inshore versus offshore analyses showed that corals were consistently larger on inshore reefs. The median of the posterior distributions of tabular *Acropora* and *P. damicornis* colony sizes was consistently larger inshore compared to offshore locations for all size classes and regions. Especially for median size colonies, there was strong evidence that inshore corals were larger. The consistency of the patterns found among regions and morphotaxa with contrasting life-history strategies suggest a strong environmental influence on demographic processes (Meesters et al., 2001). The consistently larger size of inshore colonies is also a reliable indicator that the environmental variables that affect size structure differ between inshore and offshore reefs. Small colonies are larger on Inshore Central than on Offshore Central reefs, which could indicate recent low recruitment rates inshore. However, this does not seem to be the case in the southern region. Previous studies have suggested that the combination of higher growth rates and lower rates of partial mortality in inshore habitats

provides an explanation for the presence of larger colonies (Anthony, 2006; Edinger et al., 2000; Lirman & Fong, 2007; Lough & Barnes, 1992).

Though considered remote, the reefs in the Torres Strait exhibit inshore characteristics such as high turbidity (Petus et al., 2022) and low wave exposure due to island geography. Both the latitudinal and inshore/offshore gradients analyses suggest that corals tend to be larger in reefs with these inshore characteristics. Interestingly, we also found that inshore reefs tend to lack small colonies in general. Even smaller colonies in Torres Strait and Inshore Central reefs were relatively large compared to those in other clusters, despite the skew of size distributions toward smaller colonies in these clusters. While this skew is evident, the smallest and median colony sizes in inshore reefs are still closer in size and are generally larger than their offshore counterparts. This suggests that inshore reefs not only have fewer small corals but also a size distribution that skews toward larger colonies compared to other reef clusters. These results align with previous research suggesting that coral populations are skewed towards large colonies in turbid environments through the negative impact of sedimentation on coral recruitment (Babcock & Smith, 2000). Inshore reefs are also characterised by higher incidence of recruitment 'inhibitors' such as macroalgae and algal turfs (Birrell et al., 2005; Doropoulos et al., 2014; Tebbett et al., 2025). Complementing the present study with local measures of vital rates across size classes (*i.e.* survival, growth and recruitment) would provide insights into the underlying processes resulting in larger colonies inshore.

2.5.2 Influence of wave exposure and depth gradients

Our results partially support the hypothesis that larger corals were expected to be found in less exposed habitats and that top-heavy morphologies were more susceptible to wave exposure compared to bottom heavy taxa (Madin et al., 2014; Madin & Connolly, 2006). The absence of size disparity in relation to exposure for massive *Porites* and *S. pistillata* also supports our

hypothesis as the sturdier morphologies of these taxa were expected to be less susceptible to hydrodynamic damage. For instance, *S. pistillata* typically inhabits sheltered microhabitats such as crevices and overhangs, which could explain why their size is not influenced by variations in wave exposure at the plot or site level (Rich et al., 2022). Interestingly, however, the influence of habitat seemed to increase with size for all morphotaxa. We found a general trend for larger corals to be observed in sites with low wave exposure. Collectively, these results indicate that exposure-related processes in addition to mechanical breakage (e.g., tissue abrasion from suspended particles and coarse sediments that is likely to be greater at high wave energy, or inability to trap heterotrophic food at high exposure) could also affect coral size distributions. However, further research is required to test this hypothesis.

Tabular *Acropora* colonies exhibited the highest variations in size between habitats. Specifically, in shallow habitats, colonies in low exposure were larger than in high exposure. Furthermore, the size structure of tabular *Acropora* changed from being skewed towards large colonies in low exposure habitats to being skewed towards small colonies in exposed habitats. These results support the hypothesis and rationale that the mechanical vulnerability of this taxon increases with size (Madin et al. 2014). Surprisingly, there was strong evidence to suggest that tabular *Acropora* were larger in lowest exposure habitats compared to mid exposure. This contradicts prior findings indicating that this morphotaxa requires high flow to thrive, with maximum dominance in intermediate to high wave exposure environments (Roelfsema et al., 2018). This indicates that there may be subtle differences in the processes that control abundance compared to the process that control growth and survival post-settlement. Further research assessing environmental controls on settlement could help disentangle this contradiction.

Corals were larger in shallow compared to deep habitats at equivalent exposure levels (e.g., corals were larger in shallow, low exposure sites when compared to deep, low exposure sites). However, these patterns were only evident in tabular *Acropora* and for the largest size class of *P. damicornis* and *S. pistillata*. This result contrasts with our initial hypothesis that reduced wave energy at depth would promote larger colony sizes compared to shallow sites. However, our findings suggest that other environmental factors such as light and temperature may exert a stronger influence on the size structure of tabular *Acropora*. Light attenuation with depth likely limits photosynthetic capacity and, consequently, growth, which could explain the smaller colony sizes observed in deeper habitats. Importantly, the depth bins used in this study (shallow ~5 m; deep ~12 m) were chosen to align with established habitat zones commonly used in coral reef monitoring programs and were reinforced by consistent differences in benthic community composition and visual habitat structure across sites. While the mean depths of these zones are generally well separated, they nonetheless fall within the upper 15 m of the reef profile where strong biophysical gradients still occur. These environmental shifts – especially in light, sedimentation and water flow – can shape coral demographic patterns even across modest depth differences. Future work could benefit from treating depth as a continuous variable and integrating finer-scale measurements of light and flow to better disentangle the effects of depth and exposure on coral size structure.

2.5.3 Ecological implications

Our results align with previous research, offering critical validation and refinement of existing knowledge across a broader spatial and environmental context. By demonstrating consistent patterns in coral colony size variation across diverse gradients—latitudinal, cross-shelf, wave exposure, and depth—this study strengthens the generality of findings that were previously

more localised. Such replication is essential in landscape ecology, particularly for coral reefs, where environmental conditions vary markedly over small spatial scales.

Using photogrammetry, we developed a large and spatially extensive colony size dataset that allowed precise quantification of planar area across a wide range of taxa and environments. While our method excluded colonies smaller than 10 cm in diameter – thereby omitting recruits, juveniles and small adults that can play important roles in recovery dynamics – it still captured a broad portion of the size spectrum, particularly large, fecund colonies that are difficult to measure accurately with traditional field methods. These larger colonies play a disproportionate role in population persistence through their reproductive output and structural contributions to reef habitat.

The size structures observed varied across environmental gradients and among taxa but reflect only a snapshot in time. Colony size structure is shaped not only by life-history traits and environmental conditions, but also by past disturbances, such as bleaching, storms or disease which we were unable to account for directly in this study. As such, these patterns should not be interpreted as definitive indicators of reef conditions or demographic processes. Instead, they provide a valuable spatial baseline for identifying variation across habitats and for generating testable hypotheses about the factors influencing coral population structure.

Despite these limitations, the observed distributions can inform future monitoring and management. For example, a higher relative abundance of large colonies in some habitats may suggest areas of demographic stability or potential source reefs, while their absence may indicate recent disturbances or recruitment failure. These patterns can serve as initial benchmarks to track temporal change or evaluate restoration outcomes, especially when complemented by long-term data. Integrating such metrics into monitoring programs may enhance early detection of demographic shifts – before declines in coral cover are visible – and

support more proactive and targeted reef conversation efforts. To improve the utility of size-based indicators, future research should pair spatial surveys with disturbance histories and repeated measurements to better understand the drivers of size structure and improve the predictive utility of these metrics for assessing reef resilience and recovery.

Chapter 3. Evaluating error sources to improve precision in the co-registration of underwater 3D models

This chapter is published in Ecological Informatics as:

Lechene, M. A., Figueira, W. F., Murray, N. J., Aston, E. A., Gordon, S. E., & Ferrari, R. (2024). Evaluating error sources to improve precision in the co-registration of underwater 3D models. **Ecological Informatics**, 81, 102632. https://doi.org/10.1016/j.ecoinf.2024.102632

3.1 Abstract

Change detection is an essential and widely used approach for investigating ecosystem dynamics. Multi-temporal 3D models increasingly underpin photogrammetry-based analyses of change for many ecologically relevant attributes. To detect change, it is necessary to accurately align 3D models collected at different times using a process referred to as co-registration. However, achieving precise co-registration is difficult in underwater habitats due to practical challenges intrinsic to surveying them. These include a lack of accurate georeferencing information, variable light, turbidity and weather conditions, and diving restrictions dictated by the diver's pressure exposure over time. Here we present an efficient co-registration workflow for 3D models that directly addresses these challenges, derived from underwater structure-from-motion methods. To test our approach, we used 3D models from across a wide range of coral reef habitats covering all those that one may encounter in shallow reefs (15 m depth and above). We then identified and empirically estimated four key sources of error: co-registration, 3D processing, image acquisition, and reference and scaling features (RSF) placement, and quantified their relative contributions to the overall error. Our proposed co-registration workflow had a mean precision of 1.37 ± 16.55 mm. Image acquisition and RSF placement errors contributed the most to the total workflow error (37 % and 53 %,

respectively), while the contribution of co-registration and 3D processing errors was minimal (3 % and 7 %, respectively). As a result of our analysis, we provide 'good practice' guidelines to reduce errors associated with photogrammetric workflows and to facilitate efficient and reliable detection of 3D change in complex underwater ecosystems.

3.2 Introduction

Time-series data are essential in ecology (Wauchope et al., 2021). Long-term records of ecological data are used to quantify trends in historical change, characterize habitats, and estimate future responses to environmental change or estimate future conditions (Magurran et al., 2010; Wolfe et al., 1987). In the past two decades, the growing availability of digital photographic sensors such as digital single-lens reflex (DSLR) cameras, along with the development of topographic survey techniques have substantially increased the use of three-dimensional (3D) reconstructions in terrestrial and aquatic ecology (Carrivick & Smith, 2019; Fonstad et al., 2013). The production of high-resolution 3D datasets in time-series sampling regimes has similarly increased, as it enables the characterization of change in 3D structure, and therefore allows more robust detections of temporal change in systems where structural integrity holds importance, such as forests and coral reefs (Graham & Nash, 2013; Shugart et al., 2010). For example, studies aimed at detecting rates of change occurring in the structural properties of key ecological attributes have tracked the gain or loss in 3D structure of habitat engineers (e.g., trees and corals), or shifts in ground or benthic community composition (Burns et al., 2016; Fukunaga et al., 2022; Hardiman et al., 2013; Hernández-Landa et al., 2020; Tompalski et al., 2021).

In recent years, the use of close-range structure-from-motion photogrammetry, hereafter referred to as photogrammetry, has enabled fine spatial scale and high-resolution (0.1 - 10 mm pixel resolution) topographic reconstructions from overlapping photographs. Model

reconstruction techniques applied in photogrammetry utilize paired, overlapping photographs captured within a network to convert overlapping features into a 3D 'point cloud'. Subsequently, these points are interpolated to generate a series of interconnected triangles which create the 3D model. Scaling and orientation of the resultant 3D products (point cloud or model) is provided by the camera positions and/or by reference and scaling features of known dimensions placed in the scene (Westoby et al., 2012). Three-dimensional photogrammetry products store complex information regarding the surface structure of organisms and environments and thus provide the opportunity to investigate spatio-temporal dynamics of habitats at very fine spatial scales in four dimensions.

To enable detection of fine-scale changes in surveyed surfaces, 3D models must be aligned to a common coordinate system, a process called 'co-registration'. In terrestrial environments, co-registration techniques for land-based 3D products are well established (Dong et al., 2020). These typically use multiple georeferenced point locations obtained by Global Positioning Systems (GPS) (e.g., Coulter & Stow, 2008; Hannam & Moskal, 2015). However, co-registration of underwater 3D models remains a challenge, primarily due to the inability of GPS radio signals to penetrate water (Taraldsen et al., 2011). Moreover, errors in diver-based underwater photogrammetry data can be caused by a range of factors associated with image collection methods in the field. These factors include user-decisions (e.g., camera choice, diver experience, swimming patterns and speed) and environmental conditions (e.g., turbidity, sunlight reflections and shadows) (Bryson et al., 2017; Mangeruga et al., 2018). Any sources of error in co-registration can strongly influence the accuracy and precision of metrics extracted from 3D models, which can ultimately influence their utility for studying environmental change.

Accurate and precise co-registration is particularly essential for multi-temporal analyses of 3D structure dynamics in marine environments such as coral reefs. Typically, establishing mechanically stable reference features to support co-registration is crucial for achieving high accuracy and precision in multi-temporal surveys, but is a significant challenge (Nocerino et al., 2020; Skarlatos et al., 2017). Current methods focus on the installation of physical reference features, which are sometimes extensively developed as a geodetic reference network. Establishing physical features in coral reef environments is typically achieved by drilling and cementing anchors of known coordinates into the reef matrix (e.g., Kopecky et al., 2023; Neyer et al., 2018; Nocerino et al., 2020; Rossi et al., 2020). These studies highlighted the importance, but also the difficulty, of developing reference features that are stable over time and secured in the reef structure to verify the precision and accuracy of successive 3D models. As a result of these limitations, time-series dynamics of marine environments such as coral reefs have typically been studied at small scales.

An alternative to the physical installation or reference features is the synchronization of underwater cameras with GPS devices floating on the surface (e.g., (Abadie et al., 2018; González-Rivero et al., 2014). This innovative approach allows for the coverage of larger spatial areas (albeit often with a trade-off in image resolution) but is impractical for deep or remote habitats due to challenges diving with tethered instruments. To survey deep ecosystems, it has been necessary to develop workflows that combine a range of sensors, including acoustic sensors and imaging systems, that allow the development of 3D photogrammetric reconstructions from diverse data sources (e.g., Conti et al., 2019).

The use of 3D models in time-series studies within marine environments has been limited primarily due to challenges in the establishment of stable reference features and field data collection. These challenges introduce various errors throughout the process, spanning from

initial data collection to the subsequent 3D model processing stages. Although some studies have attempted to quantify the error associated with specific steps of the workflow (Aston et al., 2022; Figueira et al., 2015) and/or to develop a robust geodetic reference system (Marre et al., 2019; Nocerino et al., 2020), they have not addressed all known error sources. Consequently, there is still a clear need to develop new, robust, and scalable techniques for the co-registration of multi-temporal, large-area, high-resolution photogrammetry products.

This study aims to empirically estimate the main errors influencing the precision of an efficient field protocol for multi-temporal analyses of 3D underwater models and provide best practices guidelines to ecologist and conservationists (non-experts in computer vision or photogrammetry) using similar approaches. We used custom designed underwater reference features and efficient co-registration techniques specifically tailored for large-area applications (10s – 100s of square meters), and the generation of high-resolution, time-series 3D models. To evaluate the repeatability of this protocol, we empirically estimated four key sources of error that can influence the precision of temporal comparison of 3D models: 1) co-registration error, 2) 3D processing error, 3) image acquisition error, and 4) reference and scaling features (RSF) placement error. We present and discuss our findings in the form of 'good practice' guidelines for reliable and effective 3D model change detection using multi-temporal photogrammetry surveys across 10s – 100s of square meters.

3.3 Methods

This study was conducted as part of the Ecological Intelligence for Reef Restoration and Adaptation Program (EcoRRAP) (https://gbrrestoration.org/program/ecorrap/). Underwater imagery was collected using EcoRRAP 3D photogrammetry techniques described by Gordon et al. (2023). Study plot setup, field data collection and 3D processing are further detailed in sections 3.3.2, 3.3.3 and 3.3.4 below.

3.3.1 Sources of error examined

The current study evaluated the total error in a proposed workflow for temporally co-registering underwater 3D models. We partitioned the error focusing on practical units rather than theoretical frameworks to provide actionable guidance for field ecologists. This involved dividing the total error into four key sources: 1) co-registration error, 2) 3D processing error, 3) image acquisition error, and 4) reference and scaling features (RSF) placement error, which were empirically tested (Figure 3.1, Table 3.1). The co-registration error is evaluating the error introduced during the co-registration process. The '3D processing error' refers to the error introduced by the software workflow for Structure-from-Motion using Agisoft Metashape Professional v. 1.8.4 (Agisoft LLC, 2023) and with settings detailed in Appendix B: Table S2. The 'image acquisition error' refers to the error introduced during the image collection and is specific to the camera network used. All camera settings and processing parameters and statistics are presented in Appendix B: Tables S1-3. The 'RSF placement error' is accounting for the precision of placing and re-placing reference features consistently between surveys, as well as the impact of scaling features placement throughout the surveyed area. These four sources of error were selected based on expectations that they would be the primary sources of real-world discrepancies that can be mitigated or managed in photogrammetry workflows. While there are many other factors that could influence the precision of temporal data surveys (e.g., environmental conditions; Mangeruga et al., 2018), controlling these variables in the field is challenging and not always possible.

To test the influence of each of the four sources of error, we co-registered the test models (subsequent imaging) with reference models (first imaging) and calculated the model-to-model deviation between the models' surfaces (see section 3.3.5). In all cases, we used images from contiguous dates (or the same date where available), and similar environmental conditions (i.e.,

sea state, brightness, time of day, tide height), with no changes in the areas of interest. Ten pairs of models were created, co-registered and compared for each of the four sources of error tested (total of 40 pairs, or 80 models). All 3D models were processed in Agisoft Metashape Professional, hereafter referred to as Metashape.

Table 3. 1. The four key sources of error examined in this study, how test models were created, what the inferred error was, and if each of the key sources of error included other sources of error.

Error	Source	Models co-registered	Error inferred	Other error included
Co-registration	Introduced by the co-registration method in CloudCompare	Test models created by duplicating 10 reference models and resetting their orientation at random (i.e., dictated by the position and rotation of the first image taken during the imaging session).	Because each model is co-registered with an exact copy of itself, any model-to-model deviation will be a result of the co-registration step alone (Figure 3.1a, Figure 3.2).	None
3D processing	Introduced by the stochastic error associated with the reconstruction algorithms in Metashape	Test models created by duplicating 10 photosets used to create reference models and re-processing them using the same reconstruction parameters.	Because each model is processed twice using identical photosets and co-registered with the first version processed, any model-to-model deviation will be a result of the 3D processing and the co-registration steps (Figure 3.1b, Figure 3.2).	Co-registration
Image acquisition	Introduced by variability in conditions during image acquisition (e.g., swim patterns, camera positions and angles)	Test models created by re-imaging plots consecutively	Because the same plots were imaged consecutively within the same dive, any model-to-model deviation will be a result of the image acquisition, the 3D processing and the co-registration step (Figure 3.1c, Figure 3.2).	Co-registration, 3D processing
RSF placement	Introduced by the placement of the reference and scaling features in the plot before each imaging	Test models created by re-imaging plots with scaling features moved in different locations within the plot and reference features taken down and put back up	Because the same plots were imaged consecutively but with the reference and scaling features taken down/moved between imaging, the model-to-model deviation will be a result of the image acquisition, the 3D processing, the co-registration and the RSF placement steps (Figure 3.1d, Figure 3.2).	Co-registration, 3D processing Image acquisition

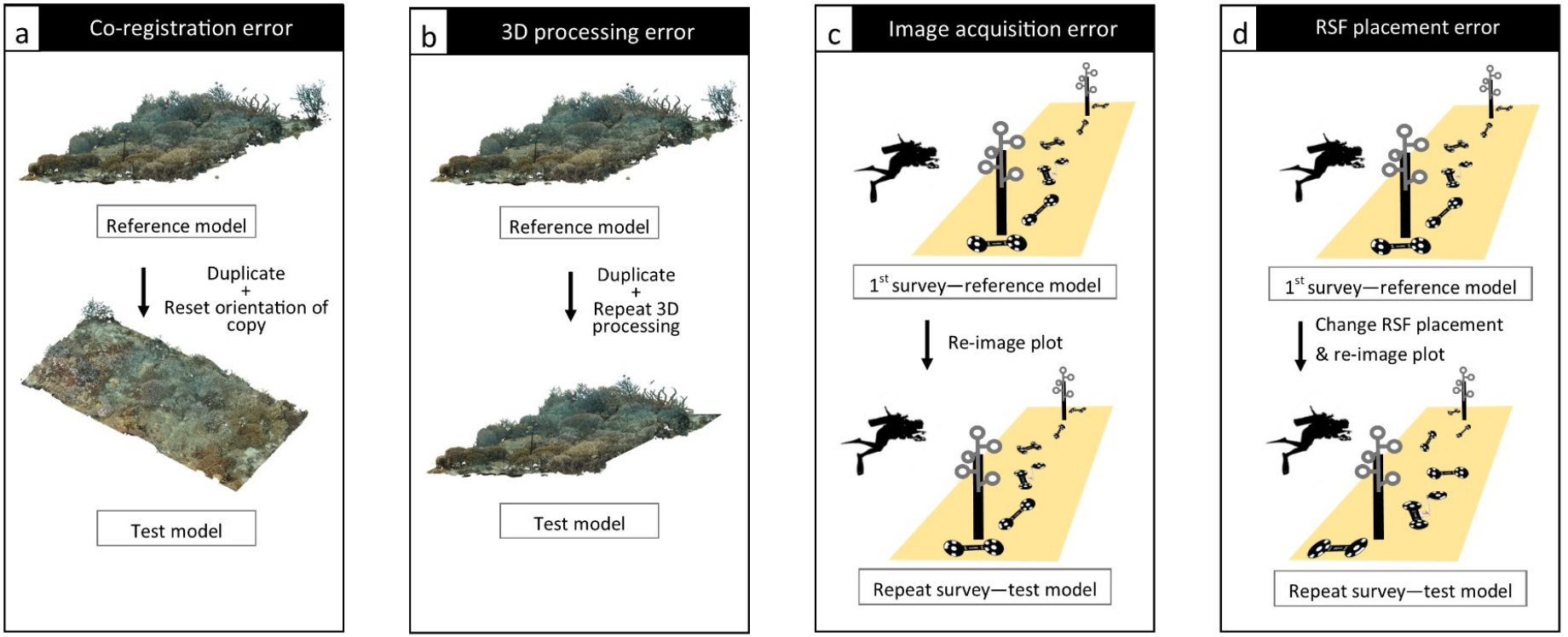


Figure 3. 1. Conceptual diagram detailing the experimental design around the four sources of error tested in the field and in the office.

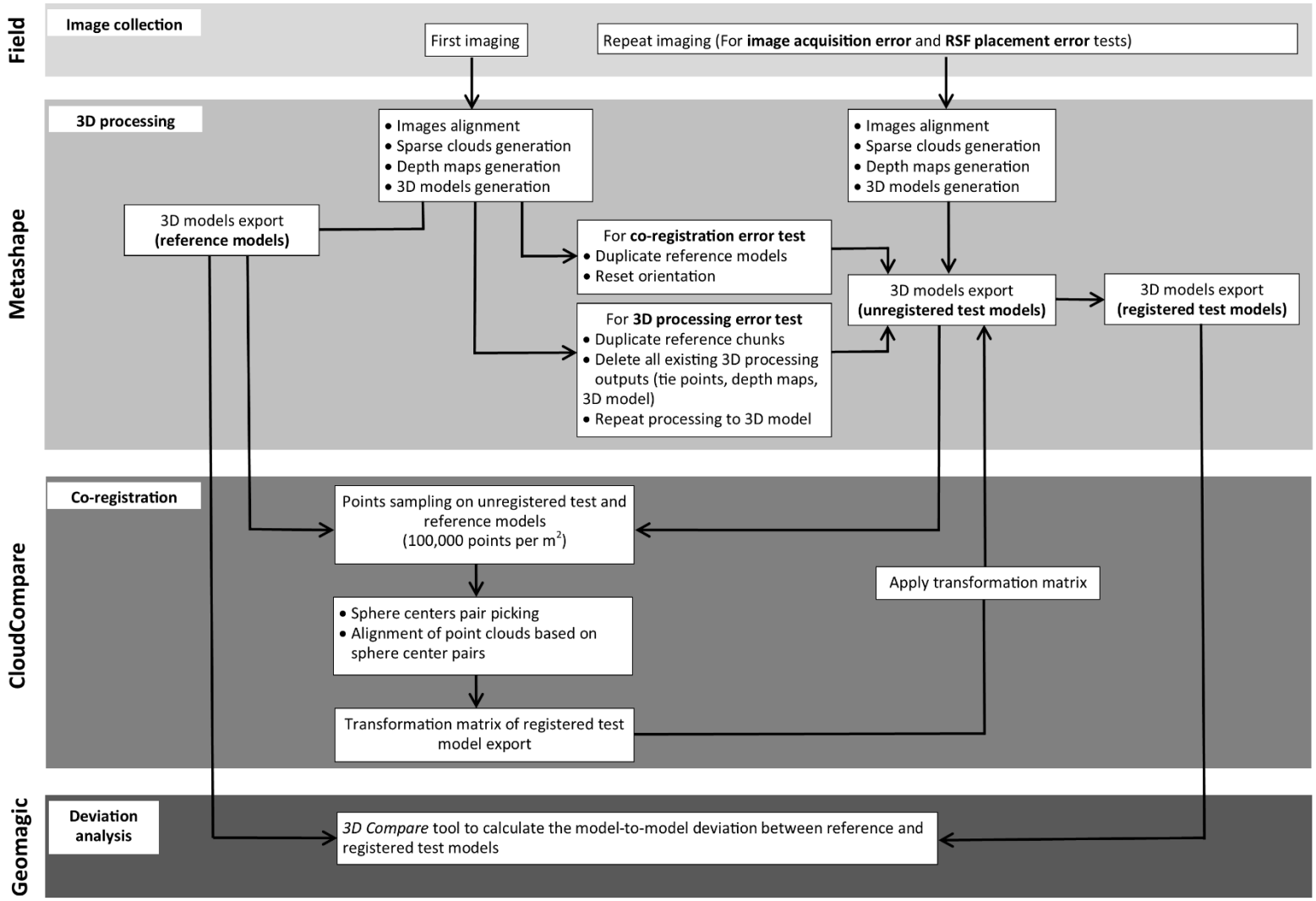


Figure 3. 2. In-depth workflow diagram detailing all the steps and parameters used from image collection in the field to precision evaluation.

3.3.2 Study plots

Permanent plots (12 x 6 m) were located between 3 – 15 m depth on exposed and sheltered reef slopes and lagoons at multiple reefs on the Great Barrier Reef (GBR). Plots ranged across the most common water visibility conditions found on the GBR (1 – 20 m vertical visibility). Five stainless steel spheres covered with patterned stickers were mounted on branches to central rod to make sphere-trees references used for plot co-registration (Figure 3.3). The top three spheres of each tree were sealed while the two bottom were hollow to achieve near neutral buoyancy underwater. At each permanent plot, two sphere-trees were attached to permanent pickets hammered into the reef substrate along the central line of each plot and roughly 6 m apart. Sphere-trees were mounted on pickets along the small angle of the star-picket, with the second branch (3rd sphere) resting against the top of the picket. The main "trunk" of the sphere-tree was attached against the star picket between its 2nd and the 3rd branches (from the top), using a 3D printed plastic clamp with a T-bolt (Figure 3.3a). The sphere-trees and clamps were designed in a way that ensured there was only one possible way they could be mounted on the picket, ensuring repeatability from one setup to the next. Additionally, we deployed in each plot six reference features: five 'dumbbell'-shaped features with two coded targets each and one 'triad'-shaped feature with three targets and two bubble-levels (Figure 3.4a, c). Coded targets were printed from Metashape. We recorded the depth of one target per feature which was then used in model reconstruction to provide vertical scale and model orientation to real-world up using Metashape.

3.3.3 Data collection

Photogrammetric surveys of permanent coral reef plots were conducted on SCUBA. Divers used a custom-designed camera platform consisting of two Nikon D850 DSLR cameras with Nikon 20mm Prime lenses housed in Nauticam underwater housings with 8-inch Nauticam

acrylic dome ports. Cameras were mounted 57 cm apart, which ensured more than 80 % lateral overlap when swimming between 1.5 – 2 m altitude. Images were taken every half a second with settings adjusted to each dive conditions (see Appendix B: Table S1 and Gordon et al., 2023 for camera characteristics and settings details). Image acquisition for the whole plot and sphere-trees was done within the same dive. The diver swam in a 'lawn mower' pattern consisting of five passes in each of the long and short-directions of the plot and swam conical spirals around the sphere-trees at multiple camera angles to achieve accurate reconstruction of all 5 spheres (Figure 3.4e).

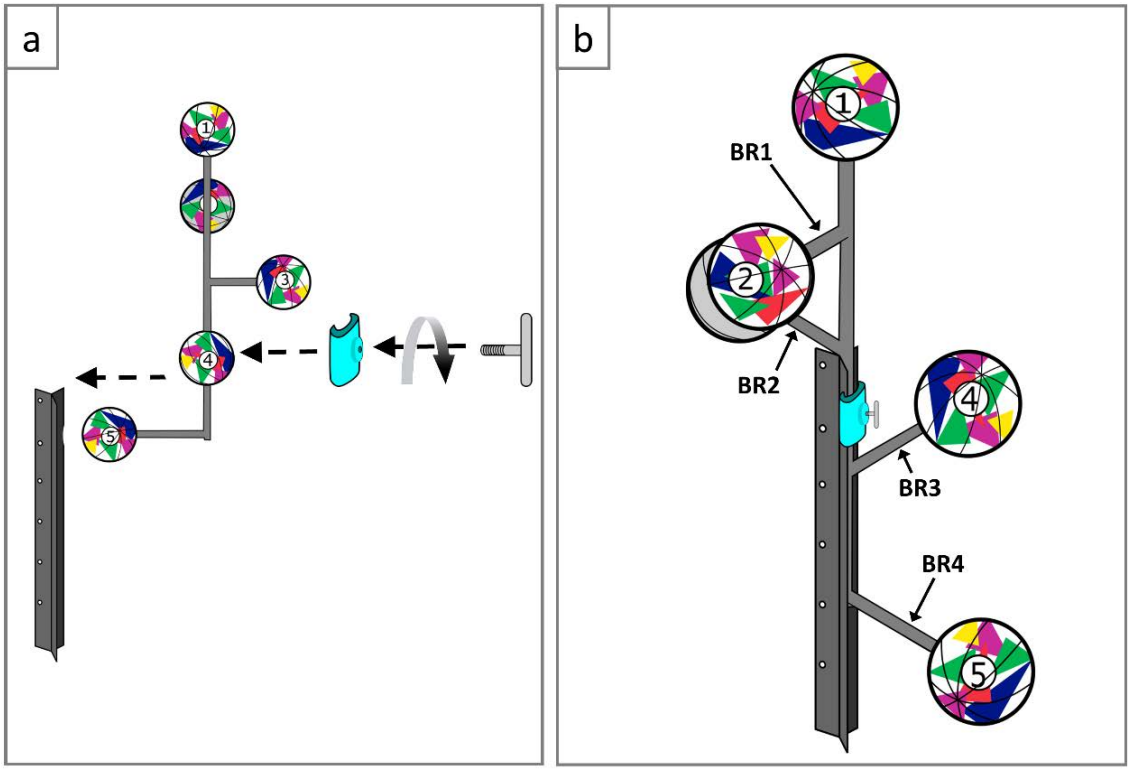


Figure 3. 3. Design and setup of a sphere-tree. (a) The sphere-tree is mounted on a permanent picket with its second branch resting on top of the picket. It is secured with a plastic clamp and tightened with a T-bolt. (b) A sphere-tree has five spheres covered with patterned stickers and four branches (BR1-BR4) to ensure enough spheres will be well reconstructed and used as co-registration targets.

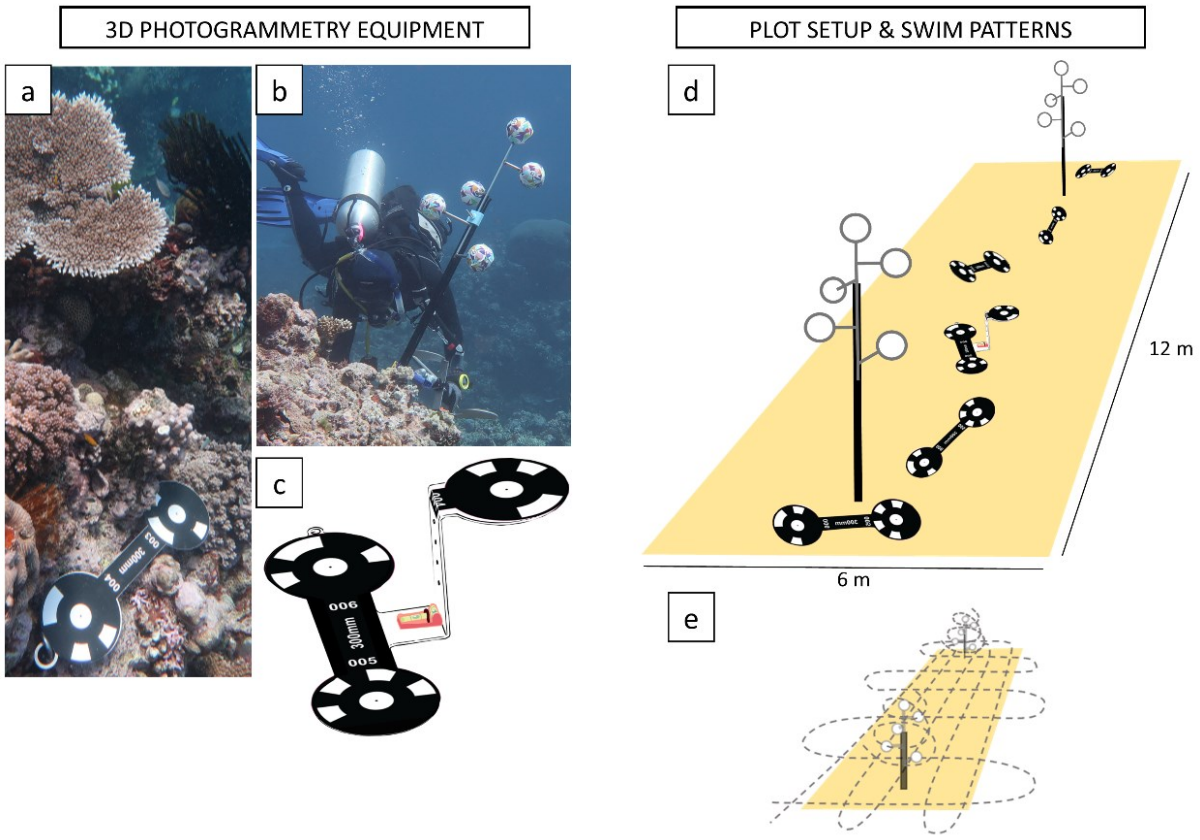


Figure 3. 4. Diagram of equipment, plot setup and swim patterns used during image acquisition. (a) example of a dumbbell with a pair of Metashape coded-targets used to record depth and scale, (b) example of a sphere-tree on which the co-registration spheres were mounted using a plastic clamp, set on a permanent picket, (c) illustration of a triad comprising three markers and a spirit level to measure depth and orientation, (d) illustration of a plot setup and (e) swim patterns above the plot and around the sphere-trees during image capture to ensure sufficient overlap between images. Photo credit: K. Fabricius.

3.3.4 3D processing

Underwater images were processed to generate 3D models in Metashape using custom Python scripts with the parameters detailed in Appendix B: Table S2. Reference and unregistered test models were imported into the Open Source software CloudCompare v2.11.3 (Anoia) with default settings. Unregistered test models were co-registered with reference models using the *point-pair picking registration* tool in CloudCompare. By enabling the 'white sphere' icon and setting a search radius, this tool automatically detects the best-fit sphere radius after the user has clicked on the location of the sphere center on the point cloud. Each sphere

on the reference model and its equivalent on the test model was selected by clicking on the center of each sphere on the point clouds. The centers of the best-fit sphere were then calculated by the software using a set search radius of 0.05 meters because each sphere is 10 centimeters in diameter. Based on the alignment of the 10 pairs of spheres, CloudCompare then created a transformation matrix for each test model. These matrices were exported and applied to the test model in Metashape via a custom Python script. Once the transformation matrix was applied, both reference and registered test models were exported from Metashape as PLY for model-to-model deviation analysis (Figure 3.2).

3.3.5 Deviation analysis

Each of the four sources of error (Figure 3.1) were estimated using the *3D Compare* deviation tool in Geomagic Control X (2020 © 3D Systems) between reference and registered models (Figure 3.6). The *3D Compare* deviation tool calculates a deviation value for every (depending on the sampling ratio) vertex of the test model compared to the reference model. Each measured vertex is defined by a set of coordinates (x_{test}, y_{test}, z_{test}) and is associated with a reference set of coordinates of the reference model ($x_{control}$, $y_{control}$, $z_{control}$), which is defined by the projection direction chosen (here we chose the shortest distance). For each point-pair, the tool calculates a gap vector GV defined in Eq. (1).

$$GV = (x_{test} - x_{control}, y_{test} - y_{control}, z_{test} - z_{control}) \quad (1)$$

Where x, y and z correspond to the coordinates on the x, y or z planes of the reference or the test model. GV is then converted to a deviation value between point-pairs D defined in Eq. (2).

$$D = \sqrt{(GV_x^2 + GV_y^2 + GV_z^2)} \quad (2)$$

For each comparison we reported the arithmetic mean, median, standard deviation (SD) and median absolute deviation (MAD) of all model-to-model deviation (***D***) between models. We report these four statistics because the mean and SD are common descriptive statistics that any user will be familiar with, but they are influenced by extreme values. In this study, the distributions of model-to-model deviations are expected to be skewed (long tails), even after removing outliers, causing the mean and SD to become biased in some cases. The median and the MAD are more robust to the influence of outliers and long-tails. Instead of using all the point-pairs, we chose a random point-pair sampling ratio of 25 % because it represented sufficient data points to observe patterns (22,171,195 to 35,036,902 point-pairs). Outliers' detection was based on model-to-model deviations. Outliers are expected, especially on the edges of the 3D models, as the reconstruction quality can be poor in these areas due to distortion at the edges of photos (Menna et al., 2016) and lower photo overlap caused by the swim patterns (Pizarro et al., 2017). Point-pairs with ***D*** falling outside of the 5-95 percentiles were considered as outliers and removed from the dataset for subsequent analyses. We also visually evaluated the spatial distribution of model-to-model deviations between the reference and test models using heatmaps. Distance heatmaps were used to examine if deviations are equally spatially distributed across the models' surfaces.

To gain insight into the distribution of model-to-model deviations within ecologically significant thresholds, we examined the proportion of deviations within specific ranges: -1 to 1mm, -10 to 10mm, and -30 to 30mm. These ranges were selected in accordance with the typical rates of micro change observed in coral reef environments, such as coral growth (~1-60 mm yr^{-1})(Ferrari et al., 2017; Lange et al., 2022), and reef bioerosion (e.g., ~10 mm over a 13-year period)(Roff et al., 2015). Larger changes in the reef 3D structure have been recorded, notably due to mechanical damage from storms or mass coral mortality event (Burns et al., 2016). However, in such instances, the changes observed were at least one order of magnitude

greater than the average model-to-model deviations expected to be found in this study; hence, we opted not to incorporate them into our analysis.

The last step was to quantify the contribution of each source of error to the total protocol error. We assumed that errors were additive between each source of error examined because they correspond to independent steps of the protocol. This allowed us to methodically isolate and evaluate the impact of each source of error by sequentially removing them from consideration. This stepwise approach enabled us to approximate the contribution of each step to the overall error based on the absolute mean model-to-model deviations. To calculate the different contributions of each source of error to the overall error, we first calculated each sub-component error by subtracting the error of the previous step. For example, if the mean error associated with the 3D processing step is 0.1, and the 3D processing step also includes the co-registration step that has an error of 0.03, the error introduced by the 3D processing step only is 0.07. We then divided each sub-component mean by the sum of all sub-component means and multiplied it by 100. Knowing the contribution of each step to the overall error allows users to determine where effort should be focused to improve the co-registration workflow.

3.4. Results

To empirically estimate the main errors influencing the precision of our protocol, we first plotted the distributions of the model-to-model deviations by plots (P01-P10) and source of error (a-d) (figure 3.5). The ranges of deviation values increased from the co-registration error (Figure 3.5a) to the RSF placement error (Figure 3.5d). The mean model-to-model deviation was 0.038 mm (± 0.602), 0.13 mm (± 0.982), -0.642 mm (± 4.418) and -1.368 mm (± 16.552) for the co-registration, 3D processing, image acquisition and RSF placement error sources respectively (Table 3.2). The overall precision of the workflow was 13.4 mm (Table 3.2, RSF placement error row) for co-registered models derived from independent imaging sessions of

the same plot where scale and reference features had been independently placed for each session (Figure 3.5, Table 3.2, RSF placement error row).

The contribution of each source of error to the overall error is presented in table 3.2 (% Contribution column). The proportion that each source of error contributed to the overall error was estimated by calculating the absolute mean of each sub-component (source) in a stepwise manner and dividing each sub-component absolute mean by the sum of all sub-component means assuming error is additive between each source. Most of the proposed workflow error can be attributed to two primary sources: 37.43% arises from the image acquisition step, while 53.07% can be attributed to the placement of reference and scaling features (Table 3.2, % contribution column).

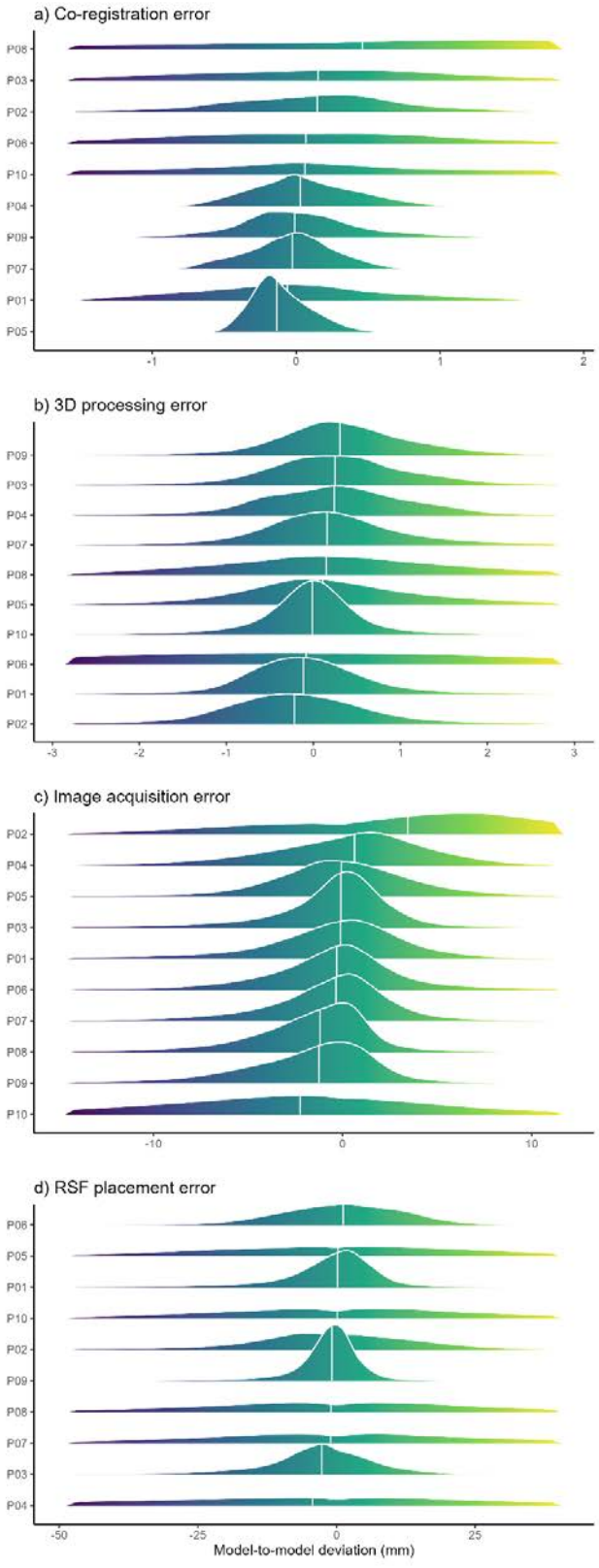


Figure 3. 5. Distributions of the model-to-model deviations by plots (P01-P10) and source of error (a-d), ranked by model-to-model deviation median values. The white vertical lines correspond to the median of each distribution. Units are in mm. Note that the range along the x-axis is different between sources of error.

Table 3. 2. Summary statistics (mean, median, standard deviation - SD - and median absolute deviation - MAD -) of model-to-model deviations calculated across all 10 plot pairs for each source of error. The contribution of each source of error to the overall error was estimated by calculating the absolute mean of each sub-component (source) in a stepwise manner and dividing each sub-component absolute mean by the sum of all (1.368), assuming error is additive between each source. For instance, the first row of the % Contribution column was calculated as 0.038/1.368*100. All units are in mm.

Source of error	Mean	Median	SD	MAD	Sub-component absolute mean	% Contribution
Co-registration	0.038	-0.001	0.602	0.495	0.038	2.78
3D processing	0.13	0.111	0.982	0.848	0.092	6.72
Image acquisition	-0.642	-0.357	4.418	3.537	0.512	37.43
RSF placement	-1.368	-0.721	16.552	13.407	0.726	53.07

The heatmaps in figure 3.6 are a visual output of the deviation analysis and show the model-to-model deviations between the reference and test models for all the point pairs sampled across the models' surfaces (each colored point represents the deviation, or 3D distance, between a given point on the surface of the reference model and its closest equivalent on the test model's surface). These heatmaps are an efficient visual way of assessing whether the size of the distance between the reference and test models increase with distance from the sphere-trees. They revealed that model-to-model deviations were evenly distributed across the 3D models' surfaces for the co-registration error (Figure 3.6a). However, for the three other sources, the smallest deviations tended to be located along the centre line of the plot that correspond to the line between the sphere-trees (prevalence of yellow or light blue points around the centre of the plot) (Figure 3.6b-d).

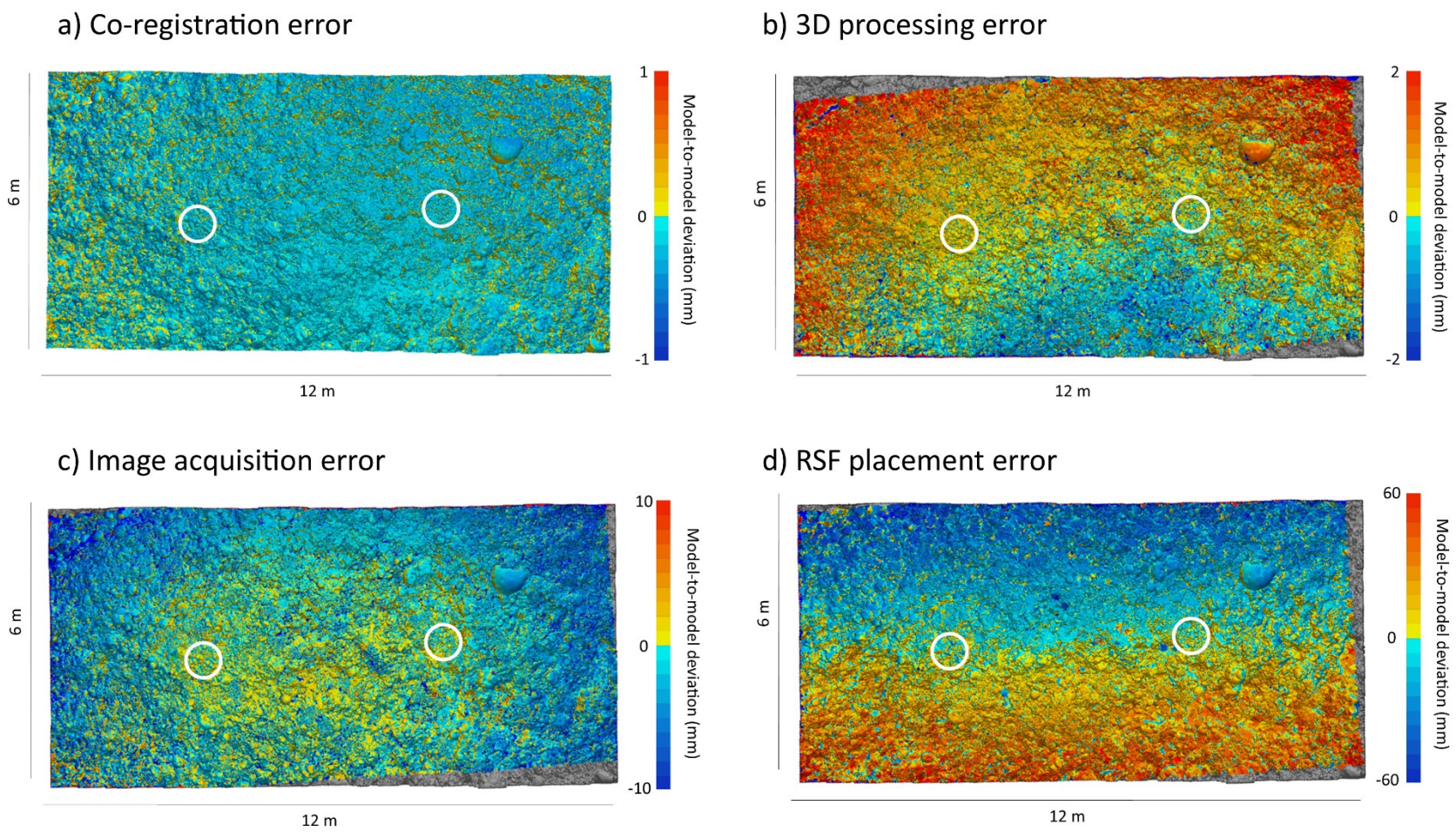


Figure 3. 6. Example of deviation analysis output using the 3D Compare tool in Geomagic Control X. The heatmaps show the model-to-model deviations (mm) between the reference and test models (note the difference in scale of the heat color ramp). The white circles mark the location of the sphere-trees. Gray areas denote areas of no overlap between models.

Finally, the proportion of model-to-model deviations within specific ranges are presented in figure 3.7. They revealed that most of the values fell between -1 and 1 mm for the co-registration error (88%) and most values fell between -10 and 10 mm for the 3D processing and image acquisition errors (100% and 96% respectively). However, only about half of model-to-model deviations fell between -10 and 10 mm for the RSF placement error, for which 90 % of deviations fell between -30 to 30 mm (Appendix B: Table S2, Figure 3.7).

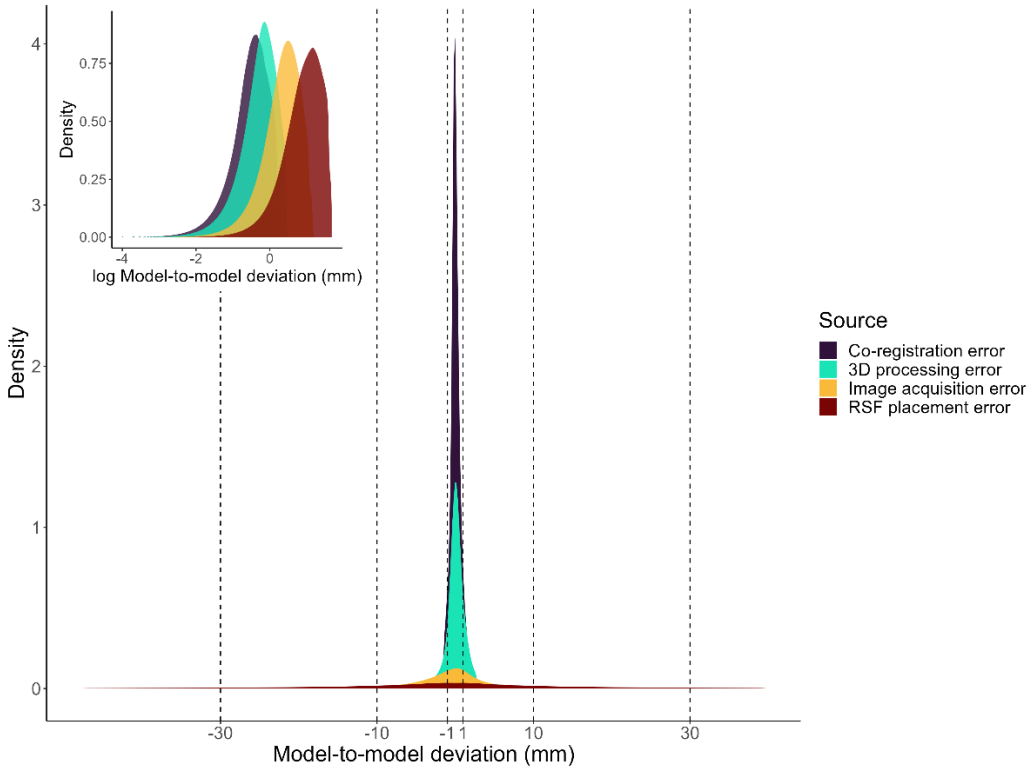


Figure 3. 7. Distribution of model-to-model deviations. The dashed lines mark the specific ranges evaluated: -1 to 1 mm, -10 to 10, and -30 to 30 mm. The inset plot shows the model-to-model deviations on a log-transform x-axis for better visualisation.

3.5 Discussion

3.5.1 Context of study

In this study we empirically estimated the main errors influencing the precision of an efficient field protocol for multi-temporal analyses of underwater 3D models. Our analysis revealed that when following the presented protocol, the absolute mean of model-to-model deviation was 1.37 mm and standard deviation of 16.55 mm, meaning that the change detection threshold of this methodology is 33 mm (standard deviation x 2). This suggests that differences greater or lesser than 33 mm at the plot level (across 72 m^2) likely represents a real change in the 3D structure of the reef (Table 3.2). Thus, the proposed protocol may be sufficient for detecting growth of fast-growing coral taxa (e.g., branching morphologies, Anderson et al., 2017) or the impact of a storm (Pascoe et al., 2021; Yuval et al., 2023), but may not be sufficient for recording slow-growing taxa (e.g., massive morphologies, Cooper et al., 2008) or dissolution of dead corals unless enough time is allowed between surveys to record such changes. The practical and ecological implications of the change detection threshold of the proposed protocol are further discussed in section 4.2 below.

It is important to note that a lower threshold might have been attainable had we based the model-to-model deviation on point-pairs pre-filtered by a confidence interval (James et al., 2017; Lague et al., 2013), instead we used random point-pairs which could encompass bad points (e.g., edges or overhangs). The significance threshold could also have been lowered if we had based our comparisons on cloud-to-cloud or cloud-to-mesh distances (Lague et al., 2013). The decision to use model-to-model comparisons was made however, as 3D models, and not point clouds, are used to derive key habitat metrics in coral reefs such as surface rugosity (Price et al., 2019; Young et al., 2017).

The results presented here are for a single acquisition system (camera, lens and waterproof housing) along with a specific suite of software. The study did not delve into comparing the influence of different camera systems and software on the accuracy of 3D models, as this has been explored in previous research (e.g., Guo et al., 2016; Maas, 2015; Neyer et al., 2018; Rossi et al., 2020). However, it is important to note that both the properties of sea water and the camera system can alter the trajectory of optical rays, thus affecting image formation and quality (Nocerino et al., 2016). Moreover, environmental conditions such as depth, wave action, light reflection, and visibility, can vary strongly and rapidly, impacting image quality (Bryson et al., 2017). To address these factors and ensure comparability, underwater 3D models used in this study were sourced from various regions of the Great Barrier Reef and surveyed around similar times of day and tide levels, representing a typical range of underwater survey conditions. To ensure transparency and reproducibility, camera settings and specific parameters employed during 3D processing in Metashape are detailed in Appendix B: Table S2, along with scale bar errors and 3D statistics in Appendix B: Table S3.

The mean of the difference between reference and test 3D models, its standard deviation, and mean absolute deviation (based on 10 3D models) for the proposed protocol are -1.34 mm, 16.5 mm and 13.4 mm (Table 3.2, RSF placement error row). Previous studies have used alternative photogrammetric workflows to detect significant changes in marine environments and found similar error estimates. For example, Neyer et al. (2018), Rossi et al. (2020) and Nocerino et al. (2020) designed and installed a geodetic reference network by cementing anchors into the reef matrix on which ground control points were screwed before imaging. Through use of this installation, they could compare the reconstructions of a reef plot between two epochs (7-months to one year apart). Neyer et al. (2018), found the mean of model-to-model difference, its standard deviation, and the MAD to be 2 mm, 69 mm, and 35 mm respectively for a single plot which are slightly higher than the model-to-model deviation found

in the present study based on 10 plots (Table 3.2, RSF placement error row). Rossi and colleagues compared two models of plots surveyed at a year interval and found the median distance between models to be 12 mm. They concluded that, considering variability introduced by the reconstruction process, only differences greater or lesser than 1 cm per year could be attributed to real change. Furthermore, Nocerino et al. (2020) found significant differences (model-to-model distances) between 50 and –30 mm corresponding to coral growth and loss that happened within a year.

These alternative workflows consistently delivered precise and accurate repeated measurements of benthic characteristics and change over time. However, the process involves time-consuming steps including the installation, collection of distance measurements and setup of the geodetic reference network within a designated plot, which typically takes two divers and between 1 to 1.5 hours to survey an area of ~ 25 m^2 (Rossi et al., 2020). In contrast, the proposed protocol here requires four divers and between 1 to 1.5 hours to survey an area of ~ 288 m^2 (four plots of 72 m^2 each surveyed per dive). This point is worth considering when scaling up the implementation of the workflow for large scale monitoring. For example, surveying an area of 1000 m^2 would take approximately 40 hours with the geodetic network workflow (workflow A) while it would take approximately 3.5 hours following the proposed workflow (workflow B). Assuming a maximum of four hours of diving per day is allowed as per most occupational diving restrictions, a 1000 m^2 area would be surveyed in ~ 10 days with workflow A and in a day or two with workflow B. The proposed workflow has been used to survey annually 360 plots of 72 m^2 each, or a total area of ~ 25000 m^2 in 30-45 field days.

The mean absolute error of the workflow presented herein is 1.4 mm (RSF placement error row, Table 3.2). Assuming that error is additive throughout the steps of the proposed workflow, we could calculate the contribution of each step to the overall error by the co-

registration (2.8%), 3D processing (6.7%), image acquisition (37.4%), and RSF placement (53.1%) (Table 3.2). Although the geodetic reference network-based workflows mentioned earlier require significant labor and time investment, the permanent reference network reduces greatly the primary source of error associated with the method described here (repositioning of the reference and scaling features). Therefore, these two methodologies highlight a trade-off between cost/scale and error.

Knowing the contribution of each step to the overall error provides insight into the factors influencing precision variability between and within surveys, suggesting which step should be modified to achieve the highest precision. Based on these different contributions, we discuss below good practices guidelines to minimize the error associated with each step of the workflow.

3.5.2 Good practices guidelines for co-registration workflows

The following section discusses the results of the current study in the context of broader applications of multi-temporal photogrammetry surveys. Specifically, we discuss how these findings can inform and shape best practices for multi-temporal imaging when using photogrammetry surveys for assessing ecological indicators.

3.5.2.1. Establish standard field protocols.

The implementation of standard operational procedure within this workflow was crucial and has enabled us to consistently capture images and construct 3D models of the same plots between different epochs and across all common coral reef habitat types between 2 – 15 m depth. The results presented here suggest that efforts should be directed towards implementation of standard protocols to minimize error introduced by the image acquisition step and the placement of reference and scaling features between surveys.

Reducing mapping error

The error introduced during the image acquisition step presents a challenge but holds strong potential for improvement. Achieving identical camera angles and positions, even with standardized imaging protocols encompassing factors like swim pattern and speed, remains a challenging task. However, there are several strategies that could be explored to enhance the consistency of data collection.

One strategy to reduce image acquisition error is to maintain the same team of observers over time, although this may be challenging to sustain for long-term monitoring. Alternatively, regular training and calibration amongst 3D imaging divers can further contribute to minimizing discrepancies. It is important to keep the swim pattern and data collection as consistent as possible while also logistically feasible and safe. For example, Pizarro et al. (2017) proposed a protocol to restrict the swimmer's movement while simultaneously imaging the plot by using a line wound around a drum affixed to a stationary pole. During the image capture, the swimmer unwinds the line resulting in a consistent spiral-like pattern. However, this workflow is best suited for down-looking surveys (only capable of achieving 2.5D, not 3D reconstructions) and would be very challenging to implement safely in most coral reef habitats (reef slopes, lagoons with high structural complexity, in depths greater than 5 m, or in low visibility habitats like inshore reefs). The use of Autonomous Underwater Vehicles (AUVs) could improve image capture patterns in some environments such as deep reef habitats, yet they are significantly more expensive and specialized.

A second strategy to reduce image acquisition error is to increasing image density. Lower density of images can result in less robust 3D reconstruction geometry (James et al., 2017) which could lead to poor co-registration quality. Indeed, in the heatmaps shown in figure 3.6, the model-to-model deviations were smaller around the center line of the plot, potentially due

to the higher photo density in this area compared to the edges of the plots. Increasing image density is a viable and easy solution to implement either by swimming slightly slower or by increasing the rate at which images are captured (for example from 1 fps to 2 fps) during image acquisition. Based on our results, if 1.4 mm error is an acceptable threshold, we recommend a minimum image density of 90 images per square meter (~ 6000 images per plot of 72 m^2) which can then be reduced to a third if photo redundancy is high (>2000 images per plot of 72 m^2).

Reducing placement of reference and scaling features (RSF) error

The importance and difficulty of setting up permanent references has been repeatedly highlighted by previous studies (e.g., Neyer et al., 2018; Nocerino et al., 2020). We suspect most of the error associated with the reference and scaling features placement is due to permanent pickets moving between imaging sessions or to the sphere-trees moving during imaging sessions, or both. Meticulous attention should be dedicated to the method by which plots are permanently marked and set up for long-term stability. This consideration is particularly crucial in dynamic settings like coral reefs, where external forces have the capacity to alter the positioning of fixed reference points used for co-registration. Introducing as much redundancy as logistically feasible in the number of permanent markers will also help. We found that the reference and scaling feature placement error, accounting for the uncertainty with which the sphere-trees are mounted and re-mounted, had a mean error of 1.37 mm (± 16.5 mm) for an area of 72 sqm. Other stable features, such as rock formations, could be used as additional static references to identify any gross issues with the permanent reference features.

One strategy to reduce RSF error is to improve the design of the permanent markers (the pickets in this study) on which co-registration features (here, sphere-trees) are mounted. While the use of star pickets as permanent anchors offered ease and cost-effectiveness, improving

their design could involve shortening their length to reduce susceptibility to hydrodynamic forces (Neyer et al., 2018). The picket's length represents the result of a trade-off between reducing the likelihood of movement and preventing overgrowth by fast-growing benthic organisms. The ideal length of a picket will also depend on the type of substrate at each site, well consolidated reef (typical of shallow exposed reefs) will require shorter pickets, while sites dominated by rubble and weaker substrate (typical of back reefs and lagoons) will require longer pickets. The type of picket should be carefully planned with site knowledge.

The structural integrity of the permanent pickets can also be compromised due to corrosion as we noticed at some of our older plots. Corroded pickets can decrease the mechanical stability of sphere-trees and thus decrease precision of co-registration. Opting for stainless-steel pickets, which are more resistant to corrosion, could present a viable solution, albeit at a higher initial material cost. In this study two pickets per plot were used, offering a little redundancy if one picket moved or corroded. Although our findings indicate that using two pickets leads to an acceptable level of error (Table 3.2), if logistically and costly feasible, it is worth considering the option of adding a third (forming a triangular arrangement within the plot) or fourth (positioned in a rhomboid arrangement) permanent picket per plot. This redundancy would safeguard against picket movement or dislodgement and allow each picket to have a sphere-tree with less spheres. Adding a third picket would also reduce the model-to-model distance around the edges of the 3D models as seen in figure 3.6 where the heatmaps showed that error generally increased with distance from the plane along which the pickets were placed.

A second strategy to reduce RSF error is to reduce the probability of co-registration features mounted onto permanent markers to move between or/and during surveys. Notably, we observed that even minor discrepancies in the way sphere-trees were mounted onto the

permanent pickets led to a slight increase in model-to-model deviation and contributed to half the total co-registration error in this study. The use of spheres as co-registration features was very efficient, offering superior alignment capabilities compared to 2D markers or any other published method to the best of our knowledge. To improve setup efficiency, the number of spheres per tree could be reduced from five to two or three (always keep the top sphere) to make sphere-trees less cumbersome and potentially mitigate the impact of water flow forces. Finally, it is also possible to better fix the permanent markers into the seafloor by cementing them for example (Nocerino et al., 2020).

3.5.2.2. Understand the 3D processing pipeline

Photogrammetry reconstruction software often operates in a black-box mode which may provide unreliable results when users lack a comprehensive understanding of the underlying technique. The error introduced during the 3D processing step using Metashape, a widely used software, was very small (mean model-to-model deviation of 0.13 ± 0.98 mm). While the task of minimizing reconstruction errors during 3D processing remains challenging, the value of obtaining insights into this error should not be understated. Such insights serve a dual purpose: they aid in compartmentalizing 3D processing error from other potential sources of error, and they provide a quantitative means to gauge the overall precision achieved. Furthermore, quantifying the error introduced during model 3D processing highlights the significant level of change that is detectable using a common processing pipeline in Metashape. We encourage photogrammetry practitioners to either quantify or, at the very least, remain aware of, the error introduced by their 3D processing pipeline, particularly when aiming for very fine change detection (mm scale).

3.5.2.3. Survey at relevant frequency

The results provide insights into the appropriate temporal frequency for sampling, emphasizing that this frequency should be informed by the rate of change in the measured variables and the error associated with the sampling protocol. Based on our results, sampling should be conducted when at least ± 30 mm of change is likely to have occurred over an area of 72 m^2 (Figure 3.7, Appendix B: Table S4). The main application for which precise co-registration is needed at the plot level is to detect changes in the 3D structural complexity over time. The 3D structural complexity of ecosystems, often created or enhanced by ecosystem engineers such as corals and trees, has a profound effect on communities of associated organisms (Graham & Nash, 2013; Romero et al., 2015). Thus, structural complexity metrics are often used as proxies for ecosystem state and resilience in coral reefs (Cheung et al., 2021; Yuval et al., 2023). There are many processes, such as storms (Madin & Connolly, 2006), coral predator outbreaks (Kayal et al., 2012), and mass bleaching (Hughes et al., 2018), that can change the 3D structure of reefs. The threshold presented here can be used as a distance cut-off when comparing models of different time points such as in Yuval et al. (2023) that used a distance cut-off of 0.05m to reliably quantify change related to the impact of a storm on a reef.

The workflow proposed in this study was not exclusively designed for detecting very fine changes such as those occurring at the organism level in 3D (e.g., coral colony growth); although the detection of such fine changes was a significant aspect under investigation. If one's primary interest lies in coral growth for instance, an optimal imaging approach would involve individual colony imaging (i.e., creating 3D models of individual coral colonies not of whole plots). Our workflow was strategically developed to facilitate the comprehensive monitoring of various critical facets of coral reef recovery and adaptation. These aspects encompassed demography, landscape ecology, structural complexity, seascape genomics, fish

shelter space availability, and spatial distribution of corallivory and herbivory, among others, across spatial extents of 100s of square meters. However, for practitioners intending to utilize this dataset for demography, a secondary fine alignment of 3D models should complement the proposed workflow. For instance, studying the growth of slow-growing coral such as massive coral morphologies, which extend at < 20 mm yr^{-1} (Cooper et al., 2008; Roff & Mumby, 2012) would require a secondary fine alignment and enough time between surveys to detect real changes.

3.5.3 Important considerations

The findings presented herein are tailored to the specific camera network, calibration parameters and suite of software used. While the outlined good practices guidelines aspire for universal applicability across similar workflows, it is important to acknowledge that using different cameras, calibration parameters, or software packages for 3D model processing will result in differences in uncertainty stemming from both random and systematic errors particular to the camera network and settings used. For instance, the use of auto-focus camera settings while the camera-to-object distance varies during image capture can result in images with different focal lengths being used to compute a unique model with a constant focal length (Ricolfe-Viala & Esparza, 2021). Consequently, this computed model may not accurately reflect the true camera location during the capture of calibration images, potentially impacting the accuracy of the resulting 3D model. Although the cumulative error encompassing random and systematic errors affecting the 3D models was captured within the overall error evaluation in this study, quantifying their individual contribution lay beyond the scope of this study.

Finally, the principal limitation identified in this study pertains to the mechanical stability of reference features. Notably, even a slight shift of one of the sphere-trees led to alignment discrepancies, as highlighted in Figure 3.6d. This underscores the main limitation of using

target-based co-registration in highly dynamic environments such as coral reefs. Therefore, our results indicate that future users could refine the co-registration method presented here by using approaches that consider the full geometry of 3D models, rather than relying solely on external features.

3.6 Conclusion

The accuracy and precision of co-registration play a pivotal role in the reliability of metric comparisons, particularly when assessing changes between time points. Precise measurements between these time points are essential because they provide the capability to determine how reefs are either accreting or eroding over time. Small errors in multi-temporal surveys and co-registration can lead to misleading interpretations, making it imperative to ensure precise survey methods and 3D models' alignment for a more robust understanding of the dynamic processes shaping reef 3D structure.

This study expands upon prior research using thorough and precise but time-consuming methodologies, proposing a complementary workflow that offers a cost-effective and time-efficient approach on a larger scale with similar error. We expect our experimental approach to estimating multi-temporal survey error can reduce a broad range of common error sources in photogrammetric analyses to improve precision. Importantly, as sources of error begin to be controlled, the value of time-series imagery data increases, and will ultimately support long-term, ultra-fine resolution, and precise studies of environmental change.

Chapter 4. Legacy effects of a mild mass bleaching event on coral survival and growth

Chapter in preparation for submission as:

Lechene M., Burn D., Álvarez-Noriega M., Becker M., Toor M., Gordon S., Aston E., Hoogenboom M., Ferrari R. Legacy effects of a mild bleaching event on coral survival and growth.

4.1 Abstract

Understanding the lethal and sublethal effects of bleaching on coral demographics is vital for predicting reef responses to climate change. This study examined the effects of a mild but spatially extensive bleaching event on corals of the central Great Barrier Reef in summer 2022. We assessed how bleaching severity influenced survival and growth of dominant coral taxa, accounting for biological, and environmental factors such as taxonomic identity, colony size, clarity, sea surface temperature, and water velocity. Results showed that initial colony size and bleaching severity were drivers of survival and growth during the year following the mild mass bleaching event, with only marginal effects of environmental conditions. Heat stress had a negative impact on both the survival probability and growth of healthy colonies. Severely bleached colonies (i.e., 'fully bleached' and 'recent partial mortality' categories) had significant declines in survival probability and growth compared to non-bleached and partially bleached colonies. By using large-area orthomosaics, we were able to virtually tag colonies and track them before, during and after bleaching to accurately quantify coral responses including bleaching-induced partial mortality. These findings offer critical insights for coral reef management, helping to identify resilient individuals, species, sizes and habitats and guiding conservation efforts for more vulnerable taxa.

4.2 Introduction

Rising sea surface temperatures pose a major threat to coral populations, leading to widespread coral bleaching events. Bleaching occurs when the relationship between corals and its symbiotic algae - dinoflagellates of the family *Symbiodiniaceae* - is disrupted. These algae provide nutritional benefits to their hosts, contributing to their energetic budget through photosynthesis and the provision of essential nutrients (Muscatine et al., 1997; Wiedenmann et al., 2023). However, environmental extremes such as elevated temperatures or irradiance, along with other stressors like low salinity, damage the algae's photosynthetic system, impairing energy provision to the host (Iglesias-Prieto et al., 1992). Eventually this leads to cellular damage in the symbionts and/or the host and can result in reduction in algae density within the coral tissue (Warner et al., 2002) or breakdown of the symbiosis (Lesser, 2006), revealing the white coral skeleton, hence the term coral 'bleaching'. Since 1998, the Great Barrier Reef (GBR) has suffered six mass coral bleaching events - four since 2016 – leaving limited time for recovery between disturbances (Emslie et al., 2024). As stress events accumulate, the trajectory of ecosystem recovery is influenced not only by present-day environmental conditions but also by ecological memory - the lasting influence or legacy of past disturbances retained through surviving organisms (Franklin et al., 2000; Johnstone et al., 2016; Monger et al., 2015; Seidl et al., 2014; Walker et al., 2024).

In coral reef ecosystems, this memory is evident in the legacy effects of repeated heat stress, which have contributed to long-term declines in coral cover (Loya et al., 2001), recruitment (Hughes et al., 2019), and habitat structural complexity (Madin et al., 2018) along with shifts in species composition and size structure (Carlot et al., 2020; Tebbett et al., 2025). At the colony level, legacy effects also include sublethal responses such as reduced growth, impaired fecundity and partial mortality (Cantin & Lough, 2014; Marshall & Baird, 2000; Ward et al.,

2002). These biological legacies constrain demographic performance and can limit a colony's contribution to population recovery and future stress resistance.

Despite broad recognition of the ecological consequences of mass bleaching, there remains a critical gap in our understanding of how mild (i.e., with sublethal effects) bleaching events influence individual-level demographic responses – specifically, coral growth and survival – across taxa and environmental gradients. Most studies have focused on severe bleaching events and mortality outcomes, with limited attention to sublethal impact that can accumulate over time and affect population trajectories. Moreover, demographic responses are known to vary with colony size, species identity, and local environmental conditions, yet few studies have simultaneously quantified these factors in situ across real-world gradients, particularly for corals that cannot be sampled using coring methods(e.g., Cantin & Lough, 2014).

Bleaching responses vary among taxa, with branching species often being more susceptible than massive morphologies (e.g., Loya et al., 2001; Marshall & Baird, 2000; Swain et al., 2016; van Woesik et al., 2011). Environmental conditions can also mediate bleaching severity, though effects are often taxon – and site-specific (Penin et al., 2007; Wooldridge & Done, 2004). For instance, deeper habitats may provide thermal refuges due to lower irradiance (Baird et al., 2018; Grimsditch et al., 2010; Smith et al., 2014), but severe bleaching has also been documented below 30 meters (e.g., Diaz et al., 2023). Turbid waters can reduce light stress and thus mitigate bleaching (Sully & van Woesik, 2020). Similarly, water flow can buffer thermal stress by enhancing heat dissipation (Fabricius, 2006) and flushing harmful photosynthetic byproducts (Finelli et al., 2006; Nakamura & van Woesik, 2001), but field evidence remains mixed – with studies showing positive (Bayraktarov et al., 2013), negative (McClanahan et al., 2005) or no clear relationship between water flow and bleaching severity (Yadav et al., 2023).

Past exposure to heat stress can also shape responses, as population with a history of disturbance may harbour more thermally tolerant individuals (Guest et al., 2012).

Bleaching response can even vary among individuals of the same species due to differences in colony size, but findings remain inconsistent across studies. In some cases, juveniles (<5 cm in diameter) have shown greater resistance to thermal stress than adults (Mumby, 1999; Shenkar et al., 2005), although this pattern is not universal and appears to be taxa-dependent (Álvarez-Noriega et al., 2018; Burn et al., 2023). Other studies report the opposite pattern, with smaller colonies bleaching more severely (Pratchett et al., 2013), or detect size effects only in specific morphologies or under particular environmental conditions (Wagner et al., 2010). Among adult colonies, some studies have found increased bleaching susceptibility (Brandt, 2009; Shenkar et al., 2005; Winslow et al., 2024), others a decrease (Johnston et al., 2020), and no clear relationship at all (Hoogenboom et al., 2017; J. C. Ortiz et al., 2009). These conflicting findings highlight the complexity of size-dependent bleaching dynamics and the importance of context – including species identity and environmental setting – in shaping these outcomes.

While much attention has focused on bleaching susceptibility and severity, what happens after bleaching - whether a colony fully recovers, partially recovers, or dies – is equally important for understanding population trajectories. Recovery capacity is influenced by biological traits, environmental conditions and legacy effects. As colonial organisms, corals exhibit size-dependent demographic rates (Hughes, 1984). Larger corals typically have higher survival probability (Meesters et al., 1997), but also face greater mechanical vulnerability. For instance, they are more prone to dislodgement storms (Madin et al., 2014; Madin & Connolly, 2006), but are better able to survive partial tissue loss and continue contributing to population processes. However, net growth in large colonies often slows or ceases due to increasing partial mortality with size (Hughes & Jackson, 1980; Meesters et al., 1997). Bleaching can reduce

growth (Cantin et al., 2010) and increase mortality either directly through physiological damage or indirectly via heightened predation (Glynn, 1985; Stimson et al., 2002) and susceptibility to disease (Miller et al., 2009). These effects can be especially pronounced in colonies already weakened by prior stress, reinforcing ecological memory through demographic feedbacks.

Despite its importance, the interaction between bleaching severity, colony size and environmental variation on coral demography remains understudied – particularly in the context of mild, sublethal bleaching events, which are increasingly common under climate change but may still generate lasting, legacy effects. Here we quantified growth and survival rates of five coral morphotaxa using high-resolution large-area orthomosaics spanning two consecutive years: one with no recorded major disturbance (2021-2022) and one following a mild mass bleaching event (2022-2023). Our objectives were to (1) compare growth and survival probability of healthy colonies (i.e., not bleached) between the year before and after bleaching and to (2) examine the effect of bleaching severity on coral survival and growth, and how this effect is influenced by initial size and key environmental variables.

4.3 Methods

4.3.1 *In situ* sampling

One inshore reef (Palm Islands 'PA') and three offshore reefs (Davies 'DA', Little Broadhurst 'LB' and Chicken 'CH') were surveyed in the central GBR between January 2021 and 2023. The main reefs (PA and DA) were initially surveyed in January 2021, while two additional offshore reefs (LB and CH) were initially surveyed in May 2021. All subsequent surveys across all four reefs took place in January 2022, April 2022 (at peak of bleaching) and in January 2023. Surveyed sites were distributed along the reef slope and around the perimeter of the reef

across a wave exposure gradient at a depth range between 3-5 m ('shallow'). At the main reefs, sites were also established at a depth range between 9-15 m ('deep'). Each site had four replicate plots of approximately 12 x 6 m (72 m^2) spaced 10 m apart and laid parallel to the depth gradient. A total of 26 sites and 98 plots were surveyed (Figure 4.1).

Photogrammetric surveys of the permanent plots were conducted on SCUBA. Two divers used a custom-designed camera rig consisting of two Nikon D850 DSLR cameras with 20 mm Nikkor lenses housed in Nauticam housing with 8" dome ports and mounted 57 cm apart (S. Gordon et al., 2023). The divers swam at 1 – 1.5 m altitude in a 'lawn mower' pattern consisting of five passes in each of the long and short-directions of the plot while taking photos every 0.5s (~ 3000 photos per plot). At each site, the cameras were white-balanced at the targeted depth before taking photos. Each plot had 13 ground control points (five pairs and one triad with bubble levels) to capture depth, scale and orientation of the 3D models. Each plot had also two reference points used to align 3D models through time (Lechene et al., 2024).

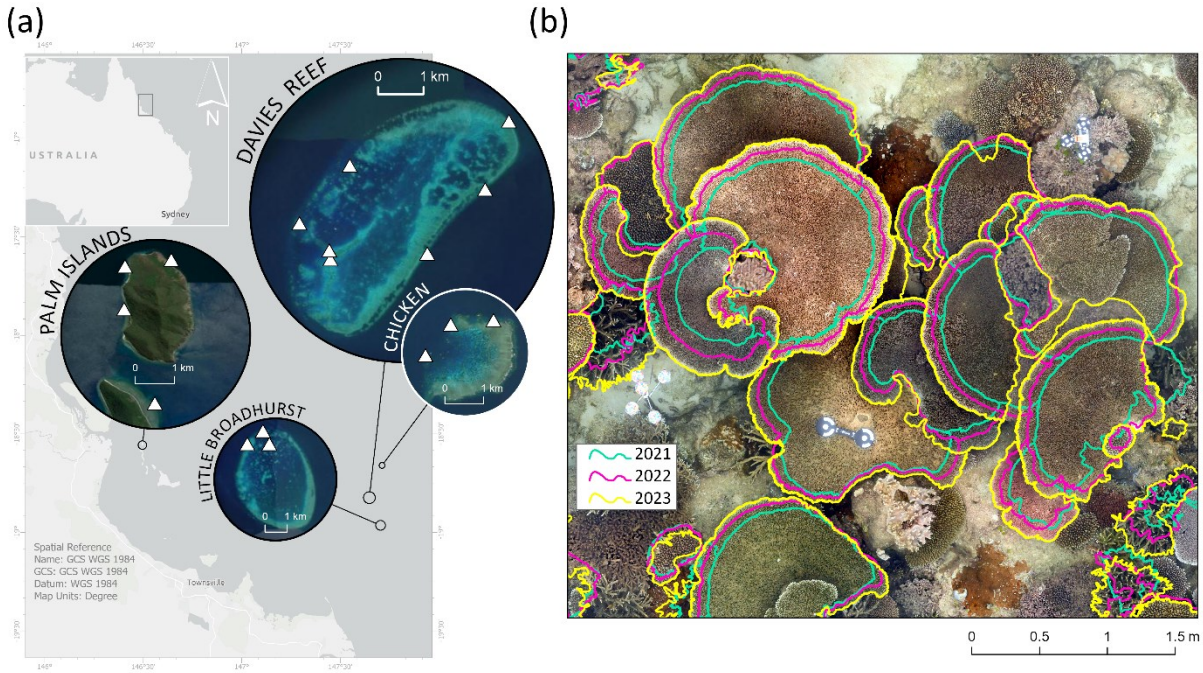


Figure 4. 1. Study sites. (a) Map of the four reefs with sites locations marked by white triangles. (b) Detail of an orthomosaic from 2023 with colonies outlines from 2021 (yellow), 2022 (pink) and 2021 (teal).

4.3.2 Image processing

The photos were processed in Agisoft Metashape Professional (v. 1.7.6) to generate a 3D model and a 2D orthomosaic per plot. Orthomosaics had an approximate resolution of 0.3 mm.pixel^{-1} and were used to estimate colony size (planar area) and assign bleaching severity categories by a single observer (categories described below). To accurately quantify changes in planar area, 3D models from different years were co-registered using the January 2022 survey as the reference and the two reference points mentioned above. This method achieved a mean precision of 1.3 mm (SD 16.5 mm) in 3D space (Lechene et al., 2024) and ensured consistent model orientation for generating orthomosaics, enabling precise size measurements by maintaining identical viewing angles for the same coral across years.

Using orthomosaics, five coral morphotaxa (staghorn *Acropora* spp., corymbose *Acropora* spp., *Pocillopora damicornis*, *Pocillopora verrucosa* and *Seriatopora hystrix*) were digitised using the high-accuracy '4-clicks' tracing tool in TagLab (Pavoni et al., 2022). We followed the workflow described in Toor et al. (2025) to extract colony size estimates and quantify bleaching severity. Colonies were digitised if they met these requirements: (i) identified with at least 80% certainty (threshold based on inter- and intra-observer error, González-Rivero et al., 2020; Williams et al., 2019, for full description of colony identification see section 5.2 in Toor et al.), (ii) clearly reconstructed (i.e., not blurry or distorted), (iii) 75% of the colony was visible (not cryptic or hidden), colonies that were obscured were noted as such and (iv) entirely within the boundaries of the orthomosaic. Only live tissue was digitised and colonies with partial mortality were noted as such.

Instead of digitising colonies every year, colony segments from 2021 were transferred onto the 2022 orthomosaic, and 2022 onto 2023. After transferring, each segment was reviewed to refine edges to align with the colony shape or to note whether the colony was now unusable (poor

quality imagery), dead, missing or with partial mortality. Colonies were noted as dead when 100% of the tissue was dead and the skeleton structure was still visible. However missing colonies were also noted as dead if they could not be found within a 2 m search radius from the original location. The segments for dead and missing colonies were left so they could be matched back to the original colony.

A single observer used the April 2022 orthomosaics to assign a bleaching category to each colony. The bleaching categories were 1) no bleaching, 2) minor bleaching (with 1-50% of the colony bleached), 3) major bleaching (with 51-95% of the colony bleached), 4) fully bleached (more than 95% of the colony bleached) and 5) fully bleached with signs of recent partial mortality (hereafter referred to as the recent partial mortality category) (modified from Gleason 1993). These categories differed from standard practice (i.e., three categories: fully bleached, partially bleached and recently dead) to better reflect differences in bleaching susceptibility, especially the "recent partial mortality" category that only includes fully bleached colonies with signs of partial mortality. This category captures taxonomic differences in injury rates, regeneration rates and bleaching susceptibility. Colonies were scored as having partial colony mortality whenever they presented mortality during the bleaching survey but did not show any signs of mortality during the January survey. Colonies that could not be assigned a bleaching category confidently were removed. Colonies that were digitised in January 2022 but not found in April 2022 were excluded from the analyses instead of classified as recently dead as we did not want to include mortality that happened prior to the bleaching event. We assumed all colonies experienced similar levels of heat stress as demonstrated by the very narrow range (4.1-5.2) of Degree Heating Weeks (DHWs) across all sites (Álvarez-Noriega et al., 2025).

Colony segments and associated data were extracted from TagLab as shapefiles, with one shapefile per orthomosaic (i.e., one shapefile per plot and year). Shapefiles were standardised

in ArcGIS Pro using custom scripts to calculate planar area of each colony in square meter, and to add metadata like plot ID and year. Colonies were matched across time using the Spatial Join tool between year pairs (2021 was joined with 2022, then this 2021-2022 join was joined with 2023). Colonies were matched based on largest overlap with a search radius of 15 cm if no overlapping colony was found. The final shapefile contained three columns for colony size (one per year) and one row per colony. Colony matches were checked, and incorrect matches and duplicates were deleted (when one polygon overlapped multiple ones, see full QA/QC steps in Toor et al. (2025)). Each colony in each year was given a survival score of 0 or 1 for dead or alive respectively. Partially dead colonies were considered survivors when they still had living tissue. Growth was estimated as the difference in planar area between sampling years via the traced outlines of colonies in the orthomosaics, thus growth can be positive (increase in planar area) or negative (decrease in planar area). The shapefiles from April 2022 only contained bleaching scores as size was not estimated in April.

4.3.3 Environmental variables

To investigate how the effect of bleaching severity on survival and growth differed across environmental gradients, we extracted modelled values of water velocity, clarity and temperature. Horizontal water velocity near the seabed ($m.s^{-1}$), referred to as "water velocity" hereafter, was derived from maps of wave metrics generated using fetch-based and process-based models, which incorporated long-term wind data and fine-scale bathymetry (Callaghan, 2023; Callaghan et al., 2015) accessible at https://espace.library.uq.edu.au/view/UQ:8246441). Since water velocity data was available only as time series summaries, the mean was used to represent routine water velocity. These estimates were provided at a 15 x 15 m horizontal resolution at the seabed, so each site and depth had a unique value. Water clarity and temperature were extracted from *eReefs*, an information platform using data and models to

estimate a series of environmental variables across the Great Barrier Reef (Steven et al., 2019). The eReefs biogeochemical model (GBR4), which as a ~ 4km pixel resolution, was used to extract daily estimates of Secchi depth (vertical integral of light attenuation at 488 nm) from 1 January 2022 to 1 January 2023 using the R package *ereefs* (Robson, 2023). The annual mean for the time period these estimates were extracted from was used and hereafter referred to as 'mean clarity'. The eReefs hydrodynamic model (GBR1) at ~1km pixel resolution was used to extract daily estimates of water temperature from 1 January 2022 to 1 January 2023. The annual mean for the time period these estimates were extracted from was used and hereafter referred to as 'mean temperature'. We acknowledge the difference in resolution at which these environmental variables were extracted. While this spatial mismatch introduces some uncertainty, particularly in fine-scale spatial interpretation (which we discuss later), our analyses focus on broader patterns in how environmental gradients mediate the effects of bleaching severity on coral growth and survival. The inclusion of a random intercept for site accounts for the unmeasured site-level variation and the hierarchical structure of the data, helping to reduce potential bias associated with resolution mismatches and spatial autocorrelation.

4.3.4 Data analyses

All statistical analyses were performed using R version 4.3.1 (R Core Team, 2023). For all analyses we fitted generalised linear mixed-effect models in a frequentist framework with the *glmmTMB* package (Brooks et al., 2017). . We plotted the models' predictions using the *ggeffects* (Lüdecke, 2018) and *ggplot2* (Wickham et al., 2016) packages. Environmental predictors were standardised (z-transformed) prior to model fitting to facilitate comparison of effect sizes and reduce multicollinearity. Model diagnostics were conducted for all models using the *DHARMa* package (Hartig, 2022). Simulated residuals were used to assess residual

distribution, dispersion, and zero-inflation, and to identify potential deviations from model assumptions. In addition, collinearity among fixed effects was assessed by calculating variance inflation factors (VIFs), and predictors with high multicollinearity (VIF > 5) were excluded or interpreted with caution. Given that our dataset is split into a before (2021-2022) and during/after bleaching (2022-2023), we split the analyses into two sets: 1) a dataset including only healthy colonies (i.e., not bleached) from the entire study period (2021-2023) and 2) a second dataset with all colonies from the post-bleaching year. The first set of analyses investigated whether heat stress had an impact on demographic rates even in the absence of bleaching. The first set of analyses compared colony-level survival and growth years (year included as fixed effect) without the correlation between year and bleaching severity (i.e., bleaching severity was always equal to 'no bleaching' for the year before bleaching). The second set of analyses investigated how bleaching severity affected survival and growth and if this relationship was modulated by colony size and the environment.

To account for variation in the number of days between annual surveys, we included a standardised variable in our models for the 2021–2022 transition, where survey intervals differed among locations. Specifically, colonies were surveyed either in January 2021 or May 2021, with all follow-up surveys conducted in January 2022. We assigned the number of days between surveys as either 365 or 240, respectively, and centred this variable around its mean to produce a variable (Days_2022c) representing deviation from the average survey interval. This covariate was included as a fixed effect in the growth and survival models to account for differences in time intervals between observations. For the 2022–2023 transition, the survey interval was fixed at 12 months across all locations, and Days_2022c was set to 0 to ensure it only influenced model estimates for the 2021–2022 transition.

Building on prior research highlighting the influence of colony size on growth and survival (Aston et al., under review; (Dornelas et al., 2017; Ferrari et al., 2012; Madin et al., 2014), we characterised growth by modelling the relationship between the log-transformed planar area at time t_1 as a function of the log-transformed planar area at time t_0. In a log-log plot, the stasis line - defined by a slope of 1 and an intercept of 0 - represents no change in size. Colonies above this line have increased in size, while those below have decreased in size between time points. A slope less than 1 indicates slowing growth and when the growth curve intersects the stasis line, colonies begin to shrink on average. The point of intersection highlights how different predictors influence the average colony size at which growth stops in a given environment, as well as how this threshold shifts with changes in environmental conditions. For instance, increased bleaching severity would be expected to flatten the slope, leading to an intersection point at a smaller colony size, indicating that the average size at which growth ceases decreases as bleaching severity intensifies.

To examine the effect of heat stress on survival and growth we ran two generalised mixed-effects models. The survival model had Survival as a binomial response and included the interaction between Taxa and Year as fixed effects along with a covariate (Days_2022c) to account for differences in the number of days between surveys in the 2021-2022 transition. A random intercept for Plot nested within Reef was included to account for the hierarchical sampling design (all random effects combinations of Reef, Site, Plot were tested). The growth model had Size at t_1 (log-transformed) as a response and included the interaction between size at t_0 (log-transformed), Taxa and Year as fixed effects along with the covariate Days_2022c. A random intercept for Colony nested within Plot was included to account for the hierarchical sampling design and non-independence between colony size measurements (all random effects combinations of Reef, Site, Plot, Colony were tested).

To estimate the effect of bleaching severity on survival, accounting for initial size, and to test the influence of the environment, we built GLMMs for each of the five taxa. We first defined a base model structure for each taxon based on prior exploratory model comparisons. Specifically, we tested whether including an interaction between initial size and bleaching severity (categorical variable) improved model performance over an additive structure. The selected base structure was retained in all subsequent models for that taxon. In addition, random intercepts were included to account for spatial structure, with (1|Site) used for all taxa except *S. hystrix* for which (1|Site/Plot) was found to better capture the nested sampling design. We then tested the influence of environmental variables on survival by comparing a set of candidate models. These models extended the base structure to include standardised estimates of mean temperature, water clarity and water velocity, both as main effects and as interactions with bleaching severity. Specifically, we fitted a full model including all three interactions, a null model with no environmental variables and a suite of intermediate models with one or more environmental variables removed. In total, this resulted in a consistent set of models across taxa that allowed evaluation of the relative importance of environmental stressors in modulating survival under varying bleaching severity and initial size. Model comparisons were based on Akaike's Information Criterion (AIC). The model with the lowest AIC was selected as the best-fit model for each taxon (Table 4.1), if AIC were similar (i.e., less than two units different), the most parsimonious model was chosen. Models that failed to converge were excluded from interpretation. Collinearity among predictors was assessed using variance inflation factors (VIFs) via the *performance* package (Lüdecke et al., 2021) and model diagnostics were performed using the DHARMa package (Hartig 2022) to evaluate residual structure and potential dispersion.

Table 4. 1. Survival model formula of the best-fit model for each taxon. Models were ranked using AIC, preference was given to simpler models when ΔAIC < 2.

Taxa	Model name	Model formula
A. staghorn	null	Survival ~ initial size : bleaching severity + (1|Site)
A. corymbose	null	Survival ~ initial size + bleaching severity + (1 | Site)
P. damicornis	null	Survival ~ initial size + bleaching severity + (1 | Site)
P. verrucosa	null	Survival ~ initial size + bleaching severity + (1 | Site)
S. hystrix	only_temp	Survival ~ initial size : bleaching severity + temperature * bleaching severity + (1 | Site/Plot)

To examine the effect of bleaching severity and the environment (water clarity, temperature and water velocity) on growth, we fitted a suite of GLMMs for each taxon. All models included log-transformed size at t0 and its interaction with bleaching severity, with colony size at time t1 as the response variable. A full model included interactions between size at t0 and all standardised environmental variables, as well as their interactions with bleaching severity. A null model included only size at t0 * bleaching severity, and intermediate models systematically excluded one or more environmental predictors or interactions. All models included site as a random intercept. Models were ranked by AIC, with preference given to simpler models when ΔAIC < 2. The best-fit models for growth of each taxon are presented in table 4.2. Model assumptions were verified using residual diagnostics and multicollinearity was assessed using VIFs. In general, collinearity was low to moderate, however, VIFs were inflated in models with higher-order interactions involving rare bleaching categories, particularly for *P. verrucosa* and *S. hystrix*. These models were retained for completeness but interpreted cautiously.

Table 4. 2. Growth model formula of the best-fit model for each taxon. Models were ranked using AIC, with preference given to simpler models when ΔAIC < 2.

Taxa	Model name	Model formula
A. staghorn	only_temp	size at t_1 ~ size at t_0 + size at t_0 : bleaching severity + size at t_0 : temperature + size at t_0 : temperature : bleaching severity + (1 | Site)
A. corymbose	additive_env	size at t_1 ~ size at t_0 + size at t_0 : bleaching severity + size at t_0 : water clarity + size at t_0 : water velocity + size at t_0 : temperature + (1 | Site)
P. damicornis	null	size at t_1 ~ size at t_0 + size at t_0 : bleaching severity + (1 | Site)
P. verrucosa	only_temp	size at t_1 ~ size at t_0 + size at t_0 : bleaching severity + size at t_0 : temperature + size at t_0 : temperature : bleaching severity + (1 | Site)
S. hystrix	only_temp	size at t_1 ~ size at t_0 + size at t_0 : bleaching severity + size at t_0 : temperature + size at t_0 : temperature : bleaching severity + (1 | Site)

4.4 Results

4.4.1 Effect of heat stress on survival and growth of healthy colonies

Survival probability was consistently lower in the bleaching year (2022-2023) compared to pre-bleaching (2021-2022) except for *P. verrucosa* but the difference in survival of healthy colonies was only significant for *S. hystrix* (Figure 4.2). *A.* staghorn had no colony mortality in 2021-2022.

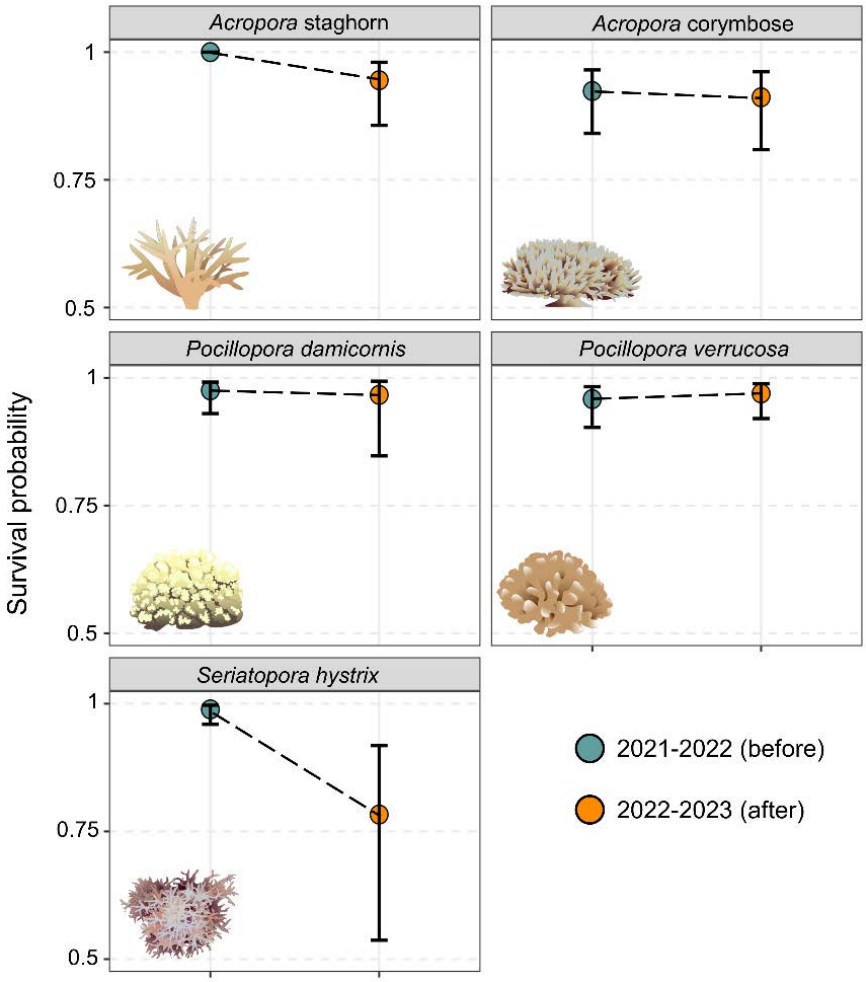


Figure 4. 2. Survival probability between years and taxa. Points represent the fitted model predictions, and the error bars represent the 95% confidence intervals.

For all models of growth of healthy colonies, the slopes were positive but less than one, with positive intercepts (Figure 4.3). This indicates that growth as a proportion of colony size decreases with increasing size, eventually intersecting the stasis line at a certain size, where colonies, on average, cease growing and can shrink. A consistent pattern was observed across most taxa, except for *A.* staghorn, where growth curves intercepted the stasis line at smaller size in 2022-2023 (year of heat stress) compared to 2021-2022 (Figure 4.3), indicating a decrease in growth during bleaching. Slopes differed significantly between years for all taxa except *P. damicornis* (Appendix C: Table S1).

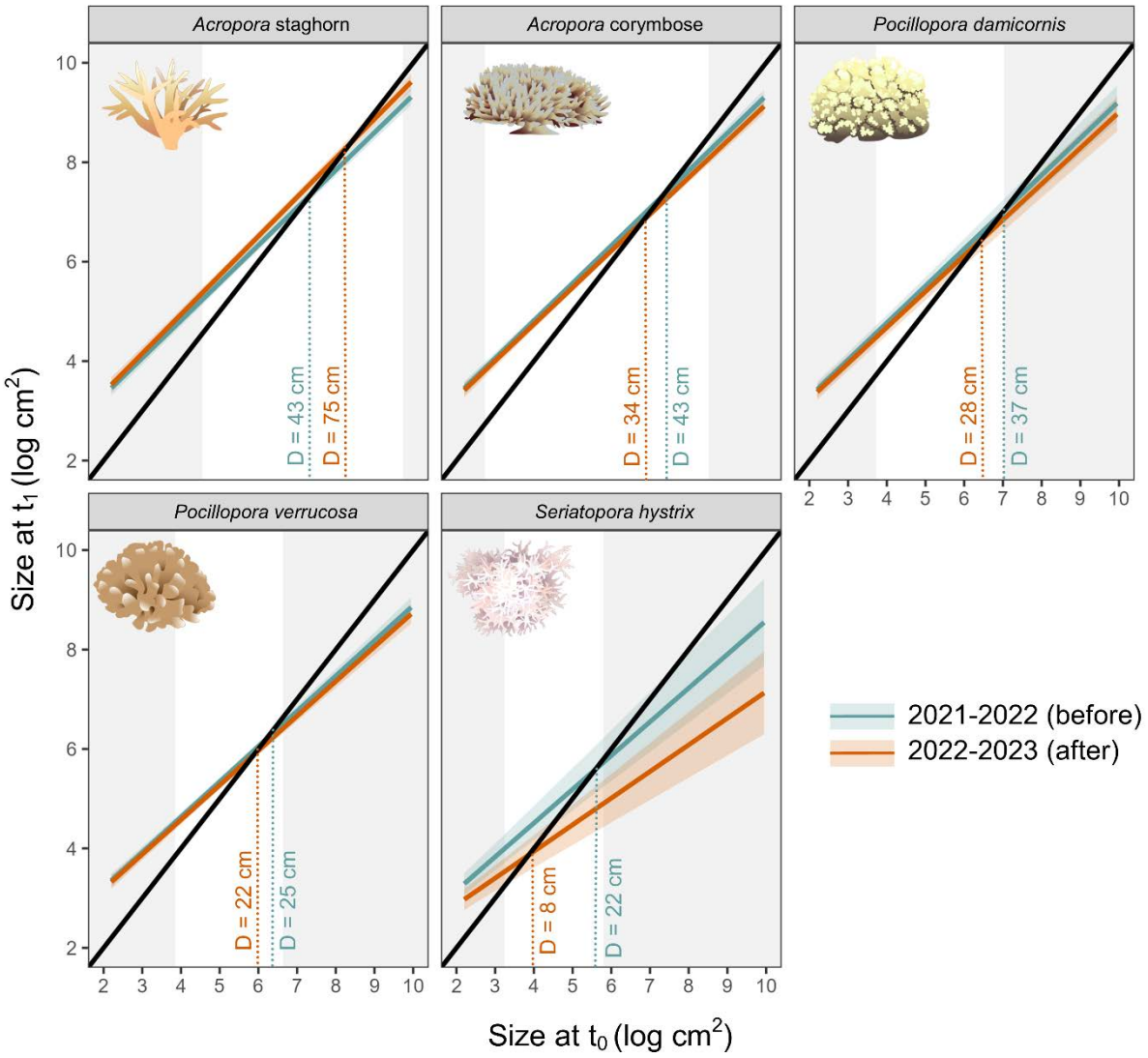


Figure 4. 3. Size at t_1 as a function of size at t_0, year and taxa. Ribbons represent the 95% confidence intervals. Diagonal black lines indicate the stasis line where size at t_1 = size at t_0. Grey-shaded regions represent areas where predictions are outside of the observed size range. The size at t_0 at which the curves cross the stasis line are indicated by the dotted vertical lines. An approximation of size in diameter (cm) is also given for ease of interpretation.

4.4.2 Effect of bleaching severity, colony size and environmental variables on survival and growth of coral colonies during a mild mass bleaching event

General trends

Across all taxa, survival probability and growth significantly increased with colony size and decreased with bleaching severity (Table 4.3). Bleaching severity had a particularly negative impact when colonies were fully bleached and/or with signs of recent partial mortality. The effect of environmental variables tested was taxa-dependent and predominantly influenced coral growth rather than survival during bleaching., The exception was *S. hystrix* for which, survival probability was also significantly influenced by mean temperature (Figure 4.8b-c).

The environmental variables tested were rarely retained in the growth best-fit models at the exception of mean temperature (Table 4.3). Mean water clarity had no effect on growth following bleaching. Mean water velocity had a significant negative effect on growth for *A.*

corymbose only (Figure 4.5d). The direction of the effect of mean temperature on growth changed depending on the bleaching category

Survival and growth did not differ significantly among colonies with no signs of bleaching, minor bleaching or major bleaching. Significant differences were observed only when colonies were severely bleached (fully bleached or fully bleached with signs of partial mortality).

Taxon-specific trends

Acropora staghorn

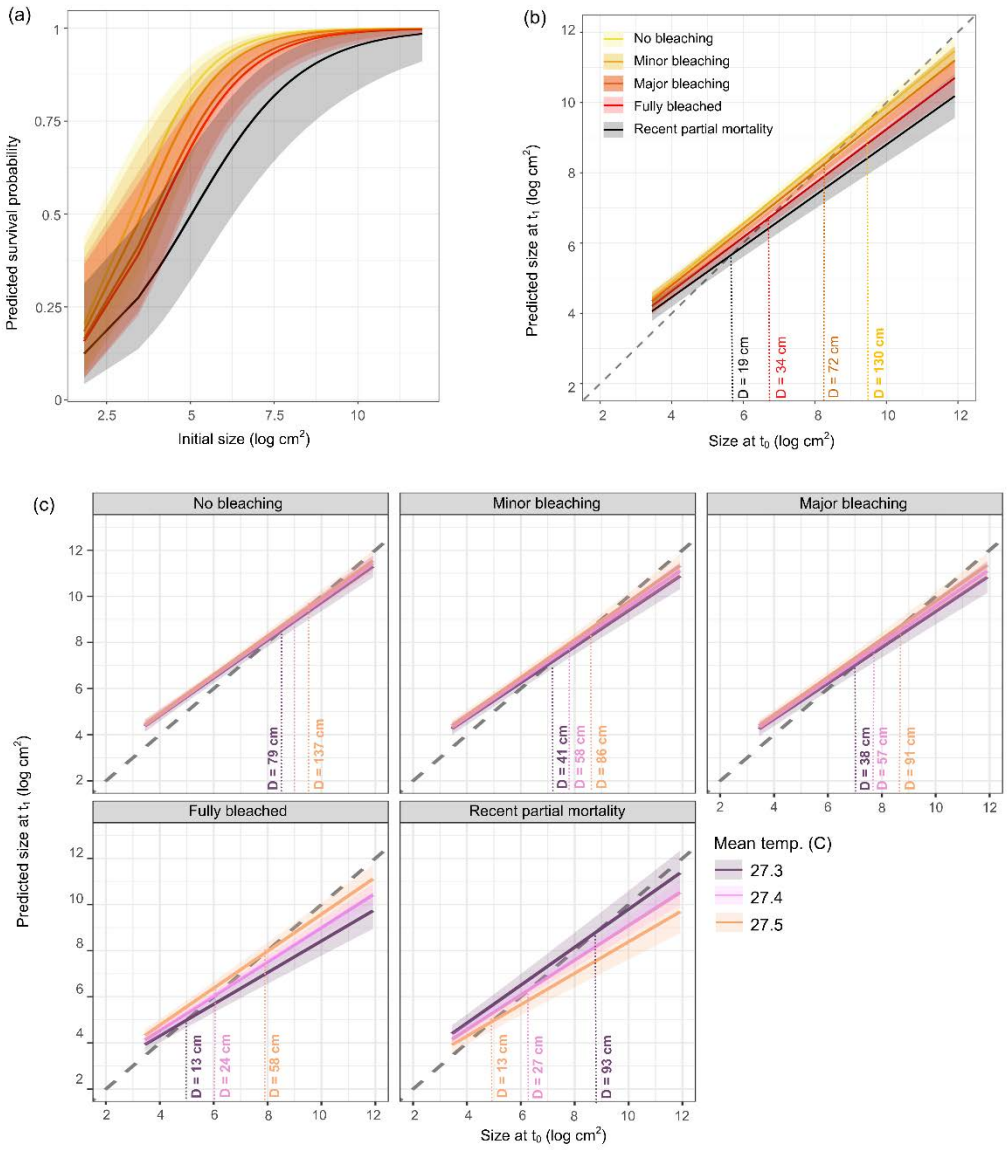


Figure 4. 4. Survival and growth model outputs for A. staghorn. (a) Predicted survival probability as a response of the interaction between initial size and bleaching severity, error bars represent 95% confidence intervals. Predicted size in 2023 as a function of size in 2022 and (b) bleaching severity and (c) mean temperature across levels of bleaching severity (facet labels). Shaded ribbons represent 95% confidence intervals. The dashed line represents the stasis line (slope = 1). Vertical dotted lines denote the approximate diameter where growth curves intersect the stasis line, indicating the size threshold beyond which colonies are expected to shrink under the given conditions.

Survival probability increased with initial size and decreased with bleaching severity (Figure 4.4a). Growth was negatively impacted by bleaching severity, particularly in the fully bleached and recent partial mortality categories (Figure 4.4b). Mean temperature positively influenced growth and interacted with bleaching severity to modulate its impact. Only for the colonies that

fully bleached with signs of partial mortality, the effect of temperature was negative (Figure 4.4c).

Acropora corymbose

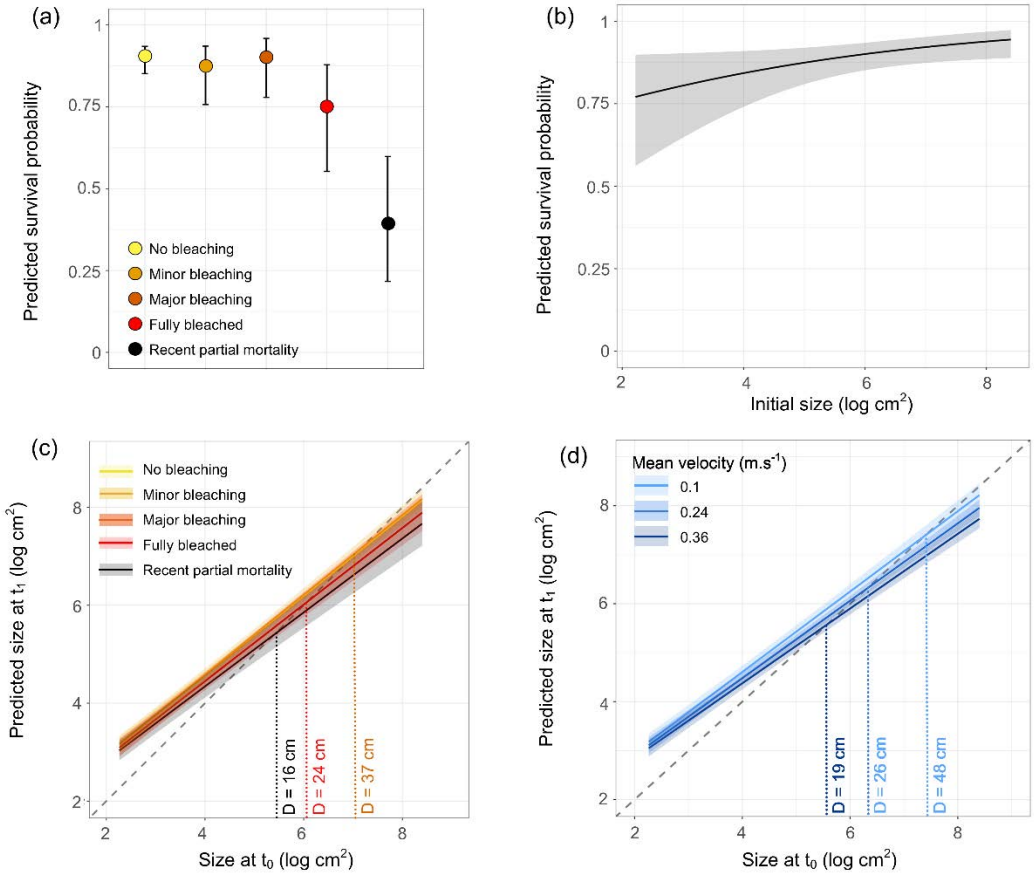


Figure 4. 5. Survival and growth model outputs for A. corymbose. (a) Predicted survival probability as a response of bleaching severity, error bars represent 95% confidence intervals. (b) Predicted survival probability as a response of initial size, shaded ribbon corresponds to 95% confidence intervals. Predicted size in 2023 as a function of size in 2022 and (c) bleaching severity, and (d) mean water velocity. Shaded ribbons correspond to 95% confidence intervals. The dashed line represents the stasis line (slope = 1). Vertical dotted lines denote the approximate diameter where growth curves cross the stasis line, indicating the size threshold beyond which colonies are expected to shrink under the given conditions.

Survival probability increased with initial size and decreased with bleaching severity, with significantly lower survival for colonies showing signs of recent partial mortality compared to non-bleached and partially bleached colonies (Figure 4.5a-b). Growth was negatively affected by bleaching severity, specifically in the major bleaching category, which was significantly

different from the non-bleaching category (Figure 4.5c). Additionally, water velocity had a significant negative effect on growth (Figure 4.5d).

Pocillopora damicornis

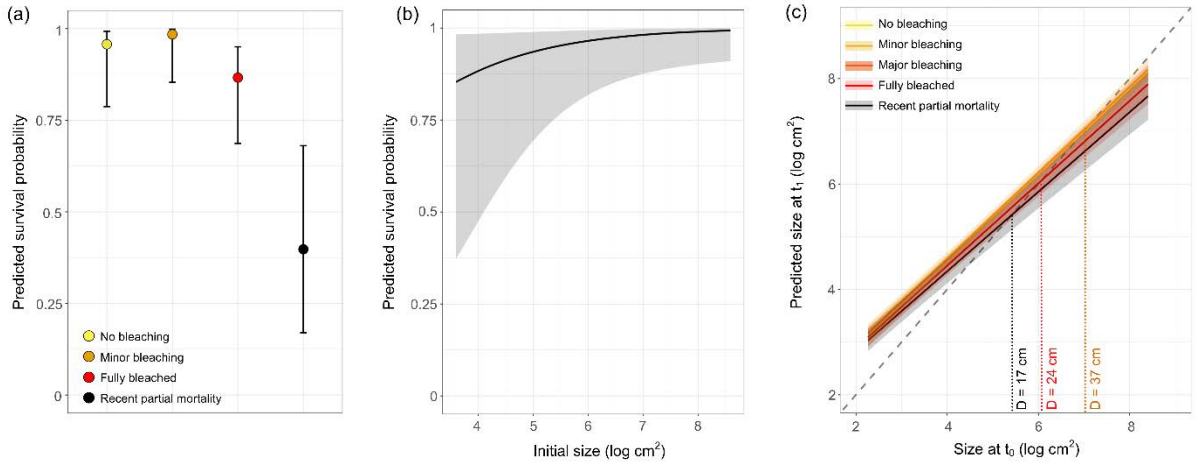


Figure 4. 6. Survival and growth model outputs for P. damicornis. (a) Predicted survival probability as a response of bleaching severity. Error bars represent 95% confidence intervals, note the absence of confidence intervals for the major bleaching category was caused by the fact that no colonies died in this category. (b) Predicted survival probability as a response of initial size, shaded ribbons represent 95% confidence intervals. (c) Predicted size at in 2023 as a function of size in 2022 and bleaching severity. Shaded ribbons correspond to 95% confidence intervals. The dashed line represents the stasis line (slope = 1). Vertical dotted lines represent the approximate diameter at which growth curves cross the stasis line, indicating the size threshold beyond which colonies are expected to shrink under the given conditions.

Survival probability increased with initial size and decreased with bleaching severity, with colonies showing signs of recent partial mortality exhibiting significantly lower survival probabilities than other categories (Figure 4.6a, b). Growth was negatively impacted by bleaching severity, particularly for colonies in the recent partial mortality category compared to the 'no bleaching' category (Figure 4.6c). Due to the limited sample size (n = 4, recent partial mortality), these results should be interpreted with caution.

Pocillopora verrucosa

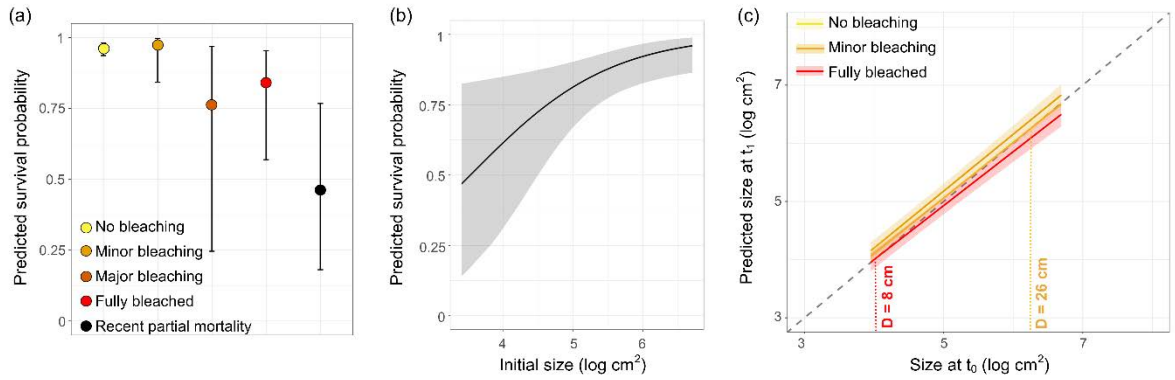


Figure 4. 7. Survival and growth model outputs for P. verrucosa. (a) Predicted survival probability as a response of bleaching severity, error bars correspond to 95% confidence intervals. (b) Predicted survival probability as a response of initial size, ribbon represents 95% confidence intervals. (c) Predicted size in 2023 as a function of size in 2022 and bleaching severity. Shaded ribbons correspond to 95% confidence intervals. The dashed line represents the stasis line (slope = 1). Vertical dotted lines represent the approximate diameter at which growth curves cross the stasis line, indicating the size threshold beyond which colonies are expected to shrink under the given conditions.

Survival probability increased with initial size and decreased with bleaching severity, especially colonies with signs of recent partial mortality (Figure 4.7a, b). Growth was negatively affected by bleaching severity, but this was significant only for the recent partial mortality category which had a very low sample size (two colonies out of 207) (Figure 4.7c). Although mean temperature was retained in the best-fit model, its effect was small and statistically inconsistent across bleaching categories (significant negative effect only for the recent partial mortality category), likely reflecting the narrow temperature range in the study (mean = 27.4 C, sd = 0.09). As a result, we visualised the more interpretable relationship between colony size and bleaching severity, with predictions shown at mean temperature (Figure 4.7c).

Seriatopora hystrix

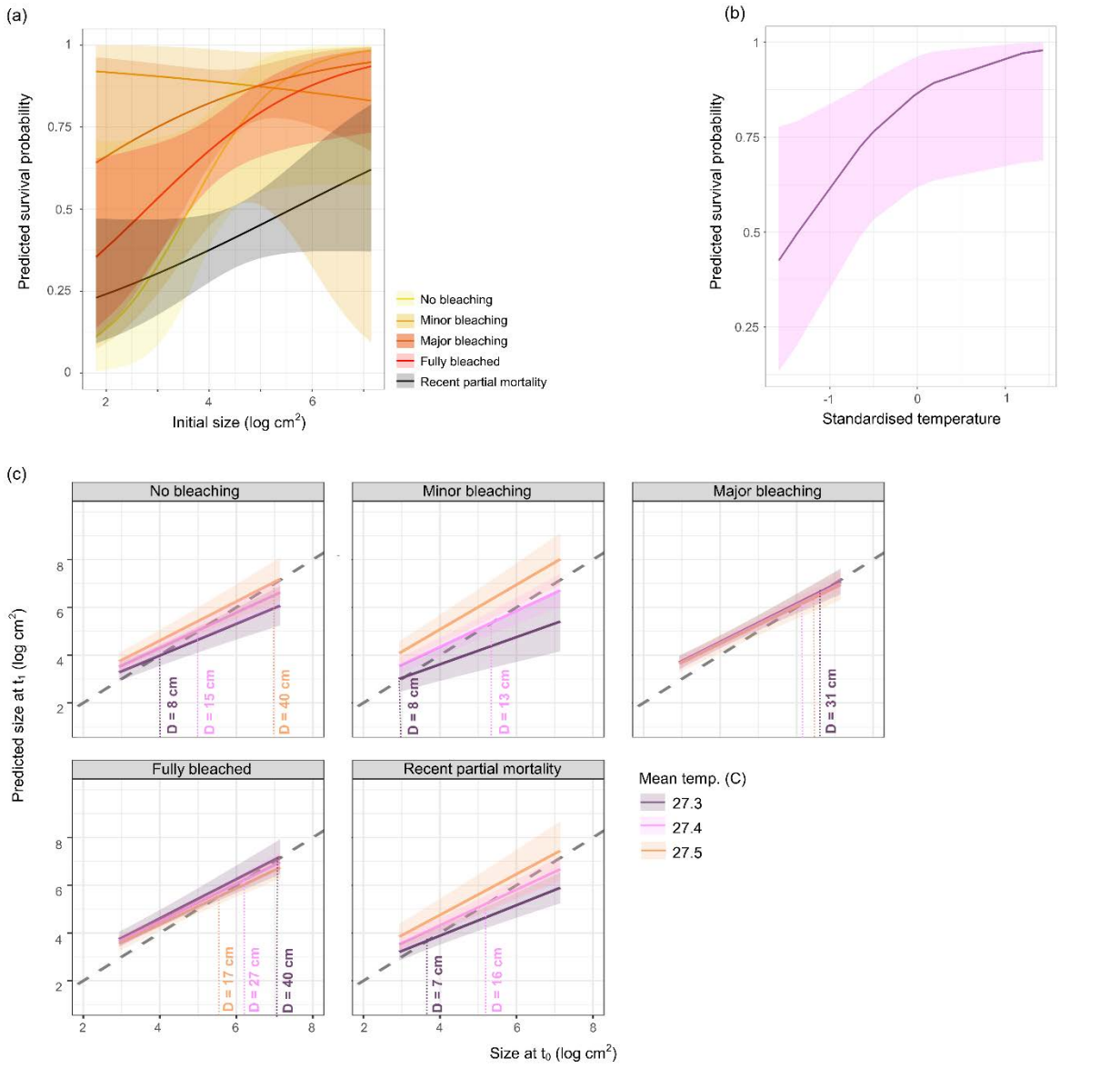


Figure 4. 8. Survival and growth model outputs for *S. hystrix*. (a) Predicted survival probability as a response of bleaching severity and initial size. (b) Predicted survival probability as a response of mean annual temperature (standardised). (c) Predicted size in 2023 as a function of size in 2022 and mean water temperature across levels of bleaching severity (facet labels). Shaded ribbons represent 95% confidence intervals. The dashed line represents the stasis line (slope = 1). Vertical dotted lines denote the approximate diameter where growth curves intersect the stasis line, indicating the size threshold beyond which colonies are expected to shrink under the given conditions.

Survival probability increased with initial size and mean temperature and decreased with bleaching severity (Figure 4.8a, b). While bleaching severity did not independently modify the size at t_1 – size at t_0 relationship, colony growth was more sensitive to small temperature differences among fully bleached colonies, with higher temperatures associated with steeper growth declines (Figure 4.8c).

Table 4. 3. Summary table of the significant effects of tested predictors on survival probability and growth of five morphotaxa

		***Acropora* staghorn**	***Acropora* corymbose**	***Pocillopora damicornis***	***Pocillopora verrucosa***	***Seriatopora hystrix***
Survival	Initial size	+	+	+	+	+
	Bleaching severity	-	-	-	-	-
	Velocity					
	Clarity					
	Temperature	-				+
Growth	Bleaching severity	-	-	-	-	
	Velocity		-		+-	
	Clarity					
	Temperature	+-				+-

4.5 Discussion

Understanding the nuanced differences in lethal and sublethal effects of bleaching on survival and growth rates of corals due to differences in taxonomic identity, colony size and across environmental gradients is key to understand recovery trajectories in a world where bleaching events are becoming more frequent. Overall, our results suggest that initial size and bleaching severity were driving survival and growth responses during the year following a mild mass bleaching event. Heat stress had a negative impact on survival probability and growth of healthy colonies even though those colonies did not show visible signs of bleaching. Severely bleached colonies (i.e., 'fully bleached' and 'recent partial mortality' categories) had significant declines in survival probability and growth compared to non-bleached and partially bleached colonies.

We found that heat stress was impacting visually healthy colonies (i.e., not bleached), with a general trend for survival and growth to be lower in the year of bleaching compared to the year before, where no known major disturbances were recorded. Although differences in survival

were not statistically significant (except for *S. hystrix*), this lack of significance supports the conclusion that we successfully captured the peak of bleaching. If colonies of the five taxa tested had bleached after our surveys, we would have expected a significant reduction in survival. There were significant differences in growth rates – represented by the slopes of the log-size at t_0 – log-size at t_1 relationship – for all taxa examined except *P. damicornis*. Thus, even though healthy colonies did not experience significantly higher mortality after bleaching, their growth was noticeably slowed. The exception to this was for *A.* staghorn colonies whose growth rates were significantly higher after bleaching across the entire size range of colonies and thus, growth rates were predicted to cross the stasis line at larger sizes. For this taxon, the modelled difference in colony diameter when crossing the stasis line was on average 28 cm larger under heat stress. Branching *Acropora* corals are known for their rapid growth (Pratchett et al., 2015) and high fecundity rates (Hall & Hughes, 1996), often driving short-term recovery after disturbances (Morais et al., 2021; Pratchett et al., 2020). Previous studies have also showed that branching *Acropora* had higher growth rates in warmer temperature regimes (temporally, Aston et al., under review; or spatially, Anderson et al., 2017). The second part of our analyses is also in favour of this pattern (i.e., higher growth rates at higher temperatures) except when colonies were in the 'recent partial mortality category' (Figure 4.4c).

Across all taxa, our study found that survival probability increased with colony size and decreased with bleaching severity. Specifically, there was a significant difference in survival probability between colonies experiencing minor bleaching (non-bleached and partially bleached corals) compared to the ones with severe bleaching including signs of recent partial mortality. For some taxa, an interaction between colony size and bleaching severity influenced survival, but the overall trend remained consistent: survival increased with size across all bleaching severity levels. The key difference was that more severely bleached colonies needed to be larger than less severely bleached ones to achieve the same survival probability. These

findings align with previous studies on coral survival, showing that survival generally increases with colony size in years with no or low heat stress (Aston et al., under review, Speare et al., 2022). Some studies also report that bleaching severity decreases with colony size (Álvarez-Noriega et al., 2025), potentially due to mechanisms such as increased tolerance from prior exposure to thermal stress (Guest et al., 2012; Maynard et al., 2008; Penin et al., 2013), greater energetic reserves that can be redistributed within the colony (Oren et al., 2001), or self-shading in branching corals, which may reduce overall bleaching severity (Kaniewska et al., 2011; Lewis et al., 2022). However, other studies have found contrasting patterns. Some research suggests that juveniles may be less susceptible to bleaching than adults (Álvarez-Noriega et al., 2018; Burn et al., 2023), and that bleaching severity increased with size (Speare et al., 2022; Winslow et al., 2024), others report high survival and bleaching tolerance of juvenile corals found in shaded understory habitats (Hoogenboom et al., 2017), supporting a 'seed-bank' hypothesis for rapid recovery following disturbance (Doropoulos et al., 2022). In cases where bleaching severity increases with colony size, this could be explained by a reduced efficiency of mass transfer of toxic by-products in larger colonies (Nakamura & van Woesik, 2001). Another possible explanation is differences in size structure among cryptic species—if larger colonies belong to a more bleaching-susceptible haplotype while smaller colonies belong to a more resistant haplotype, the observed link between size and bleaching severity could be an artifact of genetic differences rather than colony size itself (Burgess et al., 2021). These conflicting findings highlight the complexity of size-dependent bleaching responses and emphasise the need for further research to disentangle the effects of colony size, genetic variation, and environmental conditions on coral survival under thermal stress.

As supported by previous studies on growth (Dornelas et al., 2017; Aston et al., under review), planar growth rates increased with colony size up to a point where net growth ceased. Across all taxa, a general trend was observed where bleaching severity influenced the size at which

colonies, on average, ceased growing. Our results show that more severely bleached colonies exhibited the lowest maximum sizes (i.e., the model crossing point with the stasis line, where initial size and final size are equal). While these findings are not unexpected, the significantly slowed growth of more severely bleached coral has critical implications, especially as mild mass bleaching events become increasingly common. First, slowed growth affects population size structure and fecundity, ultimately impacting recovery. Smaller colonies and fewer large, highly fecund individuals – those that disproportionally contribute to population reproductive output – mean longer recovery times after disturbances because total reproductive output of the population is decreased. Second, a reduction in the abundance of medium and large colonies may impact reef carbonate budgets. This can result in net deficit in carbonate production and calcification, reducing reef accretion over time. Third, coral growth, especially fast-growing branching colonies, can be tied to habitat complexity and thus decrease in growth may result in decrease in habitat complexity (but see Ferrari et al., 2016) with cascading effects on reef associated organisms (Graham et al., 2007). Consequently, even mild mass bleaching events, which are expected to occur more frequently in the coming decades, may not be followed by mass mortality but can still compromise key functional reef ecosystem characteristics such as accretion, size structure and habitat complexity. Finally, our results also highlight an important aspect of partial mortality: even for fast-growing taxa like *Acropora* staghorn, partial mortality was so severe that it resulted in net negative growth despite nine months of subsequent growth following bleaching.

The environmental variables tested had only marginal effects on growth and survival across taxa. These findings suggest that while environmental conditions likely influence bleaching susceptibility, they do not necessarily drive post-bleaching demographic outcomes – at least not as captured by the broad-scale environmental variables used here. Instead, initial size and bleaching severity emerged as the most consistent and influential predictors of both growth and

survival in the year following the bleaching event. It is possible that the limited explanatory power of environmental variables reflects data limitations rather than an absence of ecological effects. The environmental metrics used in this study were modelled annual estimates instead of high-resolution, in situ measurements. As such, they may not reflect the fine-scale, temporally-explicit conditions that colonies experienced during the peak of thermal stress, particularly during short-term extremes. Additionally, the temperature range among sites was narrow (mean = 27.4C, sd = 0.09), which may have masked potential thermal effects; future work could explore the utility of metrics such as maximum temperature or cumulative heat exposure to better capture ecologically meaningful thresholds. Another possible limitation is observer bias in the visual classification of bleaching severity. While care was taken to apply consistent criteria when scoring colonies, some level of subjectivity is inherent in such assessments, especially when distinguishing among intermediate bleaching categories. Nonetheless, the strong and consistent influence of colony size and bleaching severity across models suggests that these factors are robust predictors of colony fate in the immediate aftermath of bleaching.

Using photogrammetry, we were able to capture a consistent snapshot of the thermal stress event across all sites and track individual coral colonies over time. By recording the state and size of colonies several months before the bleaching event, we were able to confidently attribute signs of mortality to the thermal stress event. This approach is particularly valuable for fast-growing branching taxa, which typically have fast regenerative abilities, making it challenging to quantify the prevalence of recent partial mortality accurately. Our method allowed us to quantify actual bleaching response rather than observed capacity of regeneration. Manual tracing of corals remains time-consuming and susceptible to observer bias, despite using assisted segmentation techniques aimed at minimising manual input. Future work could leverage automated segmentation and classification methods that use pixel colour to score

objectively and efficiently bleaching severity, thereby reducing observer bias and increasing throughput. We continue to track the state and size of these colonies to determine whether growth rates return to pre-bleaching levels and how recovery periods may vary based on bleaching severity.

Chapter 5. General Discussion

Ecologists have long sought to understand how ecosystems respond to and recover from disturbances, especially as the effects of climate change increasingly alter ecosystem structure and function and affect the services on which humanity depends (Grimm et al., 2013; Mooney et al., 2009). Assessing these impacts at relevant spatial and temporal scales remains a major challenge due to the complexity of ecological interactions and the cumulative effects of multiple interacting stressors. For marine ecosystems, these difficulties are compounded by a scarcity of empirical data. Coral reefs - among the most vulnerable ecosystems – face increasingly frequent and severe disturbances that threaten both their persistence and the functions they support (Ceccarelli et al., 2024; Gudka et al., 2024; Hoegh-Guldberg et al., 2018; Tebbett et al., 2025).

Coral colony size influences key demographic processes – such as reproduction, fitness and survival - and underpins critical ecosystem functions including carbonate production and habitat provisioning (Bak & Meesters, 1998; Barneche et al., 2017; Ferrari et al., 2012; Iida et al., 2014; Lange et al., 2024; Lindenmayer & Laurance, 2017). However, traditional methods such as one-dimensional maximum diameter measurements often underestimate the size of large (~ 1m or more) or irregularly shaped colonies (Chandler et al., 2024), limiting our understanding of how size shapes ecological outcomes.

While research has focused on the exposure and impacts of disturbances (e.g., Bruno & Selig, 2007; Graham et al., 2008; Hughes et al., 2017), far less is known about how reefs recover, especially beyond increases in live coral cover (e.g., McWilliam et al., 2020; Ortiz et al., 2018) or at scales larger than individual reefs (e.g., Baker et al., 2008; Connell, 1997; Osborne et al., 2017). Empirical data - rather than experimental or modelled estimates - on the recovery trajectories of specific coral taxa remain particularly limited. This thesis contributes to filling these gaps by precisely quantifying *in situ* coral colony size across dominant taxa and environmental gradients and by tracking individual colony fates before and after heat stress events. In doing so, it offers new insights into how size structure contributes to reef resilience, how sublethal disturbances leave lasting demographic impacts and how coral morphology shapes environmental sensitivity and functional contributions.

Chapter 2 revealed that coral size distributions are skewed toward smaller colonies across most reef environments, consistent with previous work (Dietzel et al., 2020; Pisapia et al., 2019). However, the consistent presence of large colonies in inshore and low-exposure habitats highlights the importance of environmental filtering in shaping potential sources of recovery and fecundity. These spatial patterns help identify habitats critical for larval dispersal, calcium carbonate production and habitat complexity provision and support their prioritisation in resilience-based management strategies.

Resilience is not only about the ability to withstand or recover from a disturbance but also about how previous disturbances shape current and future responses. These legacy effects are central to ecological memory – the influence of historical events on present-day system dynamics (Franklin et al., 2000; Johnstone et al., 2016; Monger et al., 2015; Seidl et al., 2014; Walker et al., 2024). **Chapter 4** demonstrated that initial colony size and bleaching severity interact to shape individual-level responses to thermal stress. Severely bleached colonies showed reduced growth and higher mortality, even among fast-growing taxa such as branching *Acropora* and those often considered more resilient such as *Pocillopora*. Even colonies that appear visually unaffected may incur latent demographic costs. Over time, the accumulation of such effects – especially as disturbance frequency shortens – can erode recovery potential and reduce the long-term viability of coral populations.

This thesis also highlights how morphological traits mediate coral-environment interactions. **Chapter 2** showed that taxa with top-heavy morphologies exhibited greater variation in size across environmental gradients compared to compact forms. Top-heavy colonies are typically associated with fast-growing taxa that contribute substantially to three-dimensional habitat complexity, which supports high levels of reef-associated biodiversity (Darling et al., 2017; Wedding et al., 2019). Their loss in exposed or disturbed habitats likely signals not only a demographic bottleneck but also a reduction in ecological function.

Implications and future research

This thesis underscores the importance of size-based coral demographic rates for understanding coral reef trajectories – whether towards recovery or decline – and for linking individual-level processes to ecosystem-scale functioning. The finding that heat stress reduces growth and survival even during mild events suggests that legacy effects may compromise carbonate budgets even in the absence of mass mortality. Over time, this could lead to net erosion states,

flattening reef frameworks, and reducing the reef's capacity to provide ecological services (Lange et al., 2023; Lange & Perry, 2019). Integrating such demographic insights into reef carbonate budget models would provide a more mechanistic understanding of how climate stressors impair not only population recovery but also the maintenance of reef structure itself. These results therefore have direct conservation relevance. If the goal is to support natural recovery, protecting habitats that retain large, fecund, and structurally important colonies – typically in low-exposure environments – may yield the greatest long-term benefits. If the goal is to buffer against future bleaching, then prioritising areas with historically low bleaching severity or investing in the translocation of tolerant genotypes may be more effective. In either case, size data provide a bridge between ecological processes and management strategies.

These demographic rates can inform population models, improving our understanding of the factors influencing population maintenance and recovery on reefs (Cant et al., 2022; Edmunds & Riegl, 2020; Hughes et al., 2023), as well as more accurate projections of reef futures (Edmunds et al., 2014). For example, growth and survival estimates obtained from these methods can support integral project models (IPMs), where size-based fecundity, growth and survival contribute to more accurate population projections. IPMs are data intensive, and most robust when based on large sample sizes spanning the full size or age spectrum of an organism (Merow et al., 2014). Historically, collecting detailed coral size data has been challenging due to the time and cost involved, leading long-term monitoring programs to sample only a limited portion of the reef, and potentially underestimating within-reef variability (Cresswell et al., 2024). The methods presented here enable surveys across a broader size spectrum, capturing a more comprehensive range than traditional approaches. Although extreme size classes are still underrepresented, combining these methods with juvenile surveys – and potentially targeted surveys for very large colonies, such as massive *Porites* bommies – can significantly enhance our understanding of coral demography. By providing reliable colony size estimates across multiple transitions and demonstrating the feasibility of long-term tracking, this thesis sets a new standard for demographic data collection in coral monitoring programs.

The recent mass bleaching event in early 2024, with recovery times of a year or less, raises urgent questions about the resilience of coral populations. Continued collection of individual-level data would significantly enhance our understanding of the impacts of successive heat stress events on coral fitness and the viability of coral populations in the Anthropocene. As mentioned earlier, one limitation of the method is the difficulty in locating and identifying

colonies smaller than 5 cm in diameter. Future studies could address this gap by incorporating in-situ data on juveniles to construct complete size frequency distributions or compare juvenile and adult mortality regimes. This would be crucial for understanding recruitment dynamics and the contribution of juvenile corals to population recovery (Doropoulos et al., 2015; Gouezo et al., 2019). Moreover, information on juvenile abundances and survival rates would provide explicit information about why population structures and recovery differ between habitats and through time (Speare et al., 2025).

As image-based surveys become increasingly popular, there is a growing need for more efficient automated image analysis workflows. Tools such as TagLab (Pavoni et al., 2022) used in this thesis, have reduced the time required for size data extraction, but manual colony digitisation remains a major bottleneck. Collaborating with machine learning experts could help address this challenge by developing workflows that automate tasks such as seafloor segmentation (see for example Remmers et al., 2025) and minimise user input. For instance, a pipeline that processes 3D models and digitises coral colonies with minimal manual effort would save time, reduce the need for expertise in 3D processing or segmentation, and minimise user error when identifying or digitising corals – or make such errors easier to quantify (Remmers et al., 2025). Due to the current bottleneck, corals of target species are often prioritised for digitisation while the rest of the seafloor remains unsegmented. Automating seafloor segmentation would enable the extraction of additional important variables, such as coral densities and competitive interactions, which are critical drivers of recovery (Bruno et al., 2003; Gouezo et al., 2019; Speare et al., 2025; Tebbett et al., 2025). By pairing photogrammetry with Artificial Intelligence tools, these advancements could make standardised monitoring workflows more accessible, ensuring accurate and consistent data collection while supporting the optimisation of restoration interventions for long-term reef management.

Finally, this dataset has broader applications beyond demographic studies. It can contribute to investigations into changes in the morphological composition of coral communities or ecological processes and functions influenced by colony size, such as the provision of habitat structural complexity (Chandler et al., 2024; Zawada, Dornelas, et al., 2019). It can also contribute to guiding restoration efforts. Logistical and cost constraints limit the areas that can be targeted with interventions (median restoration area size = 100 m^2, Boström-Einarsson et al., 2020), hence there is a need to prioritise areas that would generate the highest reef-wide

benefits. If the goal is to protect mature colonies and enhance larval dispersal, then these results suggest that we should prioritise low exposure environments. If the goal is to boost recovery after bleaching, then these results suggest we should prioritise areas where colonies bleached the least or transplant corals where bleaching has been the most severe. These insights underscore the wide-ranging relevance of this research for understanding and managing coral reef ecosystems.

Conclusion

Coral reefs are experiencing intensifying climate stress, and their future hinges on understanding how individual-level processes scale up to affect population persistence and ecosystem functioning. This thesis contributes to that understanding by demonstrating how colony size shape demographic responses across environmental gradients and disturbance regimes.

Through tracking coral growth and survival, I show that legacy effects of bleaching are mediated by initial size, bleaching severity and environmental conditions with potential impact on population resilience and critical ecosystem functions such as habitat provision and carbonate accretion. Moreover, variation in morphological traits among taxa mediates their demographic responses, with top-heavy colonies more sensitive to wave exposure, yet also central to reef structure and biodiversity.

Beyond methodological advancements, this work provides a framework for integrating coral demography into resilience-based management and restoration strategies. By identifying where functionally important colonies persist – and where they are most vulnerable – it enables more targeted interventions to sustain reef functions in era of compounding stress. In doing so, this thesis helps bridge the gap between fine-scale ecological monitoring and broader efforts to model, manage and ultimately sustain coral reef ecosystems under climate change. It offers both empirical tools and conceptual insights to inform a more resilient future for coral reefs.

References

Abadie, A., Boissery, P., & Christophe, V. (2018). Georeferenced underwater photogrammetry to map marine habitats and submerged artificial structures. *The Photogrammetric Record*, *33*, 448–469. https://doi.org/10.1111/phor.12263

Abrego, D., Howells, E. J., Smith, S. D. A., Madin, J. S., Sommer, B., Schmidt-Roach, S., Cumbo, V. R., Thomson, D. P., Rosser, N. L., & Baird, A. H. (2021). Factors Limiting the Range Extension of Corals into High-Latitude Reef Regions. *Diversity*, *13*(12), Article 12. https://doi.org/10.3390/d13120632

Adjeroud, M., Mauguit, Q., & Penin, L. (2015). The size-structure of corals with contrasting life-histories: A multi-scale analysis across environmental conditions. *Marine Environmental Research*, *112*, 131–139. https://doi.org/10.1016/j.marenvres.2015.10.004

Adjeroud, M., Pratchett, M. S., Kospartov, M. C., Lejeusne, C., & Penin, L. (2007). Small-scale variability in the size structure of scleractinian corals around Moorea, French Polynesia: Patterns across depths and locations. *Hydrobiologia*, *589*(1), 117–126. https://doi.org/10.1007/s10750-007-0726-2

Agisoft LLC. (2023). *Agisoft Metashape Professional* (Version 1.7.4). https://www.agisoft.com/downloads/installer/

Álvarez-Filip, L., Dulvy, N. K., Gill, J. A., Côté, I. M., & Watkinson, A. R. (2009). Flattening of Caribbean coral reefs: Region-wide declines in architectural complexity. *Proceedings of the Royal Society B: Biological Sciences*, *276*(1669), 3019–3025. https://doi.org/10.1098/rspb.2009.0339

Álvarez-Noriega, M., Aston, E. A., Becker, M., Fabricius, K. E., Figueira, W. F., Gordon, S. E., Krensel, R., Lechene, M. A., Remmers, T., Toor, M., & Ferrari, R. (2025). Challenging Paradigms Around the Role of Colony Size, Taxa, and Environment on Bleaching Susceptibility. *Global Change Biology*, *31*(2), e70090. https://doi.org/10.1111/gcb.70090

Álvarez-Noriega, M., Baird, A. H., Bridge, T. C., Dornelas, M., Fontoura, L., Pizarro, O., Precoda, K., Torres-Pulliza, D., Woods, R. M., & Zawada, K. (2018). Contrasting patterns of changes in abundance following a bleaching event between juvenile and adult scleractinian corals. *Coral Reefs*, *37*, 527–532.

Anderson, K. D., Cantin, N. E., Heron, S. F., Pisapia, C., & Pratchett, M. S. (2017). Variation in growth rates of branching corals along Australia's Great Barrier Reef. *Scientific Reports*, *7*(1), 2920. https://doi.org/10.1038/s41598-017-03085-1

Anderson, K., & Pratchett, M. (2014). Variation in size-frequency distributions of branching corals between a tropical versus sub-tropical reef. *Marine Ecology Progress Series*, *502*, 117–128. https://doi.org/10.3354/meps10697

Anthony, K. R. N. (2006). Enhanced energy status of corals on coastal, high-turbidity reefs. *Marine Ecology Progress Series*, *319*, 111–116. https://doi.org/10.3354/meps319111

Anthony, K. R. N., & Fabricius, K. E. (2000). Shifting roles of heterotrophy and autotrophy in coral energetics under varying turbidity. *Journal of Experimental Marine Biology and Ecology*, *252*(2), 221–253. https://doi.org/10.1016/S0022-0981(00)00237-9

Anthony, K. R. N., Helmstedt, K. J., Bay, L. K., Fidelman, P., Hussey, K. E., Lundgren, P., Mead, D., McLeod, I. M., Mumby, P. J., Newlands, M., Schaffelke, B., Wilson, K. A., & Hardisty, P. E. (2020). Interventions to help coral reefs under global change—A complex decision challenge. *PLOS ONE*, *15*(8), e0236399. https://doi.org/10.1371/journal.pone.0236399

Anthony, K. R. N., Ridd, P. V., Orpin, A. R., Larcombe, P., & Lough, J. (2004). Temporal variation of light availability in coastal benthic habitats: Effects of clouds, turbidity, and tides. *Limnology and Oceanography*, *49*(6), 2201–2211. https://doi.org/10.4319/lo.2004.49.6.2201

Aston, E. A., Duce, S., Hoey, A. S., & Ferrari, R. (2022). A Protocol for Extracting Structural Metrics From 3D Reconstructions of Corals. *Frontiers in Marine Science*, *9*. https://www.frontiersin.org/articles/10.3389/fmars.2022.854395

Babcock, R. C. (1991). Comparative Demography of Three Species of Scleractinian Corals Using Age- and Size-Dependent Classifications. *Ecological Monographs*, *61*(3), 225–244. https://doi.org/10.2307/2937107

Babcock, R., & Smith, L. (2000). Effects of sedimentation on coral settlement and survivorship. *Proceedings of the Ninth International Coral Reef Symposium, Bali, 23-27 October 2000*, *1*, 245–248.

Baird, A. H., Madin, J. S., Álvarez-Noriega, M., Fontoura, L., Kerry, J. T., Kuo, C.-Y., Precoda, K., Torres-Pulliza, D., Woods, R. M., Zawada, K. J. A., & Hughes, T. P. (2018). A decline in bleaching suggests that depth can provide a refuge from global warming in most coral taxa. *Marine Ecology Progress Series*, *603*, 257–264. https://doi.org/10.3354/meps12732

Bak, R., & Meesters, E. (1998). Coral population structure:the hidden information of colony size-frequency distributions. *Marine Ecology Progress Series*, *162*, 301–306. https://doi.org/10.3354/meps162301

Bak, R. P. M., & Meesters, E. H. (1999). Population Structure as a Response of Coral Communities to Global Change. *American Zoologist*, *39*(1), 56–65. https://doi.org/10.1093/icb/39.1.56

Baker, A. C., Glynn, P. W., & Riegl, B. (2008). Climate change and coral reef bleaching: An ecological assessment of long-term impacts, recovery trends and future outlook. *Estuarine, Coastal and Shelf Science*, *80*(4), 435–471. https://doi.org/10.1016/j.ecss.2008.09.003

Baltsavias, E. P., Favey, E., Bauder, A., Bosch, H., & Pateraki, M. (2001). Digital Surface Modelling by Airborne Laser Scanning and Digital Photogrammetry for Glacier Monitoring. *The Photogrammetric Record*, *17*(98), 243–273. https://doi.org/10.1111/0031-868X.00182

Barker, R., Dixon, L., & Hooke, J. (1997). Use of terrestrial photogrammetry for monitoring and measuring bank erosion. *Earth Surface Processes and Landforms*, *22*(13), 1217–1227. https://doi.org/10.1002/(SICI)1096-9837(199724)22:13<1217::AID-ESP819>3.0.CO;2-U

Barneche, D. R., White, C. R., & Marshall, D. J. (2017). Temperature effects on mass-scaling exponents in colonial animals: A manipulative test. *Ecology*, *98*(1), 103–111. https://doi.org/10.1002/ecy.1624

Bauman, A. G., Pratchett, M. S., Baird, A. H., Riegl, B., Heron, S. F., & Feary, D. A. (2013). Variation in the size structure of corals is related to environmental extremes in the Persian Gulf. *Marine Environmental Research*, *84*, 43–50. https://doi.org/10.1016/j.marenvres.2012.11.007

Bayraktarov, E., Pizarro, V., Eidens, C., Wilke, T., & Wild, C. (2013). Bleaching Susceptibility and Recovery of Colombian Caribbean Corals in Response to Water Current Exposure and Seasonal Upwelling. *PLOS ONE*, *8*(11), e80536. https://doi.org/10.1371/journal.pone.0080536

Bellwood, D. R., Hughes, T. P., Folke, C., & Nyström, M. (2004). Confronting the coral reef crisis. *Nature*, *429*(6994), 827–833. https://doi.org/10.1038/nature02691

Bellwood, D. R., Pratchett, M. S., Morrison, T. H., Gurney, G. G., Hughes, T. P., Álvarez-Romero, J. G., Day, J. C., Grantham, R., Grech, A., Hoey, A. S., Jones, G. P., Pandolfi, J. M., Tebbett, S. B., Techera, E., Weeks, R., & Cumming, G. S. (2019). Coral reef conservation in the Anthropocene: Confronting spatial mismatches and prioritizing functions. *Biological Conservation*, *236*, 604–615. https://doi.org/10.1016/j.biocon.2019.05.056

Bergmann, C. (1848). *Über die Verhältnisse der Wärmeökonomie der Thiere zu ihrer Größe*. Vandenhoeck und Ruprecht.

Birrell, C. L., McCook, L. J., & Willis, B. L. (2005). Effects of algal turfs and sediment on coral settlement. *Marine Pollution Bulletin*, *51*(1), 408–414. https://doi.org/10.1016/j.marpolbul.2004.10.022

Boström-Einarsson, L., Babcock, R. C., Bayraktarov, E., Ceccarelli, D., Cook, N., Ferse, S. C. A., Hancock, B., Harrison, P., Hein, M., Shaver, E., Smith, A., Suggett, D., Stewart-Sinclair, P. J., Vardi, T., & McLeod, I. M. (2020). Coral restoration – A systematic review of current methods, successes, failures and future directions. *PLOS ONE*, *15*(1), e0226631. https://doi.org/10.1371/journal.pone.0226631

Brandt, M. E. (2009). The effect of species and colony size on the bleaching response of reef-building corals in the Florida Keys during the 2005 mass bleaching event. *Coral Reefs*, *28*(4), 911–924. https://doi.org/10.1007/s00338-009-0548-y

Brooks, M., E., Kristensen, K., Benthem, K., J. ,van, Magnusson, A., Berg, C., W., Nielsen, A., Skaug, H., J., Mächler, M., & Bolker, B., M. (2017). GlmmTMB Balances Speed and Flexibility Among Packages for Zero-inflated Generalized Linear Mixed Modeling. *The R Journal*, *9*(2), 378. https://doi.org/10.32614/RJ-2017-066

Browne, N. K., Smithers, S. G., & Perry, C. T. (2013). Spatial and temporal variations in turbidity on two inshore turbid reefs on the Great Barrier Reef, Australia. *Coral Reefs*, *32*(1), 195–210. https://doi.org/10.1007/s00338-012-0965-1

Bruno, J. F., & Selig, E. R. (2007). Regional Decline of Coral Cover in the Indo-Pacific: Timing, Extent, and Subregional Comparisons. *PLoS ONE*, *2*(8), e711. https://doi.org/10.1371/journal.pone.0000711

Bruno, J. F., Stachowicz, J. J., & Bertness, M. D. (2003). Inclusion of facilitation into ecological theory. *Trends in Ecology & Evolution*, *18*(3), 119–125. https://doi.org/10.1016/S0169-5347(02)00045-9

Bryson, M., Ferrari, R., Figueira, W., Pizarro, O., Madin, J., Williams, S., & Byrne, M. (2017). Characterization of measurement errors using structure-from-motion and photogrammetry to measure marine habitat structural complexity. *Ecology and Evolution*, *7*(15), 5669–5681. https://doi.org/10.1002/ece3.3127

Burgess, S. C., Johnston, E. C., Wyatt, A. S., Leichter, J. J., & Edmunds, P. J. (2021). Response diversity in corals: Hidden differences in bleaching mortality among cryptic Pocillopora species. *Ecology*, *102*(6), e03324.

Burke, L., Reytar, K., Spalding, M., & Perry, A. (2011). *Reefs at risk revisited*. Washington, DC: World Resources Institute (WRI). https://bvearmb.do/handle/123456789/1787

Burn, D., Hoey, A. S., Matthews, S., Harrison, H. B., & Pratchett, M. S. (2023). Differential bleaching susceptibility among coral taxa and colony sizes, relative to bleaching severity across Australia's Great Barrier Reef and Coral Sea Marine Parks. *Marine Pollution Bulletin*, *191*, 114907.

Burns, J., Delparte, D., Gates, R., & Takabayashi, M. (2015). Integrating structure-from-motion photogrammetry with geospatial software as a novel technique for quantifying 3D ecological characteristics of coral reefs. *PeerJ*, *3*, e1077. https://doi.org/10.7717/peerj.1077

Burns, J. H. R., Delparte, D., Kapono, L., Belt, M., Gates, R. D., & Takabayashi, M. (2016). Assessing the impact of acute disturbances on the structure and composition of a coral community using innovative 3D reconstruction techniques. *Methods in Oceanography*, *15–16*, 49–59. https://doi.org/10.1016/j.mio.2016.04.001

Byrne, M., Waller, A., Clements, M., Kelly, A. S., Kingsford, M. J., Liu, B., Reymond, C. E., Vila-Concejo, A., Webb, M., Whitton, K., & Foo, S. A. (2025). Catastrophic bleaching in protected reefs of the Southern Great Barrier Reef. *Limnology and Oceanography Letters*, *n/a*(n/a). https://doi.org/10.1002/lol2.10456

Bythell, J. C., Pan, P., & Lee, J. (2001). Three-dimensional morphometric measurements of reef corals using underwater photogrammetry techniques. *Coral Reefs*, *20*(3), 193–199. https://doi.org/10.1007/s003380100157

Callaghan, D. (2023). *Great Barrier Reef non-cyclonic and on-reef wave model predictions*.

Callaghan, D. P., Leon, J. X., & Saunders, M. I. (2015). Wave modelling as a proxy for seagrass ecological modelling: Comparing fetch and process-based predictions for a bay and reef lagoon. *Estuarine, Coastal and Shelf Science*, *153*, 108–120.

Cant, J., Cook, K. M., Reimer, J. D., Mezaki, T., Nakamura, M., O'Flaherty, C., Salguero-Gómez, R., & Beger, M. (2022). Transient amplification enhances the persistence of tropicalising coral assemblages in marginal high-latitude environments. *Ecography*, *2022*(10), e06156. https://doi.org/10.1111/ecog.06156

Cantin, N. E., Cohen, A. L., Karnauskas, K. B., Tarrant, A. M., & McCorkle, D. C. (2010). Ocean Warming Slows Coral Growth in the Central Red Sea. *Science*, *329*(5989), 322–325. https://doi.org/10.1126/science.1190182

Cantin, N. E., & Lough, J. M. (2014). Surviving Coral Bleaching Events: Porites Growth Anomalies on the Great Barrier Reef. *PLoS ONE*, *9*(2), e88720. https://doi.org/10.1371/journal.pone.0088720

Cardoso, P., Borges, P. A. V., Triantis, K. A., Ferrández, M. A., & Martín, J. L. (2012). The underrepresentation and misrepresentation of invertebrates in the IUCN Red List. *Biological Conservation*, *149*(1), 147–148. https://doi.org/10.1016/j.biocon.2012.02.011

Carlot, J., Rovère, A., Casella, E., Harris, D., Grellet-Muñoz, C., Chancerelle, Y., Dormy, E., Hedouin, L., & Parravicini, V. (2020). Community composition predicts photogrammetry-based structural complexity on coral reefs. *Coral Reefs*, *39*(4), 967–975. https://doi.org/10.1007/s00338-020-01916-8

Carrivick, J. L., & Smith, M. W. (2019). Fluvial and aquatic applications of Structure from Motion photogrammetry and unmanned aerial vehicle/drone technology. *WIREs Water*, *6*(1), e1328. https://doi.org/10.1002/wat2.1328

Ceccarelli, D. M., Logan, M., Evans, R. D., Jones, G. P., Puotinen, M., Petus, C., Russ, G. R., Sinclair-Taylor, T., Srinivasan, M., & Williamson, D. H. (2024). Regional-scale disturbances drive long-term decline of inshore coral reef fish assemblages in the Great Barrier Reef Marine Park. *Global Change Biology*, *30*(10), e17506. https://doi.org/10.1111/gcb.17506

Chandler, J. F., Figueira, W. F., Burn, D., Doll, P. C., Johandes, A., Piccaluga, A., & Pratchett, M. S. (2024). Predicting 3D and 2D surface area of corals from simple field measurements. *Scientific Reports*, *14*(1), 20549. https://doi.org/10.1038/s41598-024-71580-3

Chase, T. J., Pratchett, M. S., Walker, S. P. W., & Hoogenboom, M. O. (2014). Small-scale environmental variation influences whether coral-dwelling fish promote or impede coral growth. *Oecologia*, *176*(4), 1009–1022. https://doi.org/10.1007/s00442-014-3065-9

Cheung, P.-Y., Nozawa, Y., & Miki, T. (2021). Ecosystem engineering structures facilitate ecological resilience: A coral reef model. *Ecological Research*, *36*(4), 673–685. https://doi.org/10.1111/1440-1703.12230

Chong, F., Sommer, B., Stant, G., Verano, N., Cant, J., Lachs, L., Johnson, M. L., Parsons, D. R., Pandolfi, J. M., Salguero-Gómez, R., Spencer, M., & Beger, M. (2023). High-latitude marginal reefs support fewer but bigger corals than their tropical counterparts. *Ecography*, *2023*(12), e06835. https://doi.org/10.1111/ecog.06835

Chong-Seng, K. M., Graham, N. A. J., & Pratchett, M. S. (2014). Bottlenecks to coral recovery in the Seychelles. *Coral Reefs*, *33*(2), 449–461. https://doi.org/10.1007/s00338-014-1137-2

Cinner, J. (2014). Coral reef livelihoods. *Current Opinion in Environmental Sustainability*, *7*, 65–71. https://doi.org/10.1016/j.cosust.2013.11.025

Collins, S. H., & Moon, G. C. (1979). Stereometric Measurement of Streambank Erosion. *Photogrammetric Engineering and Remote Sensing*, *45*(2), 183–190.

Connell, J. H. (1973). Population ecology of reef-building corals. In *Biology and Geology of Coral Reefs* (pp. 205–245). Elsevier. https://doi.org/10.1016/B978-0-12-395526-5.50015-8

Connell, J. H. (1997). Disturbance and recovery of coral assemblages. *Coral Reefs*, *16*(0), S101–S113. https://doi.org/10.1007/s003380050246

Connell, J. H., Hughes, T. P., & Wallace, C. C. (1997). A 30-Year Study of Coral Abundance, Recruitment, and Disturbance at Several Scales in Space and Time. *Ecological Monographs*, *67*(4), 461–488. https://doi.org/10.1890/0012-9615(1997)067[0461:AYSOCA]2.0.CO;2

Conti, L. A., Lim, A., & Wheeler, A. J. (2019). High resolution mapping of a cold water coral mound. *Scientific Reports*, *9*(1), Article 1. https://doi.org/10.1038/s41598-018-37725-x

Cooper, T. F., De'ath, G., Fabricius, K. E., & Lough, J. M. (2008). Declining coral calcification in massive Porites in two nearshore regions of the northern Great Barrier Reef. *Global Change Biology*, *14*(3), 529–538. https://doi.org/10.1111/j.1365-2486.2007.01520.x

Couch, C. (2021). *Comparing coral demographic surveys from in situ observations and Structure-from-Motion imagery shows low methodological bias*. https://doi.org/10.25923/307K-FK90

Coulter, L., & Stow, D. (2008). Assessment of the Spatial Co-registration of Multitemporal Imagery from Large Format Digital Cameras in the Context of Detailed Change Detection. *Sensors*, *8*(4), 2161–2173. https://doi.org/10.3390/s8042161

Cresswell, A. K., Orr, M., Renton, M., Haywood, M. D. E., Ospina, A. G., Slawinski, D., Austin, R., & Thomson, D. P. (2020). Structure-from-motion reveals coral growth is influenced by colony size and wave energy on the reef slope at Ningaloo Reef, Western Australia. *Journal of Experimental Marine Biology and Ecology*, *530–531*, 151438. https://doi.org/10.1016/j.jembe.2020.151438

Darling, E. S., Alvarez-Filip, L., Oliver, T. A., McClanahan, T. R., & Côté, I. M. (2012). Evaluating life-history strategies of reef corals from species traits. *Ecology Letters*, *15*(12), 1378–1386. https://doi.org/10.1111/j.1461-0248.2012.01861.x

Darling, E. S., Graham, N. A. J., Januchowski-Hartley, F. A., Nash, K. L., Pratchett, M. S., & Wilson, S. K. (2017). Relationships between structural complexity, coral traits, and reef fish assemblages. *Coral Reefs*, *36*(2), 561–575. https://doi.org/10.1007/s00338-017-1539-z

De'ath, G., Fabricius, K. E., Sweatman, H., & Puotinen, M. (2012). The 27–year decline of coral cover on the Great Barrier Reef and its causes. *Proceedings of the National Academy of Sciences*, *109*(44), 17995–17999. https://doi.org/10.1073/pnas.1208909109

Diaz, C., Foster, N. L., Attrill, M. J., Bolton, A., Ganderton, P., Howell, K. L., Robinson, E., & Hosegood, P. (2023). Mesophotic coral bleaching associated with changes in thermocline depth. *Nature Communications*, *14*(1), 6528. https://doi.org/10.1038/s41467-023-42279-2

Dietzel, A., Bode, M., Connolly, S. R., & Hughes, T. P. (2020). Long-term shifts in the colony size structure of coral populations along the Great Barrier Reef. *Proceedings of the Royal Society B: Biological Sciences*, *287*(1936), 20201432. https://doi.org/10.1098/rspb.2020.1432

Dietzel, A., Bode, M., Connolly, S. R., & Hughes, T. P. (2021). The population sizes and global extinction risk of reef-building coral species at biogeographic scales. *Nature Ecology & Evolution*, *5*(5), 663–669. https://doi.org/10.1038/s41559-021-01393-4

Dong, Z., Liang, F., Yang, B., Xu, Y., Zang, Y., Li, J., Wang, Y., Dai, W., Fan, H., Hyyppä, J., & Stilla, U. (2020). Registration of large-scale terrestrial laser scanner point clouds: A review and benchmark. *ISPRS Journal of Photogrammetry and Remote Sensing*, *163*, 327–342. https://doi.org/10.1016/j.isprsjprs.2020.03.013

Donner, S. D., Skirving, W. J., Little, C. M., Oppenheimer, M., & Hoegh-Guldberg, O. (2005). Global assessment of coral bleaching and required rates of adaptation under climate change. *Global Change Biology*, *11*(12), 2251–2265. https://doi.org/10.1111/j.1365-2486.2005.01073.x

Dornelas, M., Madin, J. S., Baird, A. H., & Connolly, S. R. (2017). Allometric growth in reef-building corals. *Proceedings of the Royal Society B: Biological Sciences*, *284*(1851), 20170053. https://doi.org/10.1098/rspb.2017.0053

Doropoulos, C., Bozec, Y.-M., Gouezo, M., Priest, M. A., Thomson, D. P., Mumby, P. J., & Roff, G. (2022). Cryptic coral recruits as dormant "seed banks": An unrecognized mechanism of rapid reef recovery. *Ecology*, *103*(3), 1–6.

Doropoulos, C., Roff, G., Bozec, Y.-M., Zupan, M., Werminghausen, J., & Mumby, P. J. (2016). Characterizing the ecological trade-offs throughout the early ontogeny of coral recruitment. *Ecological Monographs*, *86*(1), 20–44. https://doi.org/10.1890/15-0668.1

Doropoulos, C., Roff, G., Zupan, M., Nestor, V., Isechal, A. L., & Mumby, P. J. (2014). Reef-scale failure of coral settlement following typhoon disturbance and macroalgal bloom in Palau, Western Pacific. *Coral Reefs*, *33*(3), 613–623. https://doi.org/10.1007/s00338-014-1149-y

Doropoulos, C., Ward, S., Roff, G., González-Rivero, M., & Mumby, P. J. (2015). Linking Demographic Processes of Juvenile Corals to Benthic Recovery Trajectories in Two Common Reef Habitats. *PLOS ONE*, *10*(5), e0128535. https://doi.org/10.1371/journal.pone.0128535

Edinger, E. N., Limmon, G. V., Jompa, J., Widjatmoko, W., Heikoop, J. M., & Risk, M. J. (2000). Normal Coral Growth Rates on Dying Reefs: Are Coral Growth Rates Good Indicators of Reef Health? *Marine Pollution Bulletin*, *40*(5), 404–425. https://doi.org/10.1016/S0025-326X(99)00237-4

Edmunds, P. J. (2019). The demography of hurricane effects on two coral populations differing in dynamics. *Ecosphere*, *10*(9), e02836. https://doi.org/10.1002/ecs2.2836

Edmunds, P. J., Burgess, S. C., Putnam, H. M., Baskett, M. L., Bramanti, L., Fabina, N. S., Han, X., Lesser, M. P., Madin, J. S., Wall, C. B., Yost, D. M., & Gates, R. D. (2014a). Evaluating the causal basis of ecological success within the scleractinia: An integral projection model approach. *Marine Biology*, *161*(12), 2719–2734. https://doi.org/10.1007/s00227-014-2547-y

Edmunds, P. J., Burgess, S. C., Putnam, H. M., Baskett, M. L., Bramanti, L., Fabina, N. S., Han, X., Lesser, M. P., Madin, J. S., Wall, C. B., Yost, D. M., & Gates, R. D. (2014b). Evaluating the causal basis of ecological success within the scleractinia: An integral projection model approach. *Marine Biology*, *161*(12), 2719–2734. https://doi.org/10.1007/s00227-014-2547-y

Edmunds, P., & Riegl, B. (2020). Urgent need for coral demography in a world where corals are disappearing. *Marine Ecology Progress Series*, *635*, 233–242. https://doi.org/10.3354/meps13205

Emslie, M. J., Logan, M., Bray, P., Ceccarelli, D. M., Cheal, A. J., Hughes, T. P., Johns, K. A., Jonker, M. J., Kennedy, E. V., Kerry, J. T., Mellin, C., Miller, I. R., Osborne, K., Puotinen, M., Sinclair-Taylor, T., & Sweatman, H. (2024). Increasing disturbance frequency undermines coral reef recovery. *Ecological Monographs*, *94*(3), e1619. https://doi.org/10.1002/ecm.1619

ESRI. (2023). *ArcGIS Pro* (Version 3.0). ESRI. https://pro.arcgis.com/en/pro-app/latest/get-started/download-arcgis-pro.htm

Fabricius, K., De'ath, G., McCook, L., Turak, E., & Williams, D. McB. (2005). Changes in algal, coral and fish assemblages along water quality gradients on the inshore Great Barrier Reef. *Marine Pollution Bulletin*, *51*(1), 384–398. https://doi.org/10.1016/j.marpolbul.2004.10.041

Fabricius, K. E. (2006). Effects of irradiance, flow, and colony pigmentation on the temperature microenvironment around corals: Implications for coral bleaching? *Limnology and Oceanography*, *51*(1), 30–37. https://doi.org/10.4319/lo.2006.51.1.0030

Ferrari, R., Bryson, M., Bridge, T., Hustache, J., Williams, S. B., Byrne, M., & Figueira, W. (2016). Quantifying the response of structural complexity and community composition to environmental change in marine communities. *Global Change Biology*, *22*(5), 1965–1975. https://doi.org/10.1111/gcb.13197

Ferrari, R., Figueira, W. F., Pratchett, M. S., Boube, T., Adam, A., Kobelkowsky-Vidrio, T., Doo, S. S., Atwood, T. B., & Byrne, M. (2017). 3D photogrammetry quantifies growth and external erosion of individual coral colonies and skeletons. *Scientific Reports*, *7*(1), 16737. https://doi.org/10.1038/s41598-017-16408-z

Ferrari, R., Gonzalez-Rivero, M., & Mumby, P. (2012). Size matters in competition between corals and macroalgae. *Marine Ecology Progress Series*, *467*, 77–88. https://doi.org/10.3354/meps09953

Ferrari, R., Lachs, L., Pygas, D. R., Humanes, A., Sommer, B., Figueira, W. F., Edwards, A. J., Bythell, J. C., & Guest, J. R. (2021). Photogrammetry as a tool to improve ecosystem restoration. *Trends in Ecology & Evolution*, *36*(12), 1093–1101. https://doi.org/10.1016/j.tree.2021.07.004

Ferrario, F., Beck, M. W., Storlazzi, C. D., Micheli, F., Shepard, C. C., & Airoldi, L. (2014). The effectiveness of coral reefs for coastal hazard risk reduction and adaptation. *Nature Communications*, *5*(1), 3794. https://doi.org/10.1038/ncomms4794

Figueira, W., Ferrari, R., Weatherby, E., Porter, A., Hawes, S., & Byrne, M. (2015). Accuracy and Precision of Habitat Structural Complexity Metrics Derived from Underwater Photogrammetry. *Remote Sensing*, *7*(12), 16883–16900. https://doi.org/10.3390/rs71215859

Finelli, C. M., Helmuth, B. S. T., Pentcheff, N. D., & Wethey, D. S. (2006). Water flow influences oxygen transport and photosynthetic efficiency in corals. *Coral Reefs*, *25*(1), 47–57. https://doi.org/10.1007/s00338-005-0055-8

Fisher, R., O'Leary, R. A., Low-Choy, S., Mengersen, K., Knowlton, N., Brainard, R. E., & Caley, M. J. (2015). Species Richness on Coral Reefs and the Pursuit of Convergent Global Estimates. *Current Biology*, *25*(4), 500–505. https://doi.org/10.1016/j.cub.2014.12.022

Fonstad, M. A., Dietrich, J. T., Courville, B. C., Jensen, J. L., & Carbonneau, P. E. (2013). Topographic structure from motion: A new development in photogrammetric measurement. *Earth Surface Processes and Landforms*, *38*(4), 421–430. https://doi.org/10.1002/esp.3366

Fox, M. D., Cohen, A. L., Rotjan, R. D., Mangubhai, S., Sandin, S. A., Smith, J. E., Thorrold, S. R., Dissly, L., Mollica, N. R., & Obura, D. (2021). Increasing Coral Reef Resilience Through Successive Marine Heatwaves. *Geophysical Research Letters*, *48*(17), e2021GL094128. https://doi.org/10.1029/2021GL094128

Franklin, J. F., Lindenmayer, D., MacMahon, J. A., McKee, A., Magnuson, J., Perry, D. A., Waide, R., & Foster, D. (2000). Threads of Continuity: There are immense differences between even-aged silvicultural disturbances (especially clearcutting) and natural disturbances, such as windthrow, wildfire, and even volcanic eruptions. *Conservation in Practice*, *1*(1), 8–17. https://doi.org/10.1111/j.1526-4629.2000.tb00155.x

Fukunaga, A., Pascoe, K. H., Pugh, A. R., Kosaki, R. K., & Burns, J. H. R. (2022). Underwater Photogrammetry Captures the Initial Recovery of a Coral Reef at Lalo Atoll. *Diversity*, *14*(1), Article 1. https://doi.org/10.3390/d14010039

Gardner, T. A., Côté, I. M., Gill, J. A., Grant, A., & Watkinson, A. R. (2003). Long-Term Region-Wide Declines in Caribbean Corals. *Science*, *301*(5635), 958–960. https://doi.org/10.1126/science.1086050

Gillis, L. G., Bouma, T. J., Jones, C. G., Katwijk, M. M. van, Nagelkerken, I., Jeuken, C. J. L., Herman, P. M. J., & Ziegler, A. D. (2014). Potential for landscape-scale positive interactions among tropical marine ecosystems. *Marine Ecology Progress Series*, *503*, 289–303. https://doi.org/10.3354/meps10716

Gilmour, J. P. (2004). Size-structures of populations of the mushroom coral Fungia fungites: The role of disturbance. *Coral Reefs*, *23*(4), 493–504. https://doi.org/10.1007/s00338-004-0427-5

Glynn, P. W. (1985). El Nino-associated disturbance to coral reefs and post disturbance mortality by Acanthaster planci. *Mar. Ecol. Prog. Ser*, *26*(295–300), 4.

Glynn, P. W. (1991). Coral reef bleaching in the 1980s and possible connections with global warming. *Trends in Ecology & Evolution*, *6*(6), 175–179. https://doi.org/10.1016/0169-5347(91)90208-F

Golden, C. D., Allison, E. H., Cheung, W. W. L., Dey, M. M., Halpern, B. S., McCauley, D. J., Smith, M., Vaitla, B., Zeller, D., & Myers, S. S. (2016). Nutrition: Fall in fish catch threatens human health. *Nature*, *534*(7607), 317–320. https://doi.org/10.1038/534317a

González-Rivero, M., Beijbom, O., Rodriguez-Ramirez, A., Bryant, D. E. P., Ganase, A., Gonzalez-Marrero, Y., Herrera-Reveles, A., Kennedy, E. V., Kim, C. J. S., Lopez-Marcano, S., Markey, K., Neal, B. P., Osborne, K., Reyes-Nivia, C., Sampayo, E. M., Stolberg, K., Taylor, A., Vercelloni, J., Wyatt, M., & Hoegh-Guldberg, O. (2020). Monitoring of Coral Reefs Using Artificial Intelligence: A Feasible and Cost-Effective Approach. *Remote Sensing*, *12*(3), Article 3. https://doi.org/10.3390/rs12030489

González-Rivero, M., Bongaerts, P., Beijbom, O., Pizarro, O., Friedman, A., Rodriguez-Ramirez, A., Upcroft, B., Laffoley, D., Kline, D., Bailhache, C., Vevers, R., & Hoegh-Guldberg, O. (2014). The Catlin Seaview Survey – kilometre-scale seascape assessment, and monitoring of coral reef ecosystems. *Aquatic Conservation: Marine and Freshwater Ecosystems*, *24*(S2), 184–198. https://doi.org/10.1002/aqc.2505

Gordon, S., Aston, E., Lechene, M., Harianto, J., Figueira, W., Gonzalez Rivero, M., & Ferrari, R. (2023). *Field photogrammetry in 4D. Reef Restoration and Adaption Program (EcoRRAP). Standard Operational Procedure Number 1: Overview and in-field workflow.* https://doi.org/10.25845/SE7T-PS86

Gouezo, M., Golbuu, Y., Fabricius, K., Olsudong, D., Mereb, G., Nestor, V., Wolanski, E., Harrison, P., & Doropoulos, C. (2019). Drivers of recovery and reassembly of coral reef communities. *Proceedings of the Royal Society B: Biological Sciences*, *286*(1897), 20182908. https://doi.org/10.1098/rspb.2018.2908

Graham, N. A. J., McClanahan, T. R., MacNeil, M. A., Wilson, S. K., Polunin, N. V. C., Jennings, S., Chabanet, P., Clark, S., Spalding, M. D., Letourneur, Y., Bigot, L., Galzin, R., Öhman, M. C., Garpe, K. C., Edwards, A. J., & Sheppard, C. R. C. (2008). Climate Warming, Marine Protected Areas and the Ocean-Scale Integrity of Coral Reef Ecosystems. *PLOS ONE*, *3*(8), e3039. https://doi.org/10.1371/journal.pone.0003039

Graham, N. A. J., & Nash, K. L. (2013). The importance of structural complexity in coral reef ecosystems. *Coral Reefs*, *32*(2), 315–326. https://doi.org/10.1007/s00338-012-0984-y

Graham, N. a. J., Wilson, S. K., Jennings, S., Polunin, N. V. C., Robinson, J., Bijoux, J. P., & Daw, T. M. (2007). Lag Effects in the Impacts of Mass Coral Bleaching on Coral Reef Fish, Fisheries, and Ecosystems. *Conservation Biology*, *21*(5), 1291–1300. https://doi.org/10.1111/j.1523-1739.2007.00754.x

Gregg, T. M., Mead, L., Burns, J. H. R., & Takabayashi, M. (2015). Puka Mai He Koʻa: The Significance of Corals in Hawaiian Culture. In N. Narchi & L. L. Price (Eds.), *Ethnobiology of Corals and Coral Reefs* (pp. 103–115). Springer International Publishing. https://doi.org/10.1007/978-3-319-23763-3_7

Grimm, N. B., Chapin III, F. S., Bierwagen, B., Gonzalez, P., Groffman, P. M., Luo, Y., Melton, F., Nadelhoffer, K., Pairis, A., Raymond, P. A., Schimel, J., & Williamson, C. E. (2013). The impacts of climate change on ecosystem structure and function. *Frontiers in Ecology and the Environment*, *11*(9), 474–482. https://doi.org/10.1890/120282

Grimsditch, G., Mwaura, J. M., Kilonzo, J., & Amiyo, N. (2010). The Effects of Habitat on Coral Bleaching Responses in Kenya. *AMBIO*, *39*(4), 295–304. https://doi.org/10.1007/s13280-010-0052-1

Grottoli, A. G., Warner, M. E., Levas, S. J., Aschaffenburg, M. D., Schoepf, V., McGinley, M., Baumann, J., & Matsui, Y. (2014). The cumulative impact of annual coral bleaching can turn some coral species winners into losers. *Global Change Biology*, *20*(12), 3823–3833. https://doi.org/10.1111/gcb.12658

Gudka, M., Obura, D., Treml, E. A., & Nicholson, E. (2024). Strengthening resilience potential assessments for coral reef management. *Methods in Ecology and Evolution*, *15*(4), 612–627. https://doi.org/10.1111/2041-210X.14303

Guest, J. R., Baird, A. H., Maynard, J. A., Muttaqin, E., Edwards, A. J., Campbell, S. J., Yewdall, K., Affendi, Y. A., & Chou, L. M. (2012). Contrasting Patterns of Coral Bleaching Susceptibility in 2010 Suggest an Adaptive Response to Thermal Stress. *PLOS ONE*, *7*(3), e33353. https://doi.org/10.1371/journal.pone.0033353

Guo, T., Capra, A., Troyer, M., Grün, A., Brooks, A. J., Hench, J. L., Schmitt, R. J., Holbrook, S. J., & Dubbini, M. (2016). *Accuracy assessment of underwater photogrammetric three dimensional modelling for coral reefs* [Application/pdf]. https://doi.org/10.3929/ETHZ-B-000118990

Hall, V. R., & Hughes, T. P. (1996). Reproductive Strategies of Modular Organisms: Comparative Studies of Reef- Building Corals. *Ecology*, *77*(3), 950–963. https://doi.org/10.2307/2265514

Hannam, M., & Moskal, L. M. (2015). Terrestrial Laser Scanning Reveals Seagrass Microhabitat Structure on a Tideflat. *Remote Sensing*, *7*(3), Article 3. https://doi.org/10.3390/rs70303037

Hardiman, B. S., Gough, C. M., Halperin, A., Hofmeister, K. L., Nave, L. E., Bohrer, G., & Curtis, P. S. (2013). Maintaining high rates of carbon storage in old forests: A mechanism linking canopy structure to forest function. *Forest Ecology and Management*, *298*, 111–119. https://doi.org/10.1016/j.foreco.2013.02.031

Harrison, P. L., & Wallace, C. C. (1990). Reproduction, dispersal and recruitment of scleractinian corals. In *Coral reefs* (Vol. 25, pp. 133–207). Elsevier.

Hartig, F. (2022). *DHARMa: Residual Diagnostics for Hierarchical (Multi-Level / Mixed) Regression Models* (Version 0.4.6). https://CRAN.R-project.org/package=DHARMa

Hein, M. Y., Vardi, T., Shaver, E. C., Pioch, S., Boström-Einarsson, L., Ahmed, M., Grimsditch, G., & McLeod, I. M. (2021). Perspectives on the Use of Coral Reef Restoration as a Strategy to Support and Improve Reef Ecosystem Services. *Frontiers in Marine Science*, *8*. https://doi.org/10.3389/fmars.2021.618303

Hernández-Landa, R. C., Barrera-Falcon, E., & Rioja-Nieto, R. (2020). Size-frequency distribution of coral assemblages in insular shallow reefs of the Mexican Caribbean using underwater photogrammetry. *PeerJ*, *8*, e8957. https://doi.org/10.7717/peerj.8957

Hinde, A. (1998). Some Demographic Fundamentals. In *Demographic Methods*. Routledge.

Hoegh-Guldberg, O., Kennedy, E. V., Beyer, H. L., McClennen, C., & Possingham, H. P. (2018). Securing a Long-term Future for Coral Reefs. *Trends in Ecology & Evolution*, *33*(12), 936–944. https://doi.org/10.1016/j.tree.2018.09.006

Hoegh-Guldberg, O., Poloczanska, E. S., Skirving, W., & Dove, S. (2017). Coral Reef Ecosystems under Climate Change and Ocean Acidification. *Frontiers in Marine Science*, *4*, 158. https://doi.org/10.3389/fmars.2017.00158

Hoegh-Guldberg, O., Skirving, W., Dove, S. G., Spady, B. L., Norrie, A., Geiger, E. F., Liu, G., De La Cour, J. L., & Manzello, D. P. (2023). Coral reefs in peril in a record-breaking year. *Science*, *382*(6676), 1238–1240. https://doi.org/10.1126/science.adk4532

Hoekstra, J. M., Boucher, T. M., Ricketts, T. H., & Roberts, C. (2005). Confronting a biome crisis: Global disparities of habitat loss and protection. *Ecology Letters*, *8*(1), 23–29. https://doi.org/10.1111/j.1461-0248.2004.00686.x

Hoogenboom, M. O., & Connolly, S. R. (2009). Defining fundamental niche dimensions of corals: Synergistic effects of colony size, light, and flow. *Ecology*, *90*(3), 767–780. https://doi.org/10.1890/07-2010.1

Hoogenboom, M. O., Frank, G. E., Chase, T. J., Jurriaans, S., Álvarez-Noriega, M., Peterson, K., Critchell, K., Berry, K. L. E., Nicolet, K. J., Ramsby, B., & Paley, A. S. (2017). Environmental Drivers of Variation in Bleaching Severity of Acropora Species during an Extreme Thermal Anomaly. *Frontiers in Marine Science*, *4*. https://doi.org/10.3389/fmars.2017.00376

Hoshikawa, T., Suzuki, S., Yajima, J., Mochizuki, H., & Yamamoto, K. (2024). Integrating personal laser scanning with uncrewed aerial vehicle-based photogrammetry or laser scanning for accurate stem volume estimation in temperate coniferous forests. *Journal of Forest Research*, *29*(5), 343–351. https://doi.org/10.1080/13416979.2024.2346004

Hughes, T. P. (1984). Population Dynamics Based on Individual Size Rather than Age: A General Model with a Reef Coral Example. *The American Naturalist*, *123*(6), 778–795. https://doi.org/10.1086/284239

Hughes, T. P., Baird, A. H., Morrison, T. H., & Torda, G. (2023). Principles for coral reef restoration in the anthropocene. *One Earth*, *6*(6), 656–665. https://doi.org/10.1016/j.oneear.2023.04.008

Hughes, T. P., Barnes, M. L., Bellwood, D. R., Cinner, J. E., Cumming, G. S., Jackson, J. B. C., Kleypas, J., van de Leemput, I. A., Lough, J. M., Morrison, T. H., Palumbi, S. R., van Nes, E. H., & Scheffer, M. (2017). Coral reefs in the Anthropocene. *Nature*, *546*(7656), 82–90. https://doi.org/10.1038/nature22901

Hughes, T. P., & Connell, J. H. (1987). Population Dynamics Based on Size or Age? A Reef-Coral Analysis. *The American Naturalist*, *129*(6), 818–829. https://doi.org/10.1086/284677

Hughes, T. P., & Jackson, J. B. C. (1980). Do Corals Lie About Their Age? Some Demographic Consequences of Partial Mortality, Fission, and Fusion. *Science*, *209*(4457), 713–715. https://doi.org/10.1126/science.209.4457.713

Hughes, T. P., Kerry, J. T., Baird, A. H., Connolly, S. R., Chase, T. J., Dietzel, A., Hill, T., Hoey, A. S., Hoogenboom, M. O., Jacobson, M., Kerswell, A., Madin, J. S., Mieog, A., Paley, A. S., Pratchett, M. S., Torda, G., & Woods, R. M. (2019). Global warming impairs stock–recruitment dynamics of corals. *Nature*, *568*(7752), 387–390. https://doi.org/10.1038/s41586-019-1081-y

Hughes, T. P., Kerry, J. T., Baird, A. H., Connolly, S. R., Dietzel, A., Eakin, C. M., Heron, S. F., Hoey, A. S., Hoogenboom, M. O., Liu, G., McWilliam, M. J., Pears, R. J., Pratchett, M. S., Skirving, W. J., Stella, J. S., & Torda, G. (2018). Global warming transforms coral reef assemblages. *Nature*, *556*(7702), 492–496. https://doi.org/10.1038/s41586-018-0041-2

Hughes, T. P., & Tanner, J. E. (2000). Recruitment Failure, Life Histories, and Long-Term Decline of Caribbean Corals. *Ecology*, *81*(8), 2250–2263. https://doi.org/10.1890/0012-9658(2000)081[2250:RFLHAL]2.0.CO;2

Hutchings, P., Kingsford, M., & Hoegh-Guldberg, O. (2019). *The Great Barrier Reef: Biology, Environment and Management*. Csiro Publishing.

Iglesias-Prieto, R., Matta, J. L., Robins, W. A., & Trench, R. K. (1992). Photosynthetic response to elevated temperature in the symbiotic dinoflagellate Symbiodinium microadriaticum in culture. *Proceedings of the National Academy of Sciences*, *89*(21), 10302–10305. https://doi.org/10.1073/pnas.89.21.10302

Iida, Y., Kohyama, T. S., Swenson, N. G., Su, S.-H., Chen, C.-T., Chiang, J.-M., & Sun, I.-F. (2014). Linking functional traits and demographic rates in a subtropical tree community: The importance of size dependency. *Journal of Ecology*, *102*(3), 641–650. https://doi.org/10.1111/1365-2745.12221

James, M. R., Robson, S., d'Oleire-Oltmanns, S., & Niethammer, U. (2017). Optimising UAV topographic surveys processed with structure-from-motion: Ground control quality, quantity and bundle adjustment. *Geomorphology*, *280*, 51–66. https://doi.org/10.1016/j.geomorph.2016.11.021

Johnston, E. C., Counsell, C. W. W., Sale, T. L., Burgess, S. C., & Toonen, R. J. (2020). The legacy of stress: Coral bleaching impacts reproduction years later. *Functional Ecology*, *34*(11), 2315–2325. https://doi.org/10.1111/1365-2435.13653

Johnstone, J. F., Allen, C. D., Franklin, J. F., Frelich, L. E., Harvey, B. J., Higuera, P. E., Mack, M. C., Meentemeyer, R. K., Metz, M. R., Perry, G. L., Schoennagel, T., & Turner, M. G. (2016). Changing disturbance regimes, ecological memory, and forest resilience. *Frontiers in Ecology and the Environment*, *14*(7), 369–378. https://doi.org/10.1002/fee.1311

Kaniewska, P., Magnusson, S. H., Anthony, K. R. N., Reef, R., Kühl, M., & Hoegh-Guldberg, O. (2011). Importance of Macro- Versus Microstructure in Modulating Light Levels Inside Coral Colonies. *Journal of Phycology*, *47*(4), 846–860. https://doi.org/10.1111/j.1529-8817.2011.01021.x

Kayal, M., Vercelloni, J., Loma, T. L. de, Bosserelle, P., Chancerelle, Y., Geoffroy, S., Stievenart, C., Michonneau, F., Penin, L., Planes, S., & Adjeroud, M. (2012). Predator Crown-of-Thorns Starfish (Acanthaster planci) Outbreak, Mass Mortality of Corals, and Cascading Effects on Reef Fish and Benthic Communities. *PLOS ONE*, *7*(10), e47363. https://doi.org/10.1371/journal.pone.0047363

Kopecky, K. L., Pavoni, G., Nocerino, E., Brooks, A. J., Corsini, M., Menna, F., Gallagher, J. P., Capra, A., Castagnetti, C., Rossi, P., Gruen, A., Neyer, F., Muntoni, A., Ponchio, F., Cignoni, P., Troyer, M., Holbrook, S. J., & Schmitt, R. J. (2023). Quantifying the Loss of Coral from a Bleaching Event Using

Underwater Photogrammetry and AI-Assisted Image Segmentation. *Remote Sensing*, *15*(16), Article 16. https://doi.org/10.3390/rs15164077

Kramer, N., Tamir, R., Eyal, G., & Loya, Y. (2020). Coral Morphology Portrays the Spatial Distribution and Population Size-Structure Along a 5–100 m Depth Gradient. *Frontiers in Marine Science*, *7*. https://doi.org/10.3389/fmars.2020.00615

Kwiatkowski, L., Cox, P., Halloran, P. R., Mumby, P. J., & Wiltshire, A. J. (2015). Coral bleaching under unconventional scenarios of climate warming and ocean acidification. *Nature Climate Change*, *5*(8), 777–781. https://doi.org/10.1038/nclimate2655

Lachs, L., Biondi, P., Gouezo, M., Nestor, V., Olsudong, D., Guest, J., & Golbuu, Y. (2024). Demographic recovery of corals at a wave-exposed reef following catastrophic disturbance. *Coral Reefs*, *43*(1), 193–199. https://doi.org/10.1007/s00338-024-02464-1

Lague, D., Brodu, N., & Leroux, J. (2013). Accurate 3D comparison of complex topography with terrestrial laser scanner: Application to the Rangitikei canyon (N-Z). *ISPRS Journal of Photogrammetry and Remote Sensing*, *82*, 10–26. https://doi.org/10.1016/j.isprsjprs.2013.04.009

Lange, I. D., Molina-Hernández, A., Medellín-Maldonado, F., Perry, C. T., & Álvarez-Filip, L. (2022). Structure-from-motion photogrammetry demonstrates variability in coral growth within colonies and across habitats. *PLOS ONE*, *17*(11), e0277546. https://doi.org/10.1371/journal.pone.0277546

Lange, I. D., & Perry, C. T. (2019). Bleaching impacts on carbonate production in the Chagos Archipelago: Influence of functional coral groups on carbonate budget trajectories. *Coral Reefs*, *38*(4), 619–624. https://doi.org/10.1007/s00338-019-01784-x

Lange, I. D., & Perry, C. T. (2020). A quick, easy and non-invasive method to quantify coral growth rates using photogrammetry and 3D model comparisons. *Methods in Ecology and Evolution*, *11*(6), 714–726. https://doi.org/10.1111/2041-210X.13388

Lange, I. D., Perry, C. T., & Stuhr, M. (2023). Recovery trends of reef carbonate budgets at remote coral atolls 6 years post-bleaching. *Limnology and Oceanography*, *68*(S1), S8–S22. https://doi.org/10.1002/lno.12066

Lange, I. D., Razak, T. B., Perry, C. T., Maulana, P. B., Prasetya, M. E., Irwan, & Lamont, T. A. (2024). Coral restoration can drive rapid reef carbonate budget recovery. *Current Biology*, *34*(6), 1341-1348.e3. https://doi.org/10.1016/j.cub.2024.02.009

Lechene, M. A. A., Figueira, W. F., Murray, N. J., Aston, E. A., Gordon, S. E., & Ferrari, R. (2024). Evaluating error sources to improve precision in the co-registration of underwater 3D models. *Ecological Informatics*, *81*, 102632. https://doi.org/10.1016/j.ecoinf.2024.102632

Lenth, R. V. (2023). *emmeans: Estimated Marginal Means, aka Least-Squares Means* (Version 1.8.7). https://CRAN.R-project.org/package=emmeans

Leslie, P. H. (1945). On the Use of Matrices in Certain Population Mathematics. *Biometrika*, *33*(3), 183–212. https://doi.org/10.2307/2332297

Lesser, M. P. (2006). Oxidative Stress in Marine Environments: Biochemistry and Physiological Ecology. *Annual Review of Physiology*, *68*(Volume 68, 2006), 253–278. https://doi.org/10.1146/annurev.physiol.68.040104.110001

Lewis, R. E., Davy, S. K., Gardner, S. G., Rongo, T., Suggett, D. J., & Nitschke, M. R. (2022). Colony self-shading facilitates Symbiodiniaceae cohabitation in a South Pacific coral community. *Coral Reefs*, *41*(5), 1433–1447. https://doi.org/10.1007/s00338-022-02292-1

Linares, C., Pratchett, M., & Coker, D. (2011). Recolonisation of Acropora hyacinthus following climate-induced coral bleaching on the Great Barrier Reef. *Marine Ecology Progress Series*, *438*, 97–104. https://doi.org/10.3354/meps09272

Lindenmayer, D. B., & Laurance, W. F. (2017). The ecology, distribution, conservation and management of large old trees. *Biological Reviews*, *92*(3), 1434–1458. https://doi.org/10.1111/brv.12290

Lirman, D., & Fong, P. (2007). Is proximity to land-based sources of coral stressors an appropriate measure of risk to coral reefs? An example from the Florida Reef Tract. *Marine Pollution Bulletin*, *54*(6), 779–791. https://doi.org/10.1016/j.marpolbul.2006.12.014

Logan, C. A., Dunne, J. P., Eakin, C. M., & Donner, S. D. (2014). Incorporating adaptive responses into future projections of coral bleaching. *Global Change Biology*, *20*(1), 125–139. https://doi.org/10.1111/gcb.12390

Lotka, A. J. (1931). The structure of a growing population. *Human Biology*, *3*(4), 459–493. JSTOR.

Lough, J. M., & Barnes, D. J. (1992). Comparisons of skeletal density variations in *Porites* from the central Great Barrier Reef. *Journal of Experimental Marine Biology and Ecology*, *155*(1), 1–25. https://doi.org/10.1016/0022-0981(92)90024-5

Lough, J. M., & Barnes, D. J. (2000). Environmental controls on growth of the massive coral *Porites*. *Journal of Experimental Marine Biology and Ecology*, *245*(2), 225–243. https://doi.org/10.1016/S0022-0981(99)00168-9

Loya, Y., Sakai, K., Yamazato, K., Nakano, Y., Sambali, H., & van Woesik, R. (2001). Coral bleaching: The winners and the losers. *Ecology Letters*, *4*(2), 122–131. https://doi.org/10.1046/j.1461-0248.2001.00203.x

Lüdecke, D. (2018). ggeffects: Tidy data frames of marginal effects from regression models. *Journal of Open Source Software*, *3*(26), 772.

Lüdecke, D., Ben-Shachar, M. S., Patil, I., Waggoner, P., & Makowski, D. (2021). performance: An R Package for Assessment, Comparison and Testing of Statistical Models. *Journal of Open Source Software*, *6*(60), 3139. https://doi.org/10.21105/joss.03139

Maas, H.-G. (2015). On the Accuracy Potential in Underwater/Multimedia Photogrammetry. *Sensors*, *15*(8), Article 8. https://doi.org/10.3390/s150818140

Madin, J., Baird, A., Bridge, T., Connolly, S., Zawada, K., & Dornelas, M. (2018). Cumulative effects of cyclones and bleaching on coral cover and species richness at Lizard Island. *Marine Ecology Progress Series*, *604*, 263–268. https://doi.org/10.3354/meps12735

Madin, J. S., Baird, A. H., Dornelas, M., & Connolly, S. R. (2014). Mechanical vulnerability explains size-dependent mortality of reef corals. *Ecology Letters*, *17*(8), 1008–1015. https://doi.org/10.1111/ele.12306

Madin, J. S., & Connolly, S. R. (2006). Ecological consequences of major hydrodynamic disturbances on coral reefs. *Nature*, *444*(7118), 477–480. https://doi.org/10.1038/nature05328

Magurran, A. E., Baillie, S. R., Buckland, S. T., Dick, J. McP., Elston, D. A., Scott, E. M., Smith, R. I., Somerfield, P. J., & Watt, A. D. (2010). Long-term datasets in biodiversity research and monitoring: Assessing change in ecological communities through time. *Trends in Ecology & Evolution*, *25*(10), 574–582. https://doi.org/10.1016/j.tree.2010.06.016

Mangeruga, M., Bruno, F., Cozza, M., Agrafiotis, P., & Skarlatos, D. (2018). Guidelines for Underwater Image Enhancement Based on Benchmarking of Different Methods. *Remote Sensing*, *10*(10), Article 10. https://doi.org/10.3390/rs10101652

Marre, G., Holon, F., Luque, S., Boissery, P., & Deter, J. (2019). Monitoring Marine Habitats With Photogrammetry: A Cost-Effective, Accurate, Precise and High-Resolution Reconstruction Method. *Frontiers in Marine Science*, *6*, 276. https://doi.org/10.3389/fmars.2019.00276

Marshall, P. A., & Baird, A. H. (2000). Bleaching of corals on the Great Barrier Reef: Differential susceptibilities among taxa. *Coral Reefs*, *19*(2), 155–163. https://doi.org/10.1007/s003380000086

Massel, S. R., & Done, T. J. (1993). Effects of cyclone waves on massive coral assemblages on the Great Barrier Reef: Meteorology, hydrodynamics and demography. *Coral Reefs*, *12*(3), 153–166. https://doi.org/10.1007/BF00334475

Maynard, J. A., Anthony, K. R. N., Marshall, P. A., & Masiri, I. (2008). Major bleaching events can lead to increased thermal tolerance in corals. *Marine Biology*, *155*(2), 173–182. https://doi.org/10.1007/s00227-008-1015-y

McClanahan, T. R., Baird, A. H., Marshall, P. A., & Toscano, M. A. (2004). Comparing bleaching and mortality responses of hard corals between southern Kenya and the Great Barrier Reef, Australia. *Marine Pollution Bulletin*, *48*(3), 327–335. https://doi.org/10.1016/j.marpolbul.2003.08.024

McClanahan, T. R., Maina, J., Moothien-Pillay, R., & Baker, A. C. (2005). Effects of geography, taxa, water flow, and temperature variation on coral bleaching intensity in Mauritius. *Marine Ecology Progress Series*, *298*, 131–142. https://doi.org/10.3354/meps298131

McManus, J. W., & Polsenberg, J. F. (2004). Coral–algal phase shifts on coral reefs: Ecological and environmental aspects. *Progress in Oceanography*, *60*(2), 263–279. https://doi.org/10.1016/j.pocean.2004.02.014

McWilliam, M., Pratchett, M. S., Hoogenboom, M. O., & Hughes, T. P. (2020). Deficits in functional trait diversity following recovery on coral reefs. *Proceedings of the Royal Society B: Biological Sciences*, *287*(1918), 20192628. https://doi.org/10.1098/rspb.2019.2628

Meesters, E. H., Wesseling, I., & Bak, R. P. M. (1997). Coral colony tissue damage in six species of reef-building corals: Partial mortality in relation with depth and surface area. *Journal of Sea Research*, *37*(1), 131–144. https://doi.org/10.1016/S1385-1101(96)00004-4

Meesters, E., Hilterman, M., Kardinaal, E., Keetman, M., de Vries, M., & Bak, R. (2001). Colony size-frequency distributions of scleractinian coral populations: Spatial and interspecific variation. *Marine Ecology Progress Series*, *209*, 43–54. https://doi.org/10.3354/meps209043

Meiri, S. (2011). Bergmann's Rule – what's in a name? *Global Ecology and Biogeography*, *20*(1), 203–207. https://doi.org/10.1111/j.1466-8238.2010.00577.x

Mellin, C., Matthews, S., Anthony, K. R. N., Brown, S. C., Caley, M. J., Johns, K. A., Osborne, K., Puotinen, M., Thompson, A., Wolff, N. H., Fordham, D. A., & MacNeil, M. A. (2019). Spatial resilience of the Great Barrier Reef under cumulative disturbance impacts. *Global Change Biology*, *25*(7), 2431–2445. https://doi.org/10.1111/gcb.14625

Menna, F., Nocerino, E., Fassi, F., & Remondino, F. (2016). Geometric and Optic Characterization of a Hemispherical Dome Port for Underwater Photogrammetry. *Sensors*, *16*(1), Article 1. https://doi.org/10.3390/s16010048

Merow, C., Dahlgren, J. P., Metcalf, C. J. E., Childs, D. Z., Evans, M. E. K., Jongejans, E., Record, S., Rees, M., Salguero-Gómez, R., & McMahon, S. M. (2014). Advancing population ecology with integral projection models: A practical guide. *Methods in Ecology and Evolution*, *5*(2), 99–110. https://doi.org/10.1111/2041-210X.12146

Miller, J., Muller, E., Rogers, C., Waara, R., Atkinson, A., Whelan, K. R. T., Patterson, M., & Witcher, B. (2009). Coral disease following massive bleaching in 2005 causes 60% decline in coral cover on reefs in the US Virgin Islands. *Coral Reefs*, *28*(4), 925–937. https://doi.org/10.1007/s00338-009-0531-7

Miller, M., Williams, D. E., Huntington, B. E., Piniak, G. A., & Vermeij, M. J. A. (2016). Decadal comparison of a diminishing coral community: A study using demographics to advance inferences of community status. *PeerJ*, *4*, e1643. https://doi.org/10.7717/peerj.1643

Monger, C., Sala, O. E., Duniway, M. C., Goldfus, H., Meir, I. A., Poch, R. M., Throop, H. L., & Vivoni, E. R. (2015). Legacy effects in linked ecological–soil–geomorphic systems of drylands. *Frontiers in Ecology and the Environment*, *13*(1), 13–19. https://doi.org/10.1890/140269

Mooney, H., Larigauderie, A., Cesario, M., Elmquist, T., Hoegh-Guldberg, O., Lavorel, S., Mace, G. M., Palmer, M., Scholes, R., & Yahara, T. (2009). Biodiversity, climate change, and ecosystem services. *Current Opinion in Environmental Sustainability*, *1*(1), 46–54. https://doi.org/10.1016/j.cosust.2009.07.006

Morais, J., Morais, R. A., Tebbett, S. B., Pratchett, M. S., & Bellwood, D. R. (2021). Dangerous demographics in post-bleach corals reveal boom-bust versus protracted declines. *Scientific Reports*, *11*(1), 18787.

Morais, J., Tebbett, S. B., Morais, R. A., & Bellwood, D. R. (2024). Natural recovery of corals after severe disturbance. *Ecology Letters*, *27*(1), e14332. https://doi.org/10.1111/ele.14332

Mumby, P. J. (1999). Bleaching and hurricane disturbances to populations of coral recruits in Belize. *Marine Ecology Progress Series*, *190*, 27–35. https://doi.org/10.3354/meps190027

Muscatine, L., Falkowski, P. G., Porter, J. W., Dubinsky, Z., & Smith, D. C. (1997). Fate of photosynthetic fixed carbon in light- and shade-adapted colonies of the symbiotic coral Stylophora pistillata. *Proceedings of the Royal Society of London. Series B. Biological Sciences*, *222*(1227), 181–202. https://doi.org/10.1098/rspb.1984.0058

Nakamura, T., & van Woesik, R. (2001). Water-flow rates and passive diffusion partially explain differential survival of corals during the 1998 bleaching event. *Marine Ecology Progress Series*, *212*, 301–304. https://doi.org/10.3354/meps212301

Negri, A. P., & Hoogenboom, M. O. (2011). Water Contamination Reduces the Tolerance of Coral Larvae to Thermal Stress. *PLOS ONE*, *6*(5), e19703. https://doi.org/10.1371/journal.pone.0019703

Neyer, F., Nocerino, E., & Gruen, A. (2018). Monitoring coral growth—The dichotomy between underwater photogrammetry and geodetic control network. *The International Archives of the Photogrammetry, Remote Sensing and Spatial Information Sciences*, *XLII–2*, 759–766. https://doi.org/10.5194/isprs-archives-XLII-2-759-2018

Nocerino, E., Menna, F., Fassi, F., & Remondino, F. (2016). Underwater calibration of dome port pressure housings. *ISPRS - International Archives of the Photogrammetry, Remote Sensing and Spatial Information Sciences*, *XL-3/W4*, 127–134. https://doi.org/10.5194/isprsarchives-XL-3-W4-127-2016

Nocerino, E., Menna, F., Gruen, A., Troyer, M., Capra, A., Castagnetti, C., Rossi, P., Brooks, A. J., Schmitt, R. J., & Holbrook, S. J. (2020). Coral Reef Monitoring by Scuba Divers Using Underwater Photogrammetry and Geodetic Surveying. *Remote Sensing*, *12*(18), Article 18. https://doi.org/10.3390/rs12183036

Oren, U., Benayahu, Y., Lubinevsky, H., & Loya, Y. (2001). Colony Integration During Regeneration in the Stony Coral Favia Favus. *Ecology*, *82*(3), 802–813. https://doi.org/10.1890/0012-9658(2001)082[0802:CIDRIT]2.0.CO;2

Ortiz, J.-C., Gomez-Cabrera, M. del C., & Hoegh-Guldberg, O. (2009). Effect of colony size and surrounding substrate on corals experiencing a mild bleaching event on Heron Island reef flat (southern Great Barrier Reef, Australia). *Coral Reefs*, *28*(4), 999–1003. https://doi.org/10.1007/s00338-009-0546-0

Ortiz, J.-C., Wolff, N. H., Anthony, K. R. N., Devlin, M., Lewis, S., & Mumby, P. J. (2018). Impaired recovery of the Great Barrier Reef under cumulative stress. *Science Advances*, *4*(7), eaar6127. https://doi.org/10.1126/sciadv.aar6127

Osborne, K., Thompson, A. A., Cheal, A. J., Emslie, M. J., Johns, K. A., Jonker, M. J., Logan, M., Miller, I. R., & Sweatman, H. P. A. (2017). Delayed coral recovery in a warming ocean. *Global Change Biology*, *23*(9), 3869–3881. https://doi.org/10.1111/gcb.13707

Paine, R. T. (1969). A Note on Trophic Complexity and Community Stability. *The American Naturalist*, *103*(929), 91–93. https://doi.org/10.1086/282586

Painter, R., Blyth, K., Mosedale, J., & Kelly, M. (1974). The effect of afforestation on erosion processes and sediment yield. *Effects of Man on the Interface of the Hydrological Cycle with the Physical Environment*, *113*, 62–68. https://www.semanticscholar.org/paper/The-effect-of-afforestation-on-erosion-processes-Painter-Blyth/88bc7930890c24eefa642b3994c2d47d734af777

Palumbi, S. R., Barshis, D. J., Traylor-Knowles, N., & Bay, R. A. (2014). Mechanisms of reef coral resistance to future climate change. *Science*, *344*(6186), 895–898. https://doi.org/10.1126/science.1251336

Pandolfi, J. M., Connolly, S. R., Marshall, D. J., & Cohen, A. L. (2011). Projecting Coral Reef Futures Under Global Warming and Ocean Acidification. *Science*, *333*(6041), 418–422. https://doi.org/10.1126/science.1204794

Pascoe, K. H., Fukunaga, A., Kosaki, R. K., & Burns, J. H. R. (2021). 3D assessment of a coral reef at Lalo Atoll reveals varying responses of habitat metrics following a catastrophic hurricane. *Scientific Reports*, *11*(1), 12050. https://doi.org/10.1038/s41598-021-91509-4

Patterson, M. R. (1992). A Chemical Engineering View of Cnidarian Symbioses1. *American Zoologist*, *32*(4), 566–582. https://doi.org/10.1093/icb/32.4.566

Pavoni, G., Corsini, M., Ponchio, F., Muntoni, A., Edwards, C., Pedersen, N., Sandin, S., & Cignoni, P. (2022). TagLab: AI-assisted annotation for the fast and accurate semantic segmentation of coral reef orthoimages. *Journal of Field Robotics*, *39*(3), 246–262. https://doi.org/10.1002/rob.22049

Pearson, R. (1981). Recovery and Recolonization of Coral Reefs. *Marine Ecology Progress Series*, *4*, 105–122. https://doi.org/10.3354/meps004105

Penin, L., Adjeroud, M., Schrimm, M., & Lenihan, H. S. (2007). High spatial variability in coral bleaching around Moorea (French Polynesia): Patterns across locations and water depths. *Comptes Rendus Biologies*, *330*(2), 171–181.

Penin, L., Vidal-Dupiol, J., & Adjeroud, M. (2013). Response of coral assemblages to thermal stress: Are bleaching intensity and spatial patterns consistent between events? *Environmental Monitoring and Assessment*, *185*(6), 5031–5042. https://doi.org/10.1007/s10661-012-2923-3

Petus, C., Waterhouse, J., Tracey, D., Wolanski, E., & Brodie, J. (2022). Using Optical Water-Type Classification in Data-Poor Water Quality Assessment: A Case Study in the Torres Strait. *Remote Sensing*, *14*(9), Article 9. https://doi.org/10.3390/rs14092212

Pisapia, C., Burn, D., & Pratchett, M. S. (2019). Changes in the population and community structure of corals during recent disturbances (February 2016-October 2017) on Maldivian coral reefs. *Scientific Reports*, *9*(1), 8402. https://doi.org/10.1038/s41598-019-44809-9

Pizarro, O., Friedman, A., Bryson, M., Williams, S. B., & Madin, J. (2017). A simple, fast, and repeatable survey method for underwater visual 3D benthic mapping and monitoring. *Ecology and Evolution*, *7*(6), 1770–1782. https://doi.org/10.1002/ece3.2701

Pratchett, M., Anderson, K., Hoogenboom, M., Widman, E., Baird, A., Pandolfi, J., Edmunds, P., & Lough, J. (2015). Spatial, Temporal and Taxonomic Variation in Coral Growth—Implications for the Structure and Function of Coral Reef Ecosystems. *Oceanography and Marine Biology*, *53*, 215–295. https://doi.org/10.1201/b18733-7

Pratchett, M. S., McCowan, D., Maynard, J. A., & Heron, S. F. (2013). Changes in bleaching susceptibility among corals subject to ocean warming and recurrent bleaching in Moorea, French Polynesia. *PLoS One*, *8*(7), e70443.

Pratchett, M. S., McWilliam, M. J., & Riegl, B. (2020). Contrasting shifts in coral assemblages with increasing disturbances. *Coral Reefs*, *39*(3), 783–793. https://doi.org/10.1007/s00338-020-01936-4

Pratchett, M. S., Thompson, C. A., Hoey, A. S., Cowman, P. F., & Wilson, S. K. (2018). Effects of Coral Bleaching and Coral Loss on the Structure and Function of Reef Fish Assemblages. In M. J. H. van Oppen & J. M. Lough (Eds.), *Coral Bleaching* (Vol. 233, pp. 265–293). Springer International Publishing. https://doi.org/10.1007/978-3-319-75393-5_11

Pratchett, M. S., Wilson, S. K., Graham, N. A. J., Munday, P. L., Jones, G. P., & Polunin, N. V. C. (2009). Coral Bleaching and Consequences for Motile Reef Organisms: Past, Present and Uncertain Future Effects. In M. J. H. van Oppen & J. M. Lough (Eds.), *Coral Bleaching: Patterns, Processes, Causes and Consequences* (pp. 139–158). Springer. https://doi.org/10.1007/978-3-540-69775-6_9

Price, D. M., Robert, K., Callaway, A., Lo lacono, C., Hall, R. A., & Huvenne, V. A. I. (2019). Using 3D photogrammetry from ROV video to quantify cold-water coral reef structural complexity and investigate its influence on biodiversity and community assemblage. *Coral Reefs*, *38*(5), 1007–1021. https://doi.org/10.1007/s00338-019-01827-3

R Core Team. (2023). *R: A language and environment for statistical computing* (Version 4.3.1). R Foundation for Statistical Computing. https://www.R-project.org/

Régnier, C., Achaz, G., Lambert, A., Cowie, R. H., Bouchet, P., & Fontaine, B. (2015). Mass extinction in poorly known taxa. *Proceedings of the National Academy of Sciences*, *112*(25), 7761–7766. https://doi.org/10.1073/pnas.1502350112

Remmers, T., Boutros, N., Wyatt, M., Gordon, S., Toor, M., Roelfsema, C., Fabricius, K., Grech, A., Lechene, M., & Ferrari, R. (2025). RapidBenthos: Automated segmentation and multi-view classification of coral reef communities from photogrammetric reconstruction. *Methods in Ecology and Evolution*, *16*(2), 427–441. https://doi.org/10.1111/2041-210X.14477

Remmers, T., Grech, A., Roelfsema, C., Gordon, S., Lechene, M., & Ferrari, R. (2024). Close-range underwater photogrammetry for coral reef ecology: A systematic literature review. *Coral Reefs*, *43*(1), 35–52. https://doi.org/10.1007/s00338-023-02445-w

Rich, W. A., Carvalho, S., Cadiz, R., Gil, G., Gonzalez, K., & Berumen, M. L. (2022). Size structure of the coral Stylophora pistillata across reef flat zones in the central Red Sea. *Scientific Reports*, *12*(1), 13979. https://doi.org/10.1038/s41598-022-17908-3

Ricolfe-Viala, C., & Esparza, A. (2021). The Influence of Autofocus Lenses in the Camera Calibration Process. *IEEE Transactions on Instrumentation and Measurement*, *70*, 1–15. IEEE Transactions on Instrumentation and Measurement. https://doi.org/10.1109/TIM.2021.3055793

Riegl, B., Cavalcante, G., Bauman, A. G., Feary, D. A., Steiner, S., & Purkis, S. (2017). Demographic Mechanisms of Reef Coral Species Winnowing from Communities under Increased Environmental Stress. *Frontiers in Marine Science*, *4*. https://doi.org/10.3389/fmars.2017.00344

Ritchie, E. G., & Johnson, C. N. (2009). Predator interactions, mesopredator release and biodiversity conservation. *Ecology Letters*, *12*(9), 982–998. https://doi.org/10.1111/j.1461-0248.2009.01347.x

Robson, B. (2023). *Useful Functions to Handle eReefs and EMS model Output*. https://rdrr.io/github/BarbaraRobson/ereefs/

Roelfsema, C., Kovacs, E., Ortiz, J. C., Wolff, N. H., Callaghan, D., Wettle, M., Ronan, M., Hamylton, S. M., Mumby, P. J., & Phinn, S. (2018). Coral reef habitat mapping: A combination of object-based image analysis and ecological modelling. *Remote Sensing of Environment*, *208*, 27–41. https://doi.org/10.1016/j.rse.2018.02.005

Roff, G., & Mumby, P. J. (2012). Global disparity in the resilience of coral reefs. *Trends in Ecology & Evolution*, *27*(7), 404–413. https://doi.org/10.1016/j.tree.2012.04.007

Roff, G., Zhao, J., & Mumby, P. J. (2015). Decadal-scale rates of reef erosion following El Niño-related mass coral mortality. *Global Change Biology*, *21*(12), 4415–4424. https://doi.org/10.1111/gcb.13006

Romero, G. Q., Gonçalves-Souza, T., Vieira, C., & Koricheva, J. (2015). Ecosystem engineering effects on species diversity across ecosystems: A meta-analysis. *Biological Reviews*, *90*(3), 877–890. https://doi.org/10.1111/brv.12138

Romero-Torres, M., Acosta, A., Palacio-Castro, A. M., Treml, E. A., Zapata, F. A., Paz-García, D. A., & Porter, J. W. (2020). Coral reef resilience to thermal stress in the Eastern Tropical Pacific. *Global Change Biology*, *26*(7), 3880–3890. https://doi.org/10.1111/gcb.15126

Rossi, P., Castagnetti, C., Capra, A., Brooks, A. J., & Mancini, F. (2020). Detecting change in coral reef 3D structure using underwater photogrammetry: Critical issues and performance metrics. *Applied Geomatics*, *12*(S1), 3–17. https://doi.org/10.1007/s12518-019-00263-w

Roughgarden, J. (1975). A Simple Model for Population Dynamics in Stochastic Environments. *The American Naturalist*, *109*(970), 713–736. https://doi.org/10.1086/283039

Sandin, S. A., Edwards, C. B., Pedersen, N. E., Petrovic, V., Pavoni, G., Alcantar, E., Chancellor, K. S., Fox, M. D., Stallings, B., Sullivan, C. J., Rotjan, R. D., Ponchio, F., & Zgliczynski, B. J. (2020). Chapter Seven—Considering the rates of growth in two taxa of coral across Pacific islands. In B. M. Riegl (Ed.), *Advances in Marine Biology* (Vol. 87, pp. 167–191). Academic Press. https://doi.org/10.1016/bs.amb.2020.08.006

Seidl, R., Rammer, W., & Spies, T. A. (2014). Disturbance legacies increase the resilience of forest ecosystem structure, composition, and functioning. *Ecological Applications*, *24*(8), 2063–2077. https://doi.org/10.1890/14-0255.1

Shaver, E. C., McLeod, E., Hein, M. Y., Palumbi, S. R., Quigley, K., Vardi, T., Mumby, P. J., Smith, D., Montoya-Maya, P., Muller, E. M., Banaszak, A. T., McLeod, I. M., & Wachenfeld, D. (2022). A roadmap to integrating resilience into the practice of coral reef restoration. *Global Change Biology*, *28*(16), 4751–4764. https://doi.org/10.1111/gcb.16212

Shenkar, N., Fine, M., & Loya, Y. (2005). Size matters: Bleaching dynamics of the coral Oculina patagonica. *Marine Ecology Progress Series*, *294*, 181–188. https://doi.org/10.3354/meps294181

Shugart, H. H., Saatchi, S., & Hall, F. G. (2010). Importance of structure and its measurement in quantifying function of forest ecosystems. *Journal of Geophysical Research: Biogeosciences*, *115*(G2). https://doi.org/10.1029/2009JG000993

Skarlatos, D., Agrafiotis, P., Menna, F., Nocerino, E., & Remondino, F. (2017). *Ground control networks for underwater photogrammetry in archaeological excavations*.

Smith, T. B., Glynn, P. W., Maté, J. L., Toth, L. T., & Gyory, J. (2014). A depth refugium from catastrophic coral bleaching prevents regional extinction. *Ecology*, *95*(6), 1663–1673. https://doi.org/10.1890/13-0468.1

Sommer, B., Hodge, J. M., Lachs, L., Cant, J., Pandolfi, J. M., & Beger, M. (2024). Decadal demographic shifts and size-dependent disturbance responses of corals in a subtropical warming hotspot. *Scientific Reports*, *14*(1), 6327. https://doi.org/10.1038/s41598-024-56890-w

Soong, K. (1993). Colony size as a species character in massive reef corals. *Coral Reefs*, *12*(2), 77–83. https://doi.org/10.1007/BF00302106

Spalding, M., Burke, L., Wood, S. A., Ashpole, J., Hutchison, J., & zu Ermgassen, P. (2017). Mapping the global value and distribution of coral reef tourism. *Marine Policy*, *82*, 104–113. https://doi.org/10.1016/j.marpol.2017.05.014

Speare, K. E., Adam, T. C., Winslow, E. M., Lenihan, H. S., & Burkepile, D. E. (2022). Size-dependent mortality of corals during marine heatwave erodes recovery capacity of a coral reef. *Global Change Biology*, *28*(4), 1342–1358. https://doi.org/10.1111/gcb.16000

Speare, K. E., Enright, L. N., Aplin, A., Adam, T. C., Edmunds, P. J., & Burkepile, D. E. (2025). Early life stage bottleneck determines rates of coral recovery following severe disturbance. *Ecology*, *106*(1), e4510. https://doi.org/10.1002/ecy.4510

Stan Development Team. (n.d.). *RStan: The R interface to Stan* (Version 2.26.22). https://mc-stan.org/

Stella, J., Pratchett, M., Hutchings, P., & Jones, G. (2011). Coral-associated invertebrates: Diversity, ecological importance and vulnerability to disturbance. In J. Gordon (Ed.), *Oceanography and Marine Biology* (Vol. 20115434). CRC Press. https://doi.org/10.1201/b11009-3

Steven, A. D. L., Baird, M. E., Brinkman, R., Car, N. J., Cox, S. J., Herzfeld, M., Hodge, J., Jones, E., King, E., Margvelashvili, N., Robillot, C., Robson, B., Schroeder, T., Skerratt, J., Tickell, S., Tuteja, N., Wild-Allen, K., & Yu, J. (2019). eReefs: An operational information system for managing the Great Barrier Reef. *Journal of Operational Oceanography*, *12*(sup2), S12–S28. https://doi.org/10.1080/1755876X.2019.1650589

Stevens, G. C. (1989). The Latitudinal Gradient in Geographical Range: How so Many Species Coexist in the Tropics. *The American Naturalist*, *133*(2), 240–256. https://doi.org/10.1086/284913

Stimson, J., Sakai, K., & Sembali, H. (2002). Interspecific comparison of the symbiotic relationship in corals with high and low rates of bleaching-induced mortality. *Coral Reefs*, *21*, 409–421.

Suggett, D. J., Guest, J., Camp, E. F., Edwards, A., Goergen, L., Hein, M., Humanes, A., Levy, J. S., Montoya-Maya, P. H., Smith, D. J., Vardi, T., Winters, R. S., & Moore, T. (2024). Restoration as a meaningful aid to ecological recovery of coral reefs. *Npj Ocean Sustainability*, *3*(1), 1–4. https://doi.org/10.1038/s44183-024-00056-8

Sully, S., & van Woesik, R. (2020). Turbid reefs moderate coral bleaching under climate-related temperature stress. *Global Change Biology*, *26*(3), 1367–1373. https://doi.org/10.1111/gcb.14948

Sunday, J. M., Bates, A. E., & Dulvy, N. K. (2012). Thermal tolerance and the global redistribution of animals. *Nature Climate Change*, *2*(9), 686–690. https://doi.org/10.1038/nclimate1539

Swain, T. D., Vega-Perkins, J. B., Oestreich, W. K., Triebold, C., DuBois, E., Henss, J., Baird, A., Siple, M., Backman, V., & Marcelino, L. (2016). Coral bleaching response index: A new tool to standardize and compare susceptibility to thermal bleaching. *Global Change Biology*, *22*(7), 2475–2488. https://doi.org/10.1111/gcb.13276

Taraldsen, G., Reinen, T., & Berg, T. (2011). The underwater GPS problem. In *OCEANS 2011 IEEE - Spain* (p. 8). https://doi.org/10.1109/Oceans-Spain.2011.6003649

Tebbett, S. B., Emslie, M. J., Jonker, M. J., Ling, S. D., Pratchett, M. S., Siqueira, A. C., Thompson, A. A., Yan, H. F., & Bellwood, D. R. (2025). Epilithic algal composition and the functioning of Anthropocene coral reefs. *Marine Pollution Bulletin*, *210*, 117322. https://doi.org/10.1016/j.marpolbul.2024.117322

Thomas, L., Rose, N. H., Bay, R. A., López, E. H., Morikawa, M. K., Ruiz-Jones, L., & Palumbi, S. R. (2018). Mechanisms of Thermal Tolerance in Reef-Building Corals across a Fine-Grained Environmental Mosaic: Lessons from Ofu, American Samoa. *Frontiers in Marine Science*, *4*. https://doi.org/10.3389/fmars.2017.00434

Tompalski, P., Coops, N. C., White, J. C., Goodbody, T. R. H., Hennigar, C. R., Wulder, M. A., Socha, J., & Woods, M. E. (2021). Estimating Changes in Forest Attributes and Enhancing Growth Projections: A Review of Existing Approaches and Future Directions Using Airborne 3D Point Cloud Data. *Current Forestry Reports*, *7*(1), 1–24. https://doi.org/10.1007/s40725-021-00135-w

Toor, M., Lechene, M., Becker, M., Remmers, T., Gordon, S., Stratford, J., & Ferrari, R. (2025). Field Photogrammetry in 4D: Digitisation and 2D metric extraction. Reef Restoration and Adaptation Program

(EcoRRAP). Standard Operating Procedure 17 (No. 3 of series). *AIMS Reef Monitoring SOPs*. https://www.aims.gov.au/sites/default/files/2025-06/AIMS_EcoRRAP_SOP17_V1_Field-Photogrammetry4D_2D-Digitisation_Metric_Extraction.pdf

Toth, L. T., Courtney, T. A., Colella, M. A., Kupfner Johnson, S. A., & Ruzicka, R. R. (2022). The past, present, and future of coral reef growth in the Florida Keys. *Global Change Biology*, *28*(17), 5294–5309. https://doi.org/10.1111/gcb.16295

van Hooidonk, R., Maynard, J., Tamelander, J., Gove, J., Ahmadia, G., Raymundo, L., Williams, G., Heron, S. F., & Planes, S. (2016). Local-scale projections of coral reef futures and implications of the Paris Agreement. *Scientific Reports*, *6*(1), 39666. https://doi.org/10.1038/srep39666

van Oppen, M. J. H., Oliver, J. K., Putnam, H. M., & Gates, R. D. (2015). Building coral reef resilience through assisted evolution. *Proceedings of the National Academy of Sciences*, *112*(8), 2307–2313. https://doi.org/10.1073/pnas.1422301112

van Woesik, R., Sakai, K., Ganase, A., & Loya, Y. (2011). Revisiting the winners and the losers a decade after coral bleaching. *Marine Ecology Progress Series*, *434*, 67–76. https://doi.org/10.3354/meps09203

Wagner, D. E., Kramer, P., & Van Woesik, R. (2010). Species composition, habitat, and water quality influence coral bleaching in southern Florida. *Marine Ecology Progress Series*, *408*, 65–78.

Walker, A. S., Kratochwill, C. A., & van Woesik, R. (2024). Past disturbances and local conditions influence the recovery rates of coral reefs. *Global Change Biology*, *30*(1), e17112. https://doi.org/10.1111/gcb.17112

Ward, S., Harrison, P., & Hoegh-Guldberg, O. (2002). Coral bleaching reduces reproduction of scleractinian corals and increases susceptibility to future stress. *Proceedings of the Ninth International Coral Reef Symposium, Bali, 23-27 October 2000*, *2*, 1123–1128.

Warner, M., Chilcoat, G., McFarland, F., & Fitt, W. (2002). Seasonal fluctuations in the photosynthetic capacity of photosystem II in symbiotic dinoflagellates in the Caribbean reef-building coral Montastraea. *Marine Biology*, *141*(1), 31–38. https://doi.org/10.1007/s00227-002-0807-8

Wauchope, H. S., Amano, T., Geldmann, J., Johnston, A., Simmons, B. I., Sutherland, W. J., & Jones, J. P. G. (2021). Evaluating Impact Using Time-Series Data. *Trends in Ecology & Evolution*, *36*(3), 196–205. https://doi.org/10.1016/j.tree.2020.11.001

Webb, T. J., & Mindel, B. L. (2015). Global Patterns of Extinction Risk in Marine and Non-marine Systems. *Current Biology*, *25*(4), 506–511. https://doi.org/10.1016/j.cub.2014.12.023

Wedding, L. M., Jorgensen, S., Lepczyk, C. A., & Friedlander, A. M. (2019). Remote sensing of three-dimensional coral reef structure enhances predictive modeling of fish assemblages. *Remote Sensing in Ecology and Conservation*, *5*(2), 150–159. https://doi.org/10.1002/rse2.115

Westoby, M. J., Brasington, J., Glasser, N. F., Hambrey, M. J., & Reynolds, J. M. (2012). 'Structure-from-Motion' photogrammetry: A low-cost, effective tool for geoscience applications. *Geomorphology*, *179*, 300–314. https://doi.org/10.1016/j.geomorph.2012.08.021

Wickham, H., Chang, W., & Wickham, H. (2016). Package 'ggplot2.' *Create Elegant Data Visualisations Using the Grammar of Graphics*, *2*(1), 1–189.

Wiedenmann, J., D'Angelo, C., Mardones, M. L., Moore, S., Benkwitt, C. E., Graham, N. A. J., Hambach, B., Wilson, P. A., Vanstone, J., Eyal, G., Ben-Zvi, O., Loya, Y., & Genin, A. (2023). Reef-building corals farm and feed on their photosynthetic symbionts. *Nature*, *620*(7976), 1018–1024. https://doi.org/10.1038/s41586-023-06442-5

Williams, I. D., Couch, C. S., Beijbom, O., Oliver, T. A., Vargas-Angel, B., Schumacher, B. D., & Brainard, R. E. (2019). Leveraging Automated Image Analysis Tools to Transform Our Capacity to Assess Status and Trends of Coral Reefs. *Frontiers in Marine Science*, *6*. https://doi.org/10.3389/fmars.2019.00222

Winslow, E. M., Speare, K. E., Adam, T. C., Burkepile, D. E., Hench, J. L., & Lenihan, H. S. (2024). Corals survive severe bleaching event in refuges related to taxa, colony size, and water depth. *Scientific Reports*, *14*(1), 9006. https://doi.org/10.1038/s41598-024-58980-1

Wolfe, D. A., Champ, M. A., Flemer, D. A., & Mearns, A. J. (1987). Long-term biological data sets: Their role in research, monitoring, and management of estuarine and coastal marine systems. *Estuaries*, *10*(3), 181–193. https://doi.org/10.2307/1351847

Woodhead, A. J., Hicks, C. C., Norström, A. V., Williams, G. J., & Graham, N. A. J. (2019). Coral reef ecosystem services in the Anthropocene. *Functional Ecology*, *33*(6), 1023–1034. https://doi.org/10.1111/1365-2435.13331

Wooldridge, S., & Done, T. (2004). Learning to predict large-scale coral bleaching from past events: A Bayesian approach using remotely sensed data, in-situ data, and environmental proxies. *Coral Reefs*, *23*(1), 96–108. https://doi.org/10.1007/s00338-003-0361-y

Yadav, S., Roach, T. N., McWilliam, M. J., Caruso, C., de Souza, M. R., Foley, C., Allen, C., Dilworth, J., Huckeba, J., & Santoro, E. P. (2023). Fine-scale variability in coral bleaching and mortality during a marine heatwave. *Frontiers in Marine Science*, *10*, 1108365.

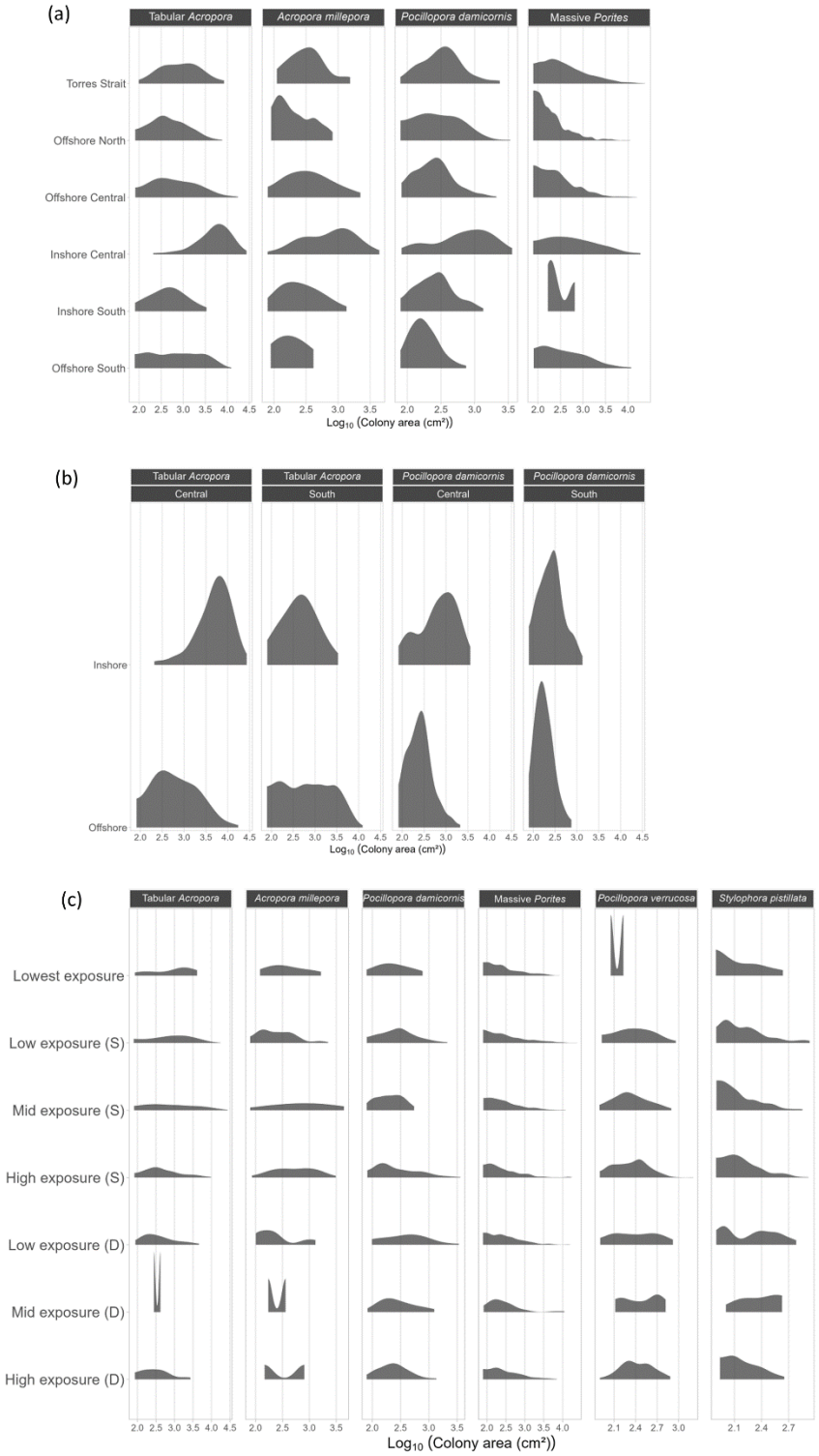
Young, G. C., Dey, S., Rogers, A. D., & Exton, D. (2017). Cost and time-effective method for multi-scale measures of rugosity, fractal dimension, and vector dispersion from coral reef 3D models. *PLOS ONE*, *12*(4), e0175341. https://doi.org/10.1371/journal.pone.0175341

Yuval, M., Pearl, N., Tchernov, D., Martinez, S., Loya, Y., Bar-Massada, A., & Treibitz, T. (2023). Assessment of storm impact on coral reef structural complexity. *Science of The Total Environment*, *891*, 164493. https://doi.org/10.1016/j.scitotenv.2023.164493

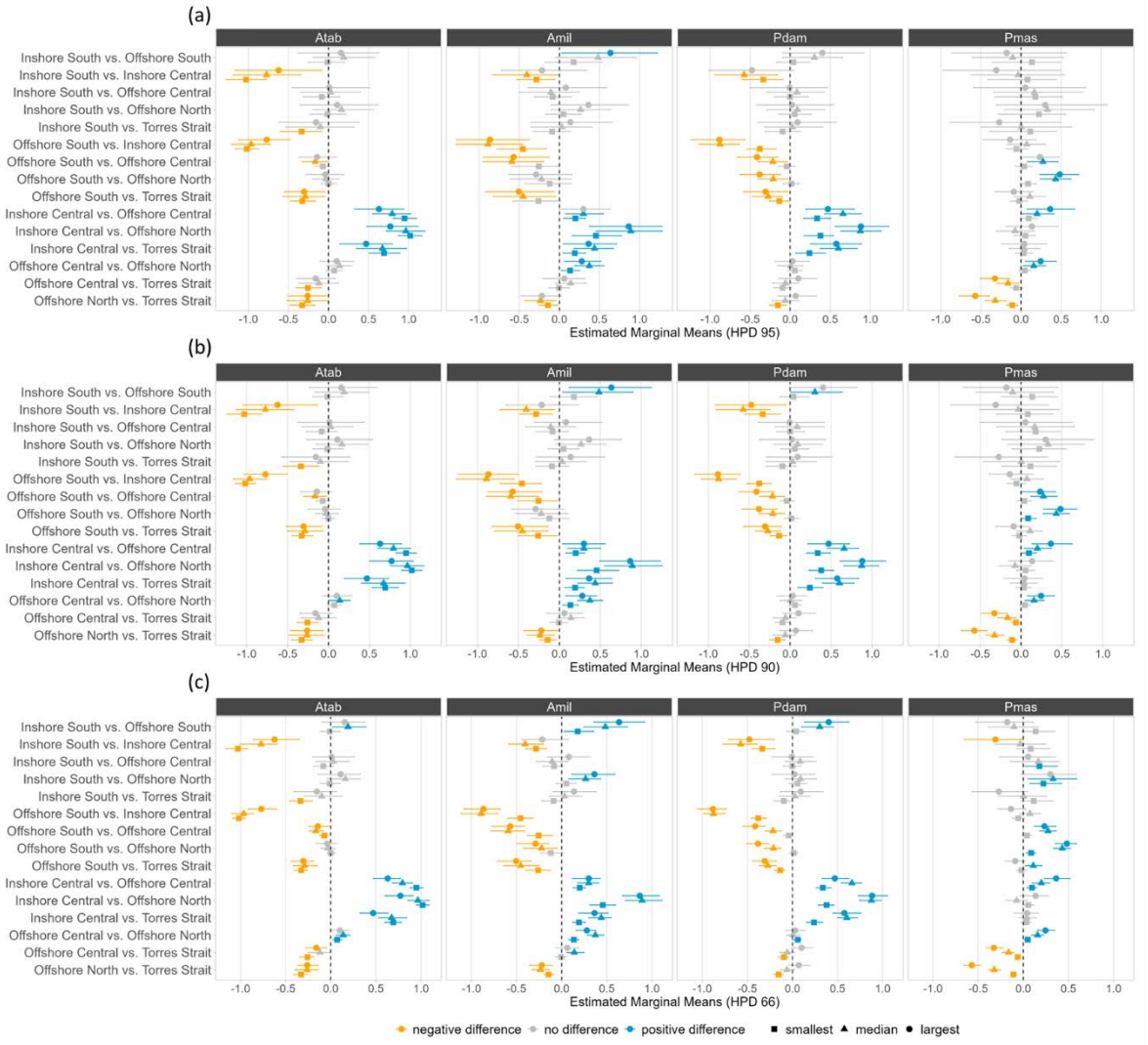
Zawada, K. J. A., Dornelas, M., & Madin, J. S. (2019). Quantifying coral morphology. *Coral Reefs*, *38*(6), 1281–1292. https://doi.org/10.1007/s00338-019-01842-4

Zawada, K. J. A., Madin, J. S., Baird, A. H., Bridge, T. C. L., & Dornelas, M. (2019). Morphological traits can track coral reef responses to the Anthropocene. *Functional Ecology*, *33*(6), 962–975. https://doi.org/10.1111/1365-2435.13358

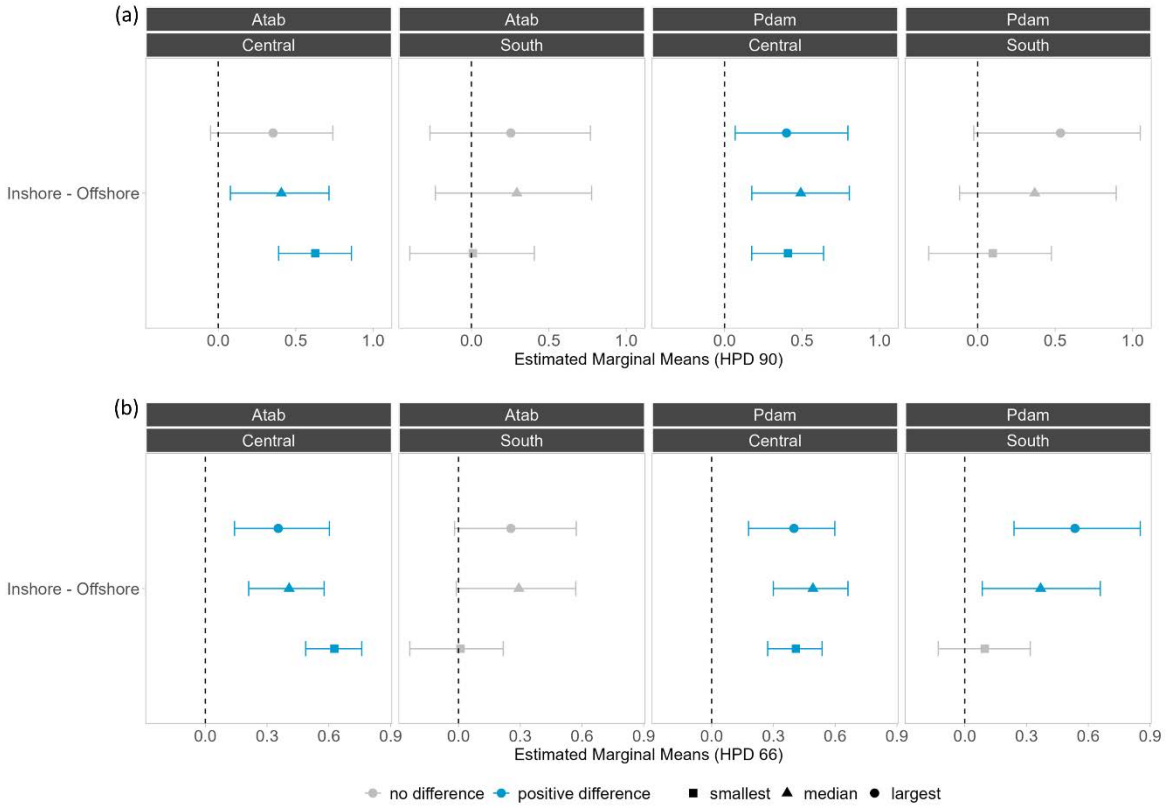
Appendix A. Supplementary material to Chapter 2



Supplementary Figure S.1. Colony size distributions (log-transformed) across (a) reef clusters, (b) cross-shelf positions, and (c) habitat types. Distributions show log10-transformed planar colony area (cm2) for colonies with estimated diameters > 10 cm. Size densities are visualised using slab plots, with each slab representing the relative distribution of sizes for a given taxon within each spatial grouping.

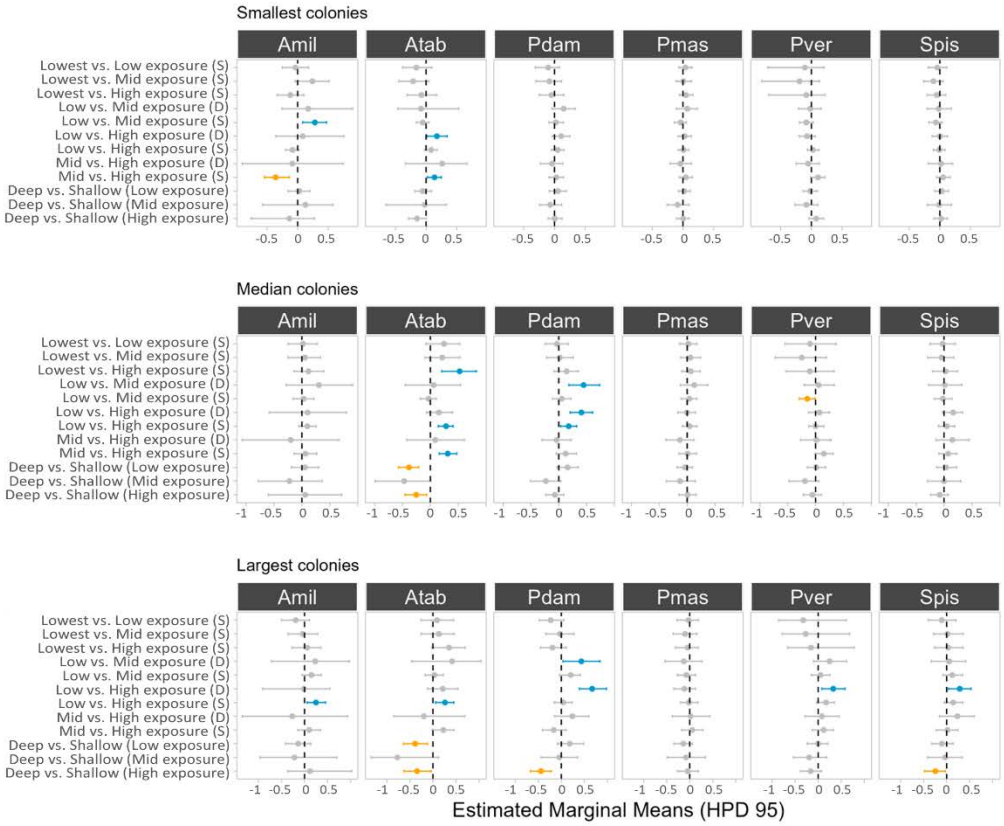


Supplementary Figure S.2. Pairwise comparisons of colony sizes (estimated marginal means) between clusters at 95% (a), 90% (b) and 66% (c) highest posterior density (HPD) credible interval. Contrasts are ordered as the cluster expected to have larger corals is the first cluster A of each pair A versus B (i.e., all differences should be positive given our hypothesis that corals are larger in higher latitude). Grey contrasts correspond to no evidence of a difference in size between clusters. Blue contrasts correspond to a positive difference and coral size is larger in the first cluster. Orange contrasts correspond to a negative difference and coral size is smaller in the first cluster. The three size classes (quantiles) are denoted by three different shapes for the estimated marginal means: square for smallest, triangle for median and circle for largest. Taxa are coded as: Atab = tabular Acropora, Amil = Acropora millepora, Pdam = Pocillopora damicornis and Pmas = massive Porites.

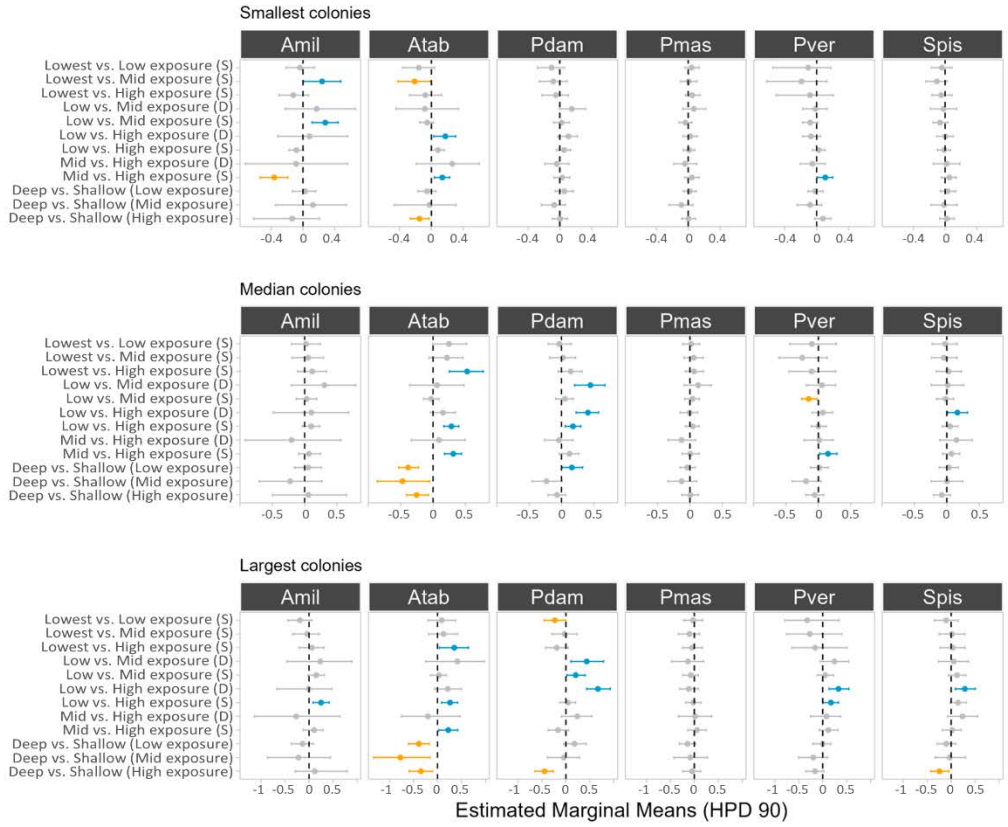


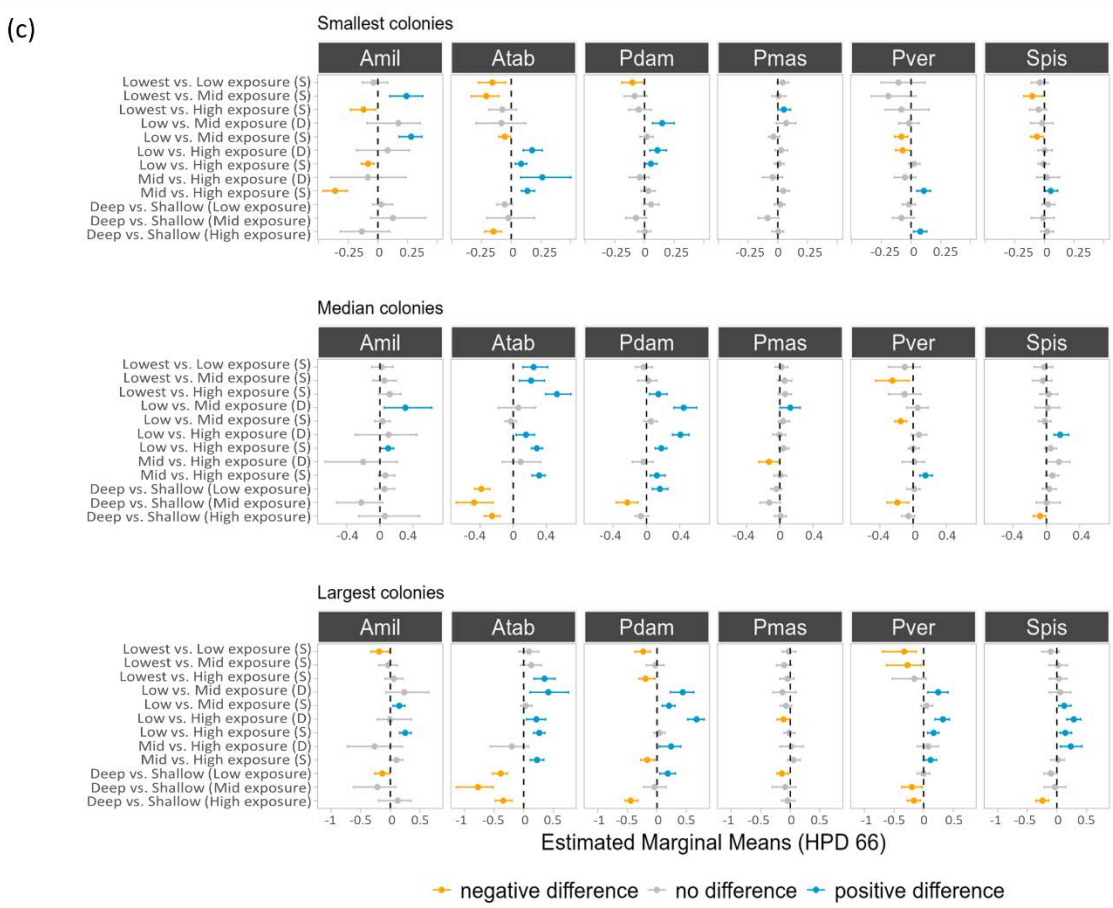
Supplementary Figure S.3. Pairwise comparisons of colony sizes (estimated marginal means) between inshore and offshore habitats for each morphotaxa and size class at HPD credible intervals 90% (a) and 66% (b). When intervals do not cross zero and are positive, there is evidence that colony size inshore is larger than offshore (hypothesis validated). Taxa are coded as: Atab = tabular Acropora, and Pdam = Pocillopora damicornis.

(a)


Smallest colonies
Median colonies
Largest colonies
Amil
Atab
Pdam
Pmas
Pver
Spis
Lowest vs. Low exposure (S)
Lowest vs. Mid exposure (S)
Lowest vs. High exposure (S)
Low vs. Mid exposure (D)
Low vs. Mid exposure (S)
Low vs. High exposure (D)
Low vs. High exposure (S)
Mid vs. High exposure (D)
Mid vs. High exposure (S)
Deep vs. Shallow (Low exposure)
Deep vs. Shallow (Mid exposure)
Deep vs. Shallow (High exposure)
Estimated Marginal Means (HPD 95)

(b)


Smallest colonies
Median colonies
Largest colonies
Amil
Atab
Pdam
Pmas
Pver
Spis
Lowest vs. Low exposure (S)
Lowest vs. Mid exposure (S)
Lowest vs. High exposure (S)
Low vs. Mid exposure (D)
Low vs. Mid exposure (S)
Low vs. High exposure (D)
Low vs. High exposure (S)
Mid vs. High exposure (D)
Mid vs. High exposure (S)
Deep vs. Shallow (Low exposure)
Deep vs. Shallow (Mid exposure)
Deep vs. Shallow (High exposure)
Estimated Marginal Means (HPD 90)



Supplementary Figure S.4. Pairwise comparisons of colony sizes (estimated marginal means) between habitats at 95% (a), 90% (b) and 66% (c) highest posterior density (HPD) credible interval. Contrasts are ordered as the habitat expected to have larger corals is the first of each pair (i.e., all differences should be positive given our hypothesis that corals are larger in less exposed habitats). Grey contrasts correspond to no evidence of a difference in size between habitats. Blue contrasts correspond to a positive difference and coral size is larger in the first habitat (to the left). Orange contrasts correspond to a negative difference and coral size is smaller in the first habitat. Taxa are coded as: Amil = Acropora millepora, Atab = tabular Acropora, Pdam = Pocillopora damicornis, Pmas = massive Porites, Pver = Pocillopora verrucosa and Spis = Stylophora pistillata.

Appendix B. Supplementary material to Chapter 3

Supplementary Table S.1. Main characteristics and settings of underwater photogrammetry systems used. See Gordon et al. (2023) for in-depth camera settings.

Camera type and body	DSLR Nikon D850
Lens	Nikkor 20 mm, f/1.8
Sensor type (Dimensions (mm))	Full frame (35.9 x 23.9)
Pixel dimensions	8256 x 5504
Pixel size (µm)	4.36
Underwater pressure housing	Nauticam 17222 NA - D850
Dome port (material)	Nauticam N120 8.5" (acrylic)
Image quality	Fine
Image size	JPEG/TIFF Large
Shooting mode	Aperture priority
Aperture value	Aperture range should be approx. f/5-f/13 (f/11 ideal)
Minimum shutter speed	1/500 (1/250 in very dark conditions)
Exposure compensation	-0.7 (-0.3 in very dark conditions, -1 in very light conditions)
ISO mode	Auto
ISO sensitivity limits	1600 (light conditions) - 2500 (dark conditions)
Focus	Autofocus continuous
Pre-calibration	No

Supplementary Table S.2. Processing steps, descriptions and settings used to build 3D models in Metashape.

Step	Description	Parameters and settings
Quality check	- Assesses the quality of photos and removes those below 0.5 - Repeatedly disables, counts, and adjusts (if required) the quality threshold to retain the 'targeted number of photos' of the maximum quality - Begins process using the 'initial quality' threshold and reduces the quality threshold (as required) by the 'quality step value,' until ≥ the 'minimum quality' threshold is reached	- Targeted number of photos to retain: > 2000 - Initial quality: 0.50 - Minimum quality: 0.35 - Quality step value: 0.05
Lowest quality alignment	Aligns photos to give the markers points in 3D space	- Accuracy: Lowest - Generic preselection: Yes - Reference preselection: Source - Key point limit: 40,000 - Tie point limit: 10,000 - Exclude stationary tie points: Yes - Reset alignment: Yes - Adaptive camera model fitting: No - Guided image matching: No - Minimum alignment: 80 %
Detect markers	Detects markers using 'initial marker tolerance' and removes markers with projections ≥ the 'marker projection error' threshold, and markers with projection numbers < the 'minimum marker projections' threshold	- Target type: Circular Target 12 bit - Initial marker tolerance: 25 - Secondary marker tolerance: 50 - Marker projection error: 50 - Minimum marker projections: 5 - Filter mask: False - Inverted: True - No parity: False - Maximum residual: 5 - Minimum size: 0 - Minimum distance: 5
Add and check scale bars	- Adds scale bars based on marker number pairings in text file - Checks the number of scale bars is ≥ the 'minimum scalebars' threshold	- Minimum scalebars: 3 - Maximum scalebar error (m): 0.01
Import depths	Imports marker X and Y coordinates, depth values (Z), and related accuracies	
High quality alignment	Resets low quality camera alignment and re-aligns at high quality	- Accuracy: High - Generic preselection: Yes - Reference preselection: Source - Key point limit: 40,000 - Tie point limit: 0 - Exclude stationary tie points: Yes - Guided image matching: No - Adaptive camera model fitting: No - Reset alignment: Yes - Minimum alignment: 80 %
Calculate scalebar error	Calculates and checks scale bar error as per step 4	
Resize bounding box	Resizes bounding box to size of required 'plot size'	Plot size: 12 x 6 x 10 m (x, y, and z, respectively)
Crops point cloud	Removes all sparse cloud points outside bounding box	
Initial camera optimization	Performs an adjustment procedure using coordinates, depths, scale bars, and corresponding accuracies, to refine exterior and interior camera orientation parameters and tie point coordinates	

Filter and re-optimize cameras	- Filters point cloud by: Selecting points with a reconstruction uncertainty > the 'maximum reconstruction uncertainty' and > 'minimum projection accuracy' Checking if the selected points > 'maximum point cloud percentage' and deletes points up to the 'maximum point cloud percentage' - Re-Optimizes cameras - Performs 5-step loop of reprojection error improvement (repeatedly removing the worst 'percentage point cloud removal' of current point cloud) by: Checking reprojection error before each iteration Optimizing after each iteration Using the 'target reprojection error' - Loop stops when either the target value is reached, or point cloud size falls < 'minimum point cloud size' of the original size (whichever comes first) - Performs final full optimization of cameras	- Maximum reconstruction uncertainty: 10 - Minimum projection accuracy: 3 - Target reprojection error: 0.5 - Maximum point cloud percentage: 50 - Percentage point cloud removal: 10 - Minimum point cloud size (%): 30
Build depth maps	Generates multiple pairwise 'depth maps' from overlapping image pairs considering their relative exterior and interior orientation parameters. These are merged into a combined depth map of the plot from which a mesh can be made.	- Filtering: Mild - Reuse depth maps: No - Maximum neighbors: 40 - Maximum group size: 100
Build mesh	Reconstructs a polygonal mesh model based on depth maps data	- Source data: Depth map - Surface type: Arbitrary (3D) - Depth map quality: Medium - Face count: High - Custom face count: 200,000 - Interpolation: Enabled (default) - Depth filtering: Mild - Point classes: All - Calculate vertex colors: Yes
Build texture	Builds different types of texture for the model	- Texture type: Diffuse map - Source data: Images - Mapping mode: Generic - Blending mode: Mosaic (default) - Texture size: 8192 - Enable hole filling: Yes - Enable ghost filter: No

Supplementary Table S.3. Survey and 3D processing statistics for all reference (Ref.) and test models. The number of images column refers to images that were aligned during the image high quality alignment processing step, ensuring at least 80% of total images were aligned.

		No. of images		Flying altitude (m)		Ground resolution (mm/pix)		Scale bar error (mm)		No. of faces	
Source of error	**Plot**	**Ref.**	**Test**	**Ref.**	**Test**	**Ref.**	**Test**	**Ref.**	**Test**	**Ref.**	**Test**
Co-registration	P01	2542	2542	1.59	1.59	0.291	0.291	1.297	1.297	37,613,686	37,613,686
Co-registration	P02	2358	2358	1.93	1.93	0.353	0.353	0.957	0.957	32,494,271	32,494,271
Co-registration	P03	2058	2058	1.95	1.95	0.357	0.357	1.319	1.319	34,341,510	34,341,510
Co-registration	P04	2469	2469	1.51	1.51	0.276	0.276	1.428	1.428	39,026,888	39,026,888
Co-registration	P05	2596	2596	2.25	2.25	0.411	0.411	0.246	0.246	25,703,619	25,703,619
Co-registration	P06	2242	2242	2.35	2.35	0.429	0.429	0.931	0.931	30,889,065	30,889,065
Co-registration	P07	2659	2659	1.86	1.86	0.341	0.341	0.957	0.957	30,961,836	30,961,836
Co-registration	P08	2901	2901	2.04	2.04	0.372	0.372	0.177	0.177	21,889,265	21,889,265
Co-registration	P09	2070	2070	1.9	1.9	0.346	0.346	0.198	0.198	16,598,998	16,598,998
Co-registration	P10	2167	2167	2.28	2.28	0.416	0.416	0.269	0.269	16,047,588	16,047,588
3D processing	P01	2678	2732	2.09	2.08	0.383	0.381	0.671	0.623	18,601,938	17,985,139
3D processing	P02	2838	2830	2	1.98	0.365	0.362	0.259	0.279	12,522,032	11,877,166
3D processing	P03	2636	2616	1.95	1.93	0.357	0.352	0.271	0.276	20,937,094	19,917,953
3D processing	P04	2474	2518	2.01	1.99	0.368	0.364	1.113	1.188	18,762,131	18,368,531
3D processing	P05	2549	2538	2.21	2.21	0.406	0.405	0.211	0.147	26,511,531	25,543,077
3D processing	P06	2902	2927	2.31	2.25	0.423	0.412	0.254	0.275	22,166,553	22,026,107
3D processing	P07	2246	2240	2.4	2.4	0.439	0.44	0.17	0.206	24,284,192	23,927,404
3D processing	P08	2757	2779	2.26	2.23	0.414	0.407	0.26	0.307	22,959,699	22,242,784
3D processing	P09	2596	2571	2.25	2.25	0.411	0.411	0.246	0.287	25,703,619	25,093,782
3D processing	P10	1892	1893	1.38	1.38	0.253	0.253	0.166	0.168	10,062,434	9,788,709
Image acquisition	P01	2861	2515	1.69	1.83	0.309	0.336	1.414	1.64	47,319,735	38,830,993
Image acquisition	P02	2732	2622	1.83	1.87	0.336	0.342	1.331	1.364	35,677,325	51,797,739
Image acquisition	P03	2358	2290	1.93	1.95	0.353	0.358	0.958	1.458	32,494,271	24,652,514
Image acquisition	P04	2526	2723	1.89	1.75	0.347	0.32	1.668	1.438	25,279,517	37,889,685
Image acquisition	P05	2469	2064	1.51	1.49	0.276	0.273	1.429	1.553	39,026,888	30,768,657
Image acquisition	P06	2068	2247	1.45	1.53	0.266	0.278	2.299	2.043	26,077,657	23,596,831
Image acquisition	P07	2636	3183	1.95	1.81	0.357	0.331	0.271	0.313	20937094	34,645,728
Image acquisition	P08	2888	2956	1.97	1.58	0.361	0.289	0.21	0.159	28,018,522	52,608,751
Image acquisition	P09	2596	3113	2.25	1.53	0.411	0.278	0.246	0.193	25,703,619	65,045,482
Image acquisition	P10	2569	3242	2.24	1.48	0.409	0.269	0.48	0.116	22,703,595	65,566,813
RSF placement	P01	2678	3089	2.09	1.98	0.383	0.362	0.671	0.182	18,601,938	31,488,521
RSF placement	P02	2838	3012	2	2.03	0.365	0.372	0.259	0.229	12,522,032	22,836,149
RSF placement	P03	2474	2881	2.01	2.08	0.368	0.381	1.113	0.226	18,762,131	23,816,278
RSF placement	P04	2474	3018	2.01	2.06	0.368	0.376	1.113	0.529	18,762,131	24,743,674
RSF placement	P05	2902	3048	2.31	2.18	0.423	0.398	0.254	0.149	22,166,553	25,991,579
RSF placement	P06	2246	2442	2.4	2.59	0.439	0.474	0.17	0.076	24,284,192	21,209,931
RSF placement	P07	2757	3341	2.26	2.03	0.414	0.372	0.26	0.118	22,959,699	30,376,192
RSF placement	P08	3341	2358	2.03	1.98	0.372	0.363	0.118	0.185	30,376,192	31,756,283
RSF placement	P09	2596	3242	2.25	1.48	0.411	0.269	0.246	0.116	25,703,619	32,816,311
RSF placement	P10	2596	2569	2.25	2.24	0.411	0.409	0.246	0.48	25,703,619	22,703,595
Averages		2556	2642	2.02	1.95	0.370	0.356	0.654	0.603	25,278,957	29,386,977

Supplementary Table S 4. Proportion (%) of model-to-model deviations within three specific ranges: -1 to 1 mm, -10 to 10 mm and -30 to 30 mm for each source of error.

Source of error	-1 and 1 mm	-10 and 10 mm	-30 and 30 mm
Co-registration	88	100	100
3D processing	72	100	100
Image acquisition	24	96	100
RSF placement	7	53	90

Appendix C. Supplementary material to Chapter 4

Supplementary Table S1. Pairwise comparisons of log size at t1 – log size at t0 slopes between years for each taxon, significant p-values are in bold.

Taxa	Estimate	p-value
Acropora staghorn	-0.18497	**0.00005**
Acropora corymbose	0.10726	**0.00012**
Pocillopora damicornis	0.13495	0.25204
Pocillopora verrucosa	0.08355	**0.03629**
Seriatopora hystrix	0.87354	**0.00315**

Appendix D. Publications arising from this thesis

Lechene, M., Figueira, W. F., Murray, N. J., Aston, E. A., Gordon, S. E., & Ferrari, R. (2024). Evaluating error sources to improve precision in the co-registration of underwater 3D models. *Ecological Informatics*, *81*, 102632. https://doi.org/10.1016/j.ecoinf.2024.102632
(Chapter 3)

Lechene M., Álvarez-Noriega M., Becker M., Toor M., Gordon S., Remmers T., Figueira W., Hoogenboom M., & Ferrari R. (2025). Colony morphology and habitat drive coral size patterns. *Under review in Ecosphere*
(Chapter 2)

Lechene M., Burn D., Álvarez-Noriega M., Becker M., Toor M., Gordon S., Aston E., Hoogenboom M., & Ferrari R. (2025). Legacy effects of a mild bleaching event on coral survival and growth. *In preparation*
(Chapter 4)

Appendix E. Publications not arising from this thesis

Gordon, S., Aston, E., **Lechene, M.**, Harianto, J., Figueira, W., Gonzalez Rivero, M., & Ferrari, R. (2023). *Field photogrammetry in 4D. Reef Restoration and Adaption Program (EcoRRAP). Standard Operational Procedure Number 1: Overview and in-field workflow.* https://doi.org/10.25845/SE7T-PS86

Remmers, T., Grech, A., Roelfsema, C., Gordon, S., **Lechene, M.**, & Ferrari, R. (2024). Close-range underwater photogrammetry for coral reef ecology: A systematic literature review. *Coral Reefs*, *43*(1), 35–52. https://doi.org/10.1007/s00338-023-02445-w

Remmers, T., Boutros, N., Wyatt, M., Gordon, S., Toor, M., Roelfsema, C., Fabricius, K., Grech, A., **Lechene, M.**, & Ferrari, R. (2025). RapidBenthos: Automated segmentation and multi-view classification of coral reef communities from photogrammetric reconstruction. *Methods in Ecology and Evolution*, *16*(2), 427–441. https://doi.org/10.1111/2041-210X.14477

Álvarez-Noriega M., Aston E., Becker M., Fabricius K., Figueira W., Gordon S., Krensel R., **Lechene M.**, Remmers T., Toor M., & Ferrari R. (2025). Challenging paradigms around the role of colony size, taxa, and environment on bleaching susceptibility. *Global Change Biology.* https://doi.org/10.1111/gcb.70090

Gordon S., Aston E., **Lechene M**., Remmers T., Piccaluga A., Brinker E., Cowasji Z., Harianto J., Bray P., Millar G., Watkin B., Figueira W., Gonzalez Rivero M., Ferrari R. (2025). *Field photogrammetry in 4D: Model Processing. Reef Restoration and Adaption Program (EcoRRAP). Standard Operational Procedure 16 (2 of series): Model processing.* Australian Institute of Marine Science, Townsville. (57 pp). https://www.aims.gov.au/sites/default/files/2025-06/AIMS_EcoRRAP_SOP16_V1_Field-Photogrammetry4D_3D-Model-Processing_2023_06.2025.pdf

Meziere Z., Prata K., **Lechene M.**, Ferrari R., Popovic I., & Riginos C. (2025). Connectivity differs by orders of magnitude among co-distributed corals, affecting spatial scales of eco-evolutionary processes. *Science Advances*. DOI: 10.1126/sciadv.adt2066

Aston E., Toor M., Gordon S., **Lechene M.**, Álvarez-Noriega M., Ortiz J.-C., Fabricius K., Gonzalez-Rivero M., & Ferrari R. (2025). Size, taxa and temperature regulate growth and survival of Indo-Pacific corals. (in preparation).

Toor, M., Lechene, M.A., Becker, M.L., Remmers-Barry, T., Gordon, S., Stratford, J., Ferrari, R. (2025). *Field Photogrammetry in 4D: Digitisation and 2D metric extraction. Reef Restoration and Adaptation Program (EcoRRAP). Standard Operating Procedure 17 (No. 3 of series).* Australian Institute of Marine Science, Townsville. (77pp). https://www.aims.gov.au/sites/default/files/2025-06/AIMS_EcoRRAP_SOP17_V1_Field-Photogrammetry4D_2D-Digitisation_Metric_Extraction.pdf